R005-01
A 会場 ：11/24　PM1 （13:15-15:15）
13:15〜13:30

遷移領域を地上から高精度に観測するレーザー計測手法: 共鳴散乱 Ca/Ca+ ライダー

#桂川 眞幸 [1,2,3], 橋本 彩香 [1], 小林 蒼汰 [1], 三好 咲也子 [1], 大饗 千彰 [1,2], 江尻 省 [3,4], 中村 卓司 [3,4]
[1] 電気通信大学・大学院情報理工学研究科, [2] 電気通信大学・量子科学研究センター, [3] 国立極地研究所, [4] 総合研究大学院大学

Laser method of precisely observing the transition region from the ground: Resonance-scattering Ca/Ca+ lidar

#Masayuki Katsuragawa[1,2,3], Ayaka Hashimoto[1], Sota Kobayashi[1], Sayako Miyoshi[1], Chiaki Ohae[1,2], Mitsumu Ejiri[3,4], Takuji Nakamura[3,4]
[1]Graduate School of Informatics and Engineering, University of Electro-Communications, [2]Institute for Advanced Science, University of Electro-Communications, [3]National Institute of Polar Research, [4]The Graduate University for Advanced Studies

Resonant-scattering lidar which utilizes meteoric atoms and/or ions as tracers, is an excellent method that enables ground-based laser observation of the transition region with a high temporal and spatial resolution. The representative tracers are iron and sodium which are relatively densely distributed in the transition region, the measurements of iron and sodium, however, are restricted to the neutral atoms as there is no available transition in the ions from the viewpoint of lidar technology. On the other hand, calcium, although not so densely distributed compared to iron or sodium, is so attractive, because both neutral atoms (Ca) and ions (Ca+) have available transitions applicable for lidar; that is, calcium as a lidar tracer, has an excellent potential to study a variety of dynamics appeared in the ultrahigh atmosphere region. Here, we report a resonant-scattering lidar that can simultaneously observe both Ca and Ca+ with a high temporal and spatial resolution. The system is based on a solid-state, dual-wavelength, injection-locked Ti:sapphire laser, being operated stably over an entire night. In our presentation, we will also discuss what new observations are expected in the near future, including a typical demonstration of the resonant-scattering Ca/Ca+ lidar examined so far.

流星を起源として遷移領域に分布する金属原子・イオンをトレーサーとする共鳴散乱ライダーは、この高層領域を地上からレーザーで高い時間・空間分解能で観測することができる優れた計測法である。相対的に高密度に分布する鉄やナトリウムをトレーサーとするものが主流であるが、使用可能な遷移波長の関係から対象は中性原子に限定される。一方で、分布密度はそれほど高くはないが、カルシウムは中性原子（Ca）と一価のイオン (Ca+) の双方にライダーとして使用可能な遷移が存在し、この高層領域におけるより多様なダイナミクスを捉えるポテンシャルを有していて魅力的である。ここでは、Ca と Ca+ の双方を同時に高い時間・空間分解能で計測する共鳴散乱ライダーについて紹介する。システムは、注入同期法を適用した固体 Ti:sapphire レーザーをもとに構成され、長時間、安定に稼働させることができる。実際におこなった観測例に加えて、今後、どのような観測が可能になると期待されるかも議論したい。

R005-02
A 会場 ：11/24　PM1 （13:15-15:15）
13:30〜13:45

#HU JINYI[1)], 津田 卓雄 [1)], 江尻 省 [2,3)], 西山 尚典 [2,3)], 中村 卓司 [2,3)], 津野 克彦 [4)], 阿保 真 [5)], 川原 琢也 [6)], 小川 貴代 [4)], 和田 智之 [4)]
([1 電通大, ([2 極地研, ([3 総研大, ([4 理研, ([5 都立大・システムデザイン, ([6 信州大・工

Investigation on K variations during wintertime observed at Syowa Station, Antarctic

#JINYI HU[1)], Takuo Tsuda[1)], Mitsumu K Ejiri[2,3)], Takanori Nishiyama[2,3)], Takuji Nakamura[2,3)], Katsuhiko Tsuno[4)], Makoto Abo[5)], Takuya Kawahara[6)], Takayo Ogawa[4)], Satoshi Wada[4)]
([1University of Electro-Communications, ([2National Institute of Polar Research, ([3SOKENDAI, ([4RIKEN, ([5Graduate School of System Design, Tokyo Meteropolitan University, ([6Faculty of Engineering, Shinshu University

Metallic layers, such as Na, Fe, K, etc., originating from meteors are valuable tracers for observations of the Earth's upper atmosphere. Through investigations on variations in such metallic layers, it would be important to advance our understanding of the dynamical and chemical processes in the upper atmosphere. Many observations for Na and Fe have been done for decades, and their variations have been widely investigated. On the other hand, observational data on K are relatively limited. As for previous K observations, there are several reports from several resonance scattering lidars located in, for example, Arecibo, Puerto Rico (18.35° N, 66.75° W), Beijing, China (40.41° N, 116.01° E), and Kühlungsborn, Germany (54.1 ° N, 11.7° E), which are the observational sites in the Northern Hemisphere. In addition, a shipboard-lidar campaign between 71° S and 45° N was carried out, and it provided limited information on the K layer variations in the Southern Hemisphere. Furthermore, there are investigations based on near-global K data, which were obtained from observations of K resonance scattering of the sunlight by a polar-orbit satellite, Odin/OSIRIS. The satellite observations were limited during the daytime, which means that the obtained data are mainly during summer at high latitudes. Thus, there are fewer K observations in winter high latitudes in the Southern Hemisphere, where there is less sunlight.

In the present work, we have investigated seasonal variations in the K layer over Syowa Station (69.0° S, 39.6° E), Antarctic, based on observational data which were obtained by a resonance scattering lidar. The resonance scattering lidar was operated from 2017 to 2018. During the period, K density data of 385 hours for 38 nights were obtained mainly during the Antarctic winter. These data were analyzed to investigate seasonal variations in the K layer over Syowa Station. As a result, the K peak density reached a maximum in June-July during wintertime. Then, a minimum of the K peak density was observed in September during springtime, The relative variation of K column density observed at Syowa Station agrees with the previous observations in the Northern Hemisphere, but those absolute values in the K column density show differences. The variation of K centroid altitude observed at Syowa Station seems to be close to the results from Odin/OSIRIS, while it was different from those from the lidar observations in the Northern Hemisphere. The variation of RMS width in K layer over Syowa Station presents the opposite of that from Arecibo, but it agrees with those from Kühlungsborn and Beijing. To discuss important factors that contribute to the observed K variations, we have investigated relationships with the background temperature and oxygen atom density and found signatures that both two factors would provide important contributions to the variation of the K density during Antarctic winter.

R005-03
A 会場 ：11/24　PM1 （13:15-15:15）
13:45〜14:00

#坂元 希優 [1)], 津田 卓雄 [1)], 西山 尚典 [2)], 南條 壮汰 [3)], 細川 敬祐 [1)], 野澤 悟徳 [4)], 川端 哲也 [4)], 水野 亮 [4)]
([1] 電通大, [2] 極地研, [3]IRF, [4] 名大・宇地研

Variations in Na D_1 and D_2 ratio based on nightglow observations at Tromsø

#Kihiro Sakamoto[1)], Takuo Tsuda[1)], Takanori Nishiyama[2)], Sota Nanjo[3)], Keisuke Hosokawa[1)], Satonori Nozawa[4)], Tetsuya Kawabata[4)], Akira Mizuno[4)]
([1]University of Electro-Communications, [2]National Institute of Polar Research, [3]Swedish Institute of Space Physics, [4]Institute for Space-Earth Environment Research, Nagoya University

The emission layer of Na nightglow is normally located at an altitude of approximately 90 km, offering valuable insights into the atmosphere near the mesopause region. The emission mechanism of Na nightglow is well known as the Chapman mechanism. In this process, Na splits into two excited states with different energy levels, leading to the double lines in the emission spectrum: the D_1 line, 589.6 nm (in air), and the D_2 line, 589.0 nm (in air). Because the ratio branching to the two excited states is theoretically considered to be constant, the intensity ratio of the D_1 and D_2 lines (defined as R_D) is expected to be constant. However, some recent works reported that the R_D was variable (not constant) from their observations. As an interpretation for the variable R_D, a modification in the Chapman mechanism has been proposed, in which R_D can vary with the balance between reactions with O and quenching with O_2. To verify the interpretation, we need more detailed investigations based on more observations.

In this study, we conducted experimental observations of R_D using a compact spectrograph at Tromsø, Norway (69.6N, 19.2E), for approximately five months from October 2017 to March 2018. To enhance the resolution of our spectrograph, we replaced the diffraction grating of 300 G/mm with one of 1200 G/mm. The replacement resulted in an improved spectral resolution of 0.4 nm. This change resulted in an improved spectral resolution of 0.4 nm. Although this made it possible to separate the Na D_1 and D_2 lines more effectively, the separation was not perfect. To separate D_1 and D_2 lines, we performed a double-gaussian fitting in the data analysis, and subsequently obtained R_D. Additionally, we analyzed all-sky images obtained during observations to examine the weather conditions and the surrounding environment affecting the observations. Such conditions over Tromsø were determined through both manual inspection and deep learning methods. We made data selections based on the determined conditions. After that, 168-hour R_D data during the five months were obtained by the data analysis including the double-gaussian fitting. In the presentation, we will show the observed R_D variations and discuss their relationships with O and O_2 effects. In addition, we will discuss the influence of contamination in the data analysis from cosmic rays and auroral N_2 emissions.

R005-04
A 会場 ：11/24　PM1 （13:15-15:15）
14:00〜14:15

#中村 卓司 [1)], 江尻 省 [1)], 木暮 優 [2)], PERWITASARI SEPTI[3)], 冨川 喜弘 [1)], 堤 雅基 [1)], 水野 亮 [4)], 津野 克彦 [5)], 小川 貴代 [5)], 和田 智之 [5)], Salvador Jacobo[6)]
([1] 極地研, [2] 九大・理・地惑, [3]NICT, [4] 名大・宇地研, [5] 理研, [6]CONICET, アルゼンチン

Gravity waves observed by OH arirglow imaging at Rio Gallegos, Argentina, near Andes: horizontal phase velocity spectrum analysis

#Takuji Nakamura[1)], Mitsumu K Ejiri[1)], Masaru Kogure[2)], SEPTI PERWITASARI[3)], Yoshihiro Tomikawa[1)], Masaki Tsutsumi[1)], Akira Mizuno[4)], Katsuhiko Tsuno[5)], Takayo Ogawa[5)], Satoshi Wada[5)], Jacobo Salvador[6)]
([1]National Institute of Polar Research, [2]Department of Earth and Planetary Sciences , Kyushu University, [3]National Institute of Information and Communications Technology, [4]Institute for Space-Earth Environmental Research, Nagoya University, [5]RIKEN, [6]CONICET, Argentina

Atmospheric gravity waves play important roles in couplings in the terrestrial whole atmosphere, by transporting momentum and energy vertically and horizontally. There are various sources of gravity waves such as meteorological disturbances, surface topography, instability of jet stream, etc. Recently the secondary wave generation caused by breaking gravity waves in the middle atmosphere has been recognized as a very important process because those waves can propagate into higher altitudes and play a great role of transporting momentum and energy to higher altitudes and furthermore efficiently propagate beyond the MLT region into the thermosphere/ionosphere to causes disturbances there. One of the gravity wave hot spots is the region of Antarctic peninsula and the Andes, where strong mountain waves are excited by the tropospheric winds and the topography.

We have been carrying out OH airglow imaging observations (˜87 km altitude) at Rio Gallegos, Patagonia, Argentine (51.6S, 69.3W) near the Andes since late 2017. In this study, we report the gravity wave horizontal phase velocity spectrum, i.e., the distribution of the gravity wave energy in the 2-D horizontal phase velocity domain observed in 2018.

In 2018, we obtained 138 nights of clear-sky and moonless images. The characteristics of the airglow images at Rio Gallegos were the quasi-stationary waves, suggesting the effect of mountain wave, and the wave breaking events, suggesting large amplitude of the waves. These suggest that the observation site, Rio Gallegos, is located under the region of strong gravity wave activity due to the Andes mountains. These characteristics show similarity with the finding by Pautet et al., (2021) by winter-time observation at Rio Grande (54S, 68W), but the quasi-stationary waves by our observation seem to be less frequent.

Horizontal phase velocity spectral analysis (M-transform, Matsuda et al., 2014) has been applied to pick up the waves with periods of 5-60 min, and with horizontal wavelengths of 10-100 km. We found that the spectrum was very widespread up to 150 m/s, and very frequently clear signal of wind filtering (wind blocking) due to the stratopause zonal wind. In summer (Nov-Feb) primary propagation was eastward. In early (Mar-April) and late (ASO) winter, phase speed is fast/broad and showing clear wind blocking. In mid-winter, spectral peaks spreads to E-W around zero. Gravity wave energy (I'/I) seems to be the largest around August-September, and larger than Syowa station where the late winter peak is not clear. Summer sub-peak also recognized.

Our observation results indicate that the horizontal phase velocity spectrum is a useful way to investigate to identify the altitude range of the generation of the gravity waves observed in the airglow layer at around 85-90 km height.

R005-05
A 会場 ：11/24　PM1 （13:15-15:15）
14:15〜14:30

#小川 泰信 [1)], 宮岡 宏 [1)], 野澤 悟徳 [2)], 橋本 大志 [1)], 大山 伸一郎 [3)], 西村 耕司 [7)], 津田 卓雄 [4)], 藤原 均 [5)], 堤 雅基 [1)], 田中 良昌 [6)], 西山 尚典 [1)], 吹澤 瑞貴 [1)], 細川 敬祐 [8)], 三好 由純 [9)], 中村 卓司 [1)], 藤井 良一 [1)]
([1] 極地研, [2] 名大・宇地研, [3] 名大 ISEE, [4] 電通大, [5] 成蹊大学, [6] 国立極地研究所/ROIS-DS/総研大, [7] 京都大学生存圏研究所, [8] 電通大, [9] 名大 ISEE

EISCAT_3D and Japan's Activities

#Yasunobu Ogawa[1)], Hiroshi Miyaoka[1)], Satonori Nozawa[2)], Taishi Hashimoto[1)], Shin ichiro Oyama[3)], Koji Nishimura[7)], Takuo Tsuda[4)], Hitoshi FUJIWARA[5)], Masaki Tsutsumi[1)], Yoshimasa Tanaka[6)], Takanori Nishiyama[1)], Mizuki Fukizawa[1)], Keisuke Hosokawa[8)], Yoshizumi Miyoshi[9)], Takuji Nakamura[1)], Ryoichi Fujii[1)]
([1]National Institute of Polar Research, [2]Institute for Space-Earth Environment Research, Nagoya University, [3]Institute for Space-Earth Environmental Research, Nagoya University, [4]University of Electro-Communications, [5]Seikei University, [6]National Institute of Polar Research, [7]RISH, Kyoto University, [8]University of Electro-Communications, [9]Institute for Space-Earth Environemental Research, Nagoya University

The European Incoherent Scatter (EISCAT) scientific association started construction of the first stage of the EISCAT_3D radar in 2017 under international collaboration. The EISCAT_3D is a new generation of incoherent scatter radar system based on phased array technology. At the first stage, a core site with a transmission power of about 3.4 MW and two receive-only remote sites will be operated. All antennas have been installed at the Skibotn site (the core site with 119 sub-arrays, Norway), the Kaiseniemi site (the remote site with 55 sub-arrays, Sweden) and the Karesuvanto site (the remote site with 54 sub-arrays, Finland) by summer 2023. A first light with 7 sub-arrays is planned at the Skibotn core site or the Kaiseniemi site. This will be followed by various testing and commissioning phases at the three sites, and then operations at the first stage will begin. In connection with the operation of EISCAT_3D, the EISCAT scientific association has taken a strategic decision to transfer its assets, operation and commitments to EISCAT AB, which will be newly established. The EISCAT_3D radar is expected to be utilized for a variety of science cases, including studies on energy and mass transport from the solar wind and magnetosphere to the ionosphere and atmosphere.

The National Institute of Polar Research (NIPR) had been contributing to the EISCAT_3D construction by supplying radar transmitter power amplifiers (SSPAs) in collaboration with the EISCAT scientific association and ISEE Nagoya University. The high energy-efficient SSPAs have been used for engineering verification tests at the EISCAT Tromsoe and Kiruna sites since 2016. In 2020, NIPR has concluded an MoU with EISCAT to supply in-kind sub-array transmitter units which are selected for the first stage by the EISCAT Headquarters through the international tendering process. In addition to these contributions to the EISCAT_3D construction, NIPR established the Advanced Radar Research Promotion Center in April 2022. Under the Center, joint usage and collaborative research of the EISCAT_3D radar are being prepared.

In this paper, we report the latest status of the EISCAT_3D project and discuss the prospects of Japan's activities for the EISCAT_3D project.

R005-06
A 会場 ：11/24　PM1 （13:15-15:15）
14:30〜14:45

#Liu Huixin[1)], Poblet Facundo[2)], Chau Jorge[2)]
(1 九大・理・地惑, (2 大気物理研究所、Rostock 大学、ドイツ

Diagnosing the dynamical structure of the thermosphere using 3rd-order structure functions

#Huixin Liu[1)], Facundo Poblet[2)], Jorge Chau[2)]
([1]Department of Earth and Planetary Science, Graduate School of Science,Kyushu University, ([2]Leibniz Institute for Atmospheric Physics, Rostock University, Germany

We use multi - year observations of cross - track winds (u) from the CHAllenging Minisatellite Payload (CHAMP) and the Gravity Field and Steady State Ocean Circulation Explorer (GOCE) to calculate third - order structure functions in the thermosphere as a function of horizontal separation (s). They are computed using the mean and the median and implemented over non - polar satellite paths in both hemispheres. On height averages is shown to scale with s2 for s $\simeq$ 80 – 1,000 km, in agreement with equivalent estimates in the lower atmosphere from aircraft observations. Conversely, med follows an s3 power law for almost the whole s range, consistent with the two - dimensional turbulence scaling law for a direct enstrophy cascade. These scaling laws appear independent of winds in distinct atmospheric regions. Furthermore, the functions are predominantly positive, indicating a preferential cyclonic motion for the wind.

R005-07
A 会場 ：11/24　PM1 （13:15-15:15）
14:45〜15:00

超小型衛星による次世代大気観測システムの構築

#高橋 幸弘 [1)], 佐藤 光輝 [2)], 杉山 玄己 [3)], 大野 辰遼 [3)], 久保田 尚之 [1)]
([1] 北大・理, [2] 北大・理, [3] 北海道大学

Next-generation atmospheric observation system by micro-/nano-satellites

#Yukihiro Takahashi[1)], Mitsuteru SATO[2)], HARUKI SUGIYAMA[3)], Tatsuharu Ono[3)], HISAYUKI KUBOTA[1)]
([1]Faculty of Science, Hokkaido University, [2]Faculty of Science, Hokkaido University, [3]Department of Cosmosciences, Graduate School of Science, Hokkaido University

In recent years, disasters caused by thunderstorms, typhoons, and linear precipitation bands has been said to be becoming more severe, but the detailed understanding of their mechanisms, high-precision and high-frequency monitoring, and prediction accuracy are insufficient, and improvements are slow. One of the major reasons for that is the lack of information obtained from observations in terms of space and time. The energy source of typhoons and many linear precipitation bands is latent heat injected from the ocean. However, the means of measuring the amount of water vapor above the ocean are limited to microwave radiometers mounted on a very small number of satellites, and observation frequency is insufficient. In addition, clouds before the start of rain cannot be captured by common weather radars (such as C-band radar). Ka-band radars with higher radio frequencies can capture cloud particles, but spatial scanning takes time, it is actually difficult to track the development of the three-dimensional structure of thunderstorm from moment to moment, and the equipment is expensive and the maintenance costs are high. The lack of improvement in the accuracy of typhoon intensity predictions may be due to the fact that the central pressure is empirically estimated from the two-dimensional cloud patterns obtained by satellites. If we could grasp the 3D (three-dimensional) structure of thunderstorm and clouds in the center of a typhoon, it could lead to a dramatic improvement in the accuracy of predictions. However, most conventional satellites only take 2D images by nadir imaging, making it difficult to estimate 3D structures.

A group led by Hokkaido University is developing a method to estimate the vertical integral value (column amount) of water vapor, including in the ocean, using water vapor absorption lines, using a super multicolor spectral camera mounted on a 50 kg-class microsatellite, and has achieved technical success. We have also mastered the technique of fixing the field of view of a camera mounted on a similar 50 kg-class microsatellite and taking continuous shots, and have succeeded in detailed 3D observation of clouds, including the center of a typhoon, from the data. In addition, the lightning observation unit (GLIMS) mounted on the International Space Station (ISS) has a track record of imaging and photometry of lightning discharge emissions in thunderstorms. Based on this experience, we are promoting a low-cost satellite constellation (coordinated operation of multiple satellites) using micro-/nano-satellites weighing 50 kg or less (6U-12U cubes). Each satellite will be equipped with a narrowband spectral camera, a thermal infrared camera, and EVS (event vision sensor) for observing lightning discharges. While being small, lightweight, and low-power consumption, they will be able to observe 3D cloud structures and horizontal water vapor distributions over the ocean with a spatial resolution of 100-200m, something that has been difficult with previous satellites, all at 1/100 to 1/10 of the cost of conventional satellites.

近年、ゲリラ雷雨や台風、線状降水帯による被害は甚大化していると言われるが、それらの詳細なメカニズムの理解や高精度・高頻度監視、さらに予測精度は十分ではなく、その改善も遅い。その大きな要因の一つが、観測から得られる情報が空間的・時間的に不足している点にある。台風や多くの線状降水帯のエネルギー源は海洋から注入される潜熱である。しかし海洋上の水蒸気量の計測手段は、ごく少数衛星に搭載されたマイクロ波放射計など限られており観測頻度は十分ではない。また、降雨開始以前の雲は、一般的な気象レーダー（C バンドレーダーなど）では捉えることができない。より周波数の高い Ka バンドレーダーは雲粒を捉えることが可能だが、空間的スキャンには時間を要し、積乱雲雲の立体構造の発達を時々刻々追うことは困難な上、装置が高価な上に維持費も高額である。台風の強度予測精度の改善が見られないのは、そもそも中心気圧が衛星で得られる雲の 2 次元パターンから経験的に推定されている事情も影響している可能性がある。もし積乱雲や台風中心部の雲の 3D（3 次元）構造が把握できれば、予測精度の飛躍的向上につながるかもしれない。しかしほとんどの従来の衛星は真上からの 2 次元（平面）撮像なので、3D 構造の推定は難しかった。

北海道大学を中心としたグループは、50kg 級の超小型衛星に搭載した超多波長スペクトルカメラを用い、水蒸気の吸収線を用いた海洋を含む水蒸気の鉛直積分値（カラム量）の推定手法の開発を進めており、技術的な目処が得られている。また、同じように 50kg 級の超小型衛星に搭載されたカメラの視野を対象に固定して連写する技術を修得しており、そのデータから、台風中心部を含む雲の詳細な 3D 観測に成功している。さらに、国際宇宙ステーション（ISS）に搭載した雷観測ユニット（GLIMS）により、積乱雲中の雷放電発光の撮像及び測光に実績がある。こうした経験を踏まえ、50kg またはそれ以下（6U-12U）の超小型衛星を用いた低コスト衛星コンステレーション（複数機の連携運用）構想を進めている。それぞれ衛星には、狭帯域スペクトルカメラ、熱赤外線カメラ、雷放電観測用の EVS（イベントビジョンセンサー）を搭載し、小型・軽量・省電力でありながら、これまでの衛星でも困難であった空間解像度 100-200m での雲の 3D 構造や海洋上水蒸気水平分布などを、従来衛星の 1/100 から 1/10 のコストで実現する。

R005-08
A 会場 ：11/24　PM2 （15:30-18:15）
15:30〜15:45

宇宙機搭載プラズマ測定器校正用超熱的イオンソースの開発

#阿部 琢美 [1)], 加藤 千晶 [1)], 小嶋 浩嗣 [1)]
[1) ＪＡＸＡ宇宙科学研究所

Development of suprathermal ion source to calibrate space-based plasma instrument

#Takumi Abe[1)], Chiaki Kato[1)], Hirotsugu Kojima[1)]
[1)Institute of Space and Astronautical Science, Japan Aerospace Exploration Agency

It is possible to simulate plasma environment in the lower ionosphere inside a vacuum chamber on the ground. In contrast, it is very difficult on the ground to simulate plasma environment which is seen from the space-based platform such as sounding rocket or satellite. If one assumes a measurement on the sounding rocket in the lower ionosphere, ions appear to be approaching with a velocity of 1.0 km/s, which is typical velocity of sounding rocket. Because a thermal velocity of O2+ ion whose temperature is 300 K is about 500 m/s, the ions would be seen as incoming ions with the bulk velocity two times faster than the thermal velocity. In general, the ion acceleration in the vacuum chamber can be made by applying negative voltage to a mesh grid whose transmission rate is high. However, such an acceleration device is unlikely feasible because of too many collisions between plasma and neutrals inside the chamber and/or difficulty in controlling a small voltage around the grid with high accuracy.

We are developing a low energy ion source which can generate such a plasma environment inside the vacuum chamber. Although our prototype model did not work as expected, we have recently succeeded to realize the very low energy ion source by applying Kaufman-type single grid ion source. We have so far generated the ions whose most probable energy exists somewhere between 1 and 6 eV. The peak energy can be controlled by a voltage setting. Since the temperature of these ions is about 1000 K, the bulk energy is considered as suprathermal. Therefore, we call this device suprathermal ion source.

The suprathermal ion source consists of 1) extreme ultraviolet radiation source to generate plasma from neutral gas, 2) stainless chamber to maintain high plasma density, and 3) grid to pull the ions outward from the stainless chamber. This ion source is placed inside a large vacuum chamber with a diameter of 2.5 m at Institute of Space and Astronautical Science of Japan Aerospace Exploration Agency. An instrument to observe the accelerated ions is installed in front of the exit grid so that the ions can enter. The ion acceleration is caused by the voltages applied to the stainless chamber and the grid. In fact, the energy and flux of the accelerated ions can be controlled by the voltage applied to the stainless chamber and the grid, respectively.

In this presentation, we will describe variation of bulk energy according to the setting voltage and characteristic feature of energy distribution of the generated ions as well as the detailed information of the suprathermal ion source.

真空チェンバーの中に電離圏下部イオンの環境を作ることはできる。しかし、飛翔体上で見えるであろう環境を作ることは難しい。例として、観測ロケット上での観測を仮定し、イオンの温度を 300K とした場合に O2+ イオンの熱速度は 500m/s であるのに対し、観測ロケットの速度は電離圏高度で 1km/s 程度であるため、熱速度の 2 倍程度のバルク速度をもつイオンを生成しなければならない。衛星からの観測の場合は数倍のバルク速度で運動するイオンを生成しなくてはならない。真空チェンバー内でイオンを加速するには開口率の高いメッシュに電圧を印加することによって行うのが一般的であるが、電離圏のような低エネルギープラズマ環境を生成するのに用いられる後方拡散型プラズマ発生装置の場合には内部に導入する中性ガスとの衝突のため、また種々の問題により１ V 以下の精度でイオンの加速を行うことは困難なために、このようなプラズマ環境を真空チャンバー内に再現することは難しい。

我々はこのようなプラズマ環境を真空チェンバー内に再現するためのイオン加速装置の開発を行ってきた。幾つかの試作を試みて期待通りには動作しなかったが、2024 年に半導体薄膜の加工などにおいて用いられるカウフマン型シングルグリッドイオン源に着目し、この原理の一部を応用し、低エネルギーのイオンビームの生成に成功した。これまで、バルクエネルギーが１〜６ eV のイオンの生成を行ってきており、イオンの温度が 1000K 程度であることを考慮すると、suprathermal（超熱的）なエネルギーということになる。

超熱的イオンの生成装置はプラズマ生成のための紫外線光源、発生したプラズマを閉じ込めるためのステンレス製容器、容器内のイオンを外側に引き出すためのグリッドから構成される。この生成装置を宇宙科学研究所の大型スペースサイエンスチェンバー内に設置し、引き出されたイオンを観測するための測定器をイオンが通過する前面に置いた。なお、この測定器は 2025 年度に打ち上げ予定の観測ロケットに搭載されるものである。イオンの加速はステンレス製容器、および引き出し用グリッドに印加する電圧により行われるが、測定器に到達する時点でのイオンのエネルギーは容器に印加する電圧で、イオンのフラックスは引き出し用グリッドに印加する電圧で各々制御される。発表では超熱的イオンソースの構成の詳細、設定電圧によるバルクエネルギーの変化、生成されたイオンエネルギー分布の特徴について述べる。

R005-09
A 会場 ：11/24　 PM2 （15:30-18:15）
15:45～16:00

取下げ

R005-10
A 会場 ：11/24　PM2 （15:30-18:15）
16:00〜16:15

FMCW 方式短波ドップラー観測を用いた夏季夜間スポラディック E 移動特性の研究

#齋藤 龍之介 [1)], 細川 敬祐 [1)], 並木 紀子 [1)], 野崎 憲朗 [1)], 中田 裕之 [2)], 坂井 純 [1)], 冨澤 一郎 [1)]
([1 電気通信大学, ([2 千葉大学

Dynamical characteristics of summer nighttime sporadic E: FMCW-based HF Doppler sounding measurements

#Ryunosuke Saito[1)], Keisuke Hosokawa[1)], Noriko Namiki[1)], Kenro Nozaki[1)], Hiroyuki Nakata[2)], Jun Sakai[1)], Ichiro Tomizawa[1)]
([1]The University of Electro-Communications, ([2]Chiba University

Sporadic E (Es) is a thin layer of extremely high electron density at around 100 km altitudes that occurs mainly in summer at mid-latitudes. Es layer has been known to cause long-range anomalous propagation of radio waves in the VHF band which enter to the ionosphere at a low elevation angle through reflection due to an extreme increase of the E region electron density. Es layer has been studied using various methods because of its influence on aeronautical navigation systems and radio broadcasts in the VHF band. It was revealed that dynamical characteristics of Es layer during daytime can be observed by using Total Electron Content (TEC) obtained by using a ground-based GNSS receiver network. Es layer during night time moves with the Medium-Scale Traveling Ionospheric Disturbances (MSTIDs), wave-like structures in the F region electron density. MSTID causes large variations in the electron density, therefore it is difficult to observe Es layers only by using GNSS-TEC observations.

In this research, we used the HF Doppler (HFD) observation in order to observe Es layers directly in a wide area. The system can detect the vertical motion of the ionosphere from ground; thus, the dynamical characteristics of various ionospheric phenomena can be visualized using variations of the Doppler frequency and received signal intensity obtained at multiple stations on the ground. The HFD sounding system transmits two radio waves, 5.006 MHz and 8.006 MHz from Chofu, Tokyo and the reflected waves are received at 11 stations in Japan. The transmitted waves consist of continuous waves and Frequency Modulated Continuous Waves (FMCW). The continuous waves are transmitted on fixed frequencies. Thus, when the radio waves are reflected by an Es layer, the observed frequency changes due to the Doppler effect and then characteristic (quasi-periodic) Doppler spectral traces are observed. The frequency of the FMCW signal is modulated in 150 kHz band periodically. Propagation distance is then calculated from frequency difference between replica of transmitted waves and received waves. The replica is synchronized with the transmit station by using GPS. The propagation distance can always be observed with high accuracy with timing of the Doppler traces. Reflection altitude is estimated from the propagation distance and distance from a transmitter to a receiver. Time resolution of the altitude is higher than conventional methods such as ionosonde. The goal of this study is to observe the dynamical characteristics of sporadic E layers from the Doppler traces from the conventional HFD sounding system and the reflection altitude from the FMCW measurement.

We conducted observations of Es layer during nighttime by using the HFD between May and August 2022. The Doppler trace was simulated by calculating the Doppler shift from the time derivative of the propagation path length. By comparing simulation of Doppler traces and the actual observations, we calculated the propagation speed and azimuth of Es layers. However, since the reflection altitude is needed to be assumed in the simulation, there was an uncertainty in the estimated propagation speed and azimuth.

Regularly transmission of the FMCW signal has started since early 2024. We conducted HFD observations of Es layer in Chiba during nighttime between May and July, 2024. We found that, when quasi-periodic Doppler spectral traces were observed, the reflection altitude estimated from FMCW signal ranged from 100 to 125 km. This reflection altitude was slightly higher than that assumed when analyzing the data in 2022 (it was assumed to be 100 km). This implies that the accuracy of simulation will be improved by using the observed reflection altitude as an input parameter for the simulation. We plan to compare these observations of HFD sounding system with those of MSTID using GNSS-TEC.

スポラディック E（Es）層は、主として夏季の中緯度の高度 100 km 付近に発生する電子密度が極端に増大した層である。Es 層の発生に伴う電子密度の増大によって、通常は電離圏を突き抜ける VHF 帯の電波が反射されてしまうことから、電離圏に低仰角で入射した電波の長距離異常伝搬を引き起こす。航空航法システムやラジオ放送に影響を及ぼすことから、Es 層の特性が様々な観測手法を用いて研究されてきた。地上 GNSS 受信機網の計測によって得られる全電子数 (Total Electron Content: TEC) 観測によって、日中の Es 層に関しては広域的な移動特性を観測できることが明らかになっている。一方、夜間の Es 層は中規模伝搬性電離圏擾乱 (Medium-Scale Traveling Ionospheric Disturbances: MSTID) と呼ばれる電離圏 F 領域における電子密度の縞状構造と連動して動くことが知られている。そのため、GNSS-TEC では MSTID に伴う電子密度変動が観測されてしまい、Es 層単独の電子密度変動を観測することが難しい。

そこで、本研究では、Es 層の広域的かつ直接的な観測を実現するために短波ドップラー観測（HF Doppler: HFD）を用いた解析を行った。HFD 観測は、電離圏に向けて短波帯の電波を送信し、その反射波を遠隔地で受信したときに得ら

れるドップラー周波数や受信電界強度の変化から、電離圏の上下動や電離圏現象の移動特性を地上から観測するシステムである。我々が運用している HFD 観測システムでは、東京都調布市から 5.006 MHz、8.006 MHz の 2 周波の電波を送信し、全国 11 箇所で受信している。観測用信号は、単一周波数の連続波と周波数連続変調波 (Frequency Modulated Continuous Wave: FMCW) から成る。連続波は一定の周波数で送信されているが、Es 層で反射する際に、Es 層の移動に伴うドップラー効果で周波数が変動し、ドップラーシフトがプラスからマイナスに変動する特徴的なドップラートレースが準周期的に見られる。FMCW 波は一定の周期でドップラー観測で用いている単一周波数を中心に 150 kHz の範囲で送信周波数に変調を与えており、GPS による同期を取った上で送信波レプリカと受信波の差周波から電離圏反射した電波の伝搬距離を、ドップラートレースのタイミングと合わせて高精度に常時測定できる。伝搬距離と送受信点間の距離から、電波の反射高度がイオノゾンデなどの従来手法より高い時間分解能で求められる。観測されたドップラートレースと反射高度から、Es 層の空間的な移動を観測することを本研究の目標とする。

2022 年 5 月から 8 月にかけて、HFD 観測を用いて夜間の Es 層の観測を実施し、ドップラートレースの観測結果とシミュレーション結果を比較することで、Es 層の移動速度と移動方向の計算を行った。Es 層の伝搬経路長の時間微分からドップラーシフトを計算し、シミュレーションを作った。シミュレーションには電波の反射高度がパラメータの一つとして必要であるが、この当時は FMCW 波の送信が行われておらず、反射高度を観測する手段がなかったため、Es 層の移動速度や移動方向に不確かさが残る状態であった。

2024 年に FMCW 波の定常的な送信が開始され、同年 5 月から 7 月にかけて千葉で HFD 観測を実施した。Es 発生時に見られる準周期的なドップラートレースが観測された夜間において、FMCW 波を用いて反射高度の観測を行った結果、確かに Es 層が高度 100—125 km の領域に出現していることが明らかになった。2022 年時点では電波の反射高度を 100 km と仮定していたが、実際には高い高度で反射が起こっており、従来のシミュレーションでは Es 層の移動速度が小さく出ていた可能性が高い。実測値をシミュレーションのパラメータに用いることでシミュレーション精度の向上が期待できる。また、GNSS-TEC を用いた MSTID の観測結果との比較も行う予定である。

R005-11
A 会場 ：11/24　PM2 （15:30-18:15）
16:15〜16:30

昭和基地上空 100-170km に観測された地磁気静穏時のスポラディック Ca^+ 層

#江尻 省 [1,2], 西山 尚典 [1,2], 津田 卓雄 [3], 津野 克彦 [4], 古城 侑季 [5], 齊藤 昭則 [5], 西岡 未知 [6], 阿保 真 [7], 川原 琢也 [8], 小川 貴代 [4], 和田 智之 [4], 中村 卓司 [1,2]
([1] 極地研, [2] 総研大, [3] 電通大, [4] 理研・光量子工学研究センター, [5] 京都大・理・地球物理, [6] 情報通信研究機構, [7] 都立大・システムデザイン, [8] 信州大・工

Sporadic Ca^+ layer observed around 100-170 km over Syowa Station during geomagnetic quiet condition

#Mitsumu K. Ejiri[1,2], Takanori Nishiyama[1,2], Takuo T. Tsuda[3], Katsuhiko Tsuno[4], Yuki Kojo[5], Akinori Saito[5], Michi Nishioka[6], Makoto Abo[7], Takuya D. Kawahara[8], Takayo Ogawa[4], Satoshi Wada[4], Takuji Nakamura[1,2]
([1]National Institute of Polar Research, [2]Graduate University for Advanced Studies, SOKENDAI, [3]University of Electro-Communications, [4]Riken, RAP, [5]Department of Geophysics, Graduate School of Science, Kyoto University, [6]National Institute of Information and Communications Technology, [7]Graduate School of System Design, Tokyo Meteropolitan University, [8]Faculty of Engineering, Shinshu University

The wind shear theory is widely accepted as the mechanism of the formation of the sporadic E layer (EsL) in the mid-latitudes. Among the ions that drift vertically due to the vertical shear of neutral horizontal winds, the long-lived ions that form the core of the EsL are metal-atom ions, such as Ca^+, Fe^+, Na^+ etc., supplied by meteoroids to the MLT region. On the other hand, in the high latitude, especially auroral oval zone, the EsL occurred with geomagnetic and auroral activity is known. However, it is unknown if there is a EsL during geomagnetic quiet condition, and a contribution of the metal-atom ions to formation and lasting of the EsL as in the mid-latitude.

A resonance scattering lidar developed by National Institute of Polar Research (NIPR) was installed at Syowa (69S, 40E), Antarctic in 2017 and observed Ca^+ density profiles in 2017 and 2018. A Ca^+ thin layer descending from ~170 to 100 km was observed on Sep. 13 in 2017 that geomagnetic activity was quiet. At the same time, a weak EsL observed with the ionozonde at Syowa operated by National Institute of Information and Communications Technology (NICT). In this presentation, we will show a relationship between Ca^+ thin layer and the EsL and discuss contributions of vertical shear of neutral wind.

R005-12
A 会場 ：11/24　PM2 （15:30-18:15）
16:30〜16:45

EISCAT レーダーで観測された地磁気静穏時の昼側極域電離圏変動の特徴について

#藤原 均 [1)], 野澤 悟徳 [2)], 小川 泰信 [3)]
([1] 成蹊大学, [2] 名古屋大学宇宙地球環境研究所, [3] 国立極地研究所

Features of disturbances in the dayside polar ionosphere during geomagnetically quiet periods observed with the EISCAT radar

#Hitoshi FUJIWARA[1)], Satonori NOZAWA[2)], Yasunobu OGAWA[3)]
([1]Seikei University, [2]Institute for Space-Earth Environmental Research, Nagoya University, [3]National Institute of Polar Research

We have been conducting dayside ionospheric observations using the EISCAT radar system since 2011. We have focused our scientific attention on ionospheric fluctuations/disturbances in the polar cap region. The EISCAT observations have revealed that the ionosphere in the polar cap region (or at higher latitudes than the auroral zone) shows some fluctuations not only during periods of disturbances such as geomagnetic storms, but also during times of geomagnetically quiet. The fluctuations, which seem to be caused by the lower atmospheric phenomena, were also observed in the polar cap ionosphere. Since there have been few observations of the ionosphere and thermosphere in the polar cap region, there are many things that we do not fully understand. Further studies are needed into the basic structure and variations of the ionosphere in the polar cap region during geomagnetically quiet periods. In this presentation, we will show some features of disturbances in the dayside polar ionosphere at higher latitude than the auroral zone observed with the EISCAT radar system.

我々の研究グループでは、EISCAT 特別実験を実施し、昼側極域電離圏について調べてきた。特に、電離圏・熱圏観測の少ない極冠域での電離圏変動に注目し、地磁気静穏時、擾乱時、太陽活動極小期、極大期での変動の成因の理解を目標としている。これまでの観測では、地磁気擾乱時に限らず、地磁気静穏時にも顕著な電離圏変動が現れる場合があることがわかった。例えば、短時間でのイオン温度の上昇や、高速イオン流などである。また、下層大気からの影響とみられる変動も検出されている。本発表では、これまでの EISCAT 観測から得られた、地磁気静穏時の昼側極域電離圏の特徴的な変動のいくつかを紹介する。

R005-13
A 会場 ：11/24　PM2 （15:30-18:15）
16:45〜17:00

#西山 尚典 [1,2], 鍵谷 将人 [3], Bag Tikemani[1], 津田 卓雄 [4], 岩佐 祐希 [5], 小川 泰信 [1,2], Sigernes Fred[6]
([1] 極地研, [2] 総研大, [3] 東北大・理・惑星プラズマ大気研究センター, [4] 電通大, [5] 計量標準総合センター/産業技術総合研究所, [6]University centre in Svalbard

Thermospheric orthohelium variations associated with a moderate storm on February 2023: the NIRAS-2 observations at Longyearbyen

#Takanori Nishiyama[1,2], Masato Kagitani[3], Tikemani Bag[1], Takuo Tsuda[4], Yuki Iwasa[5], Yasunobu Ogawa[1,2], Fred Sigernes[6]
([1]National Institute of Polar Research, [2]The Graduate University for Advanced Studies, SOKENDAI, [3]Planetary Plasma and Atmospheric Research Center, Graduate School of Science, Tohoku University, [4]University of Electro-Communications, [5]NMIJ/AIST, [6]University centre in Svalbard

Metastable orthohelium, He(2^3S) , is known to have airglow emissions by solar resonance scattering at wavelength of 388.9 nm (3^3P-2^3S) and 1083 nm (2^3P-2^3S). The emissions from the terrestrial atmosphere have been first reported more than 60 years ago during strong twilight and sunlit aurora over Moscow (Mironov et al., 1959; N. Shefov, 1961). Transition from ground state helium, He(1^1S) , to He(2^3S) is mainly caused by photoelectron impacts with energy larger than 19.8 eV (de Heer & Jansen, 1977). He(2^3S) layer is confined in the upper thermosphere and in the lower exosphere. Photoelectron impact occurs with a maximum production rate around 250 km. Generated He(2^3S) diffuses upward, but rapidly disappears above 500 km due to photo ionisation. Below 250 km, quenching due to Penning ionization is significant. As a result, He(2^3S) layer can be formed from 250 km to 800 km or above (Bishop & Link, 1993; Waldrop et al., 2005). That's why He(2^3S) is an unique and attractive candidate for remote sensing target of the neutral atmospheric dynamics in this region.

This study presents a time variability of He(2^3S) in polar region associated with a geomagnetic storm for the first time. Continuous 17-nights dataset of He(2^3S) airglow brightness at 1083 nm was obtained from a short-wavelength infrared imaging spectrograph (NIRAS-2) installed at Longyearbyen, Svalbard (78.1° N, 16.0° E). The observed He(2^3S) airglow brightness clearly displayed responses to a geomagnetic storm in different time scales. The He(2^3S) airglow brightness has began to decrease sharply within an hour of sudden commencement of the storm, and it was gradually decreased over the next few days and then recovered slowly. It was nicely agreed to helium density variations at 500-km altitude calculated by MSIS. The depletion of He(2^3S) was mainly caused by enhanced Penning ionization due to upwelling N_2 from the lower atmosphere; this was consistent with decreased O/N_2 ratio in MSIS and TIMED/GUVI measurements and electron density depletion in F region observed by EISCAT Svalbard Radar (ESR). Additionally, sudden increases in He(2^3S) airglow brightness were clearly found associated with intermittent electron precipitations observed by the ESR. Therefore, direct impact by precipitating electron injected from the space to the polar upper atmosphere can play significant roles in production of He(2^3S). The NIRAS-2 measurements have successfully demonstrated that column density of He(2^3S) from the upper thermosphere to the exosphere was drastically changed by forcing both from the lower atmosphere and from the space. He(2^3S) measurements will definitely improve our understanding of thermosphere-ionosphere coupling system and extend the coverage of space weather forecasting up to the exobase.

R005-14
A 会場 ：11/24　PM2 （15:30-18:15）
17:00〜17:15

2003 年 10 月 24 日の巨大サブストームに伴う中低緯度への電場侵入によって引き起こされた 630-nm 大気光同時増光の MAGE モデル解析

#森田 早紀 [1)], 塩川 和夫 [1)], Pham Kevin[2)], 大塚 雄一 [1)], 新堀 淳樹 [1)], 西岡 未知 [3)], Perwitasari Septi[3)], 山本 衛 [4)], 惣宇利 卓弥 [4)]
([1] 名大宇地研, [2]National Center for Atmospheric Research, [3] 情報通信研究機構, [4] 京大・生存圏研

MAGE model analysis of electric field penetration into mid-latitudes associated with a strong substorm on October 24, 2003

#Saki Morita[1)], Kazuo Shiokawa[1)], Kevin Pham[2)], Yuichi Otsuka[1)], Atsuki Shinbori[1)], Michi Nishioka[3)], Septi Perwitasari[3)], Mamoru Yamamoto[4)], Takuya Sori[4)]
([1]Institute for Space-Earth Environmental Research, Nagoya University, [2]National Center for Atmospheric Research, [3]National Institute of Information and Communications Technology, [4]Research Institute for Sustainable Humanosphere, Kyoto University

One of the causes of ionospheric and thermospheric variations at mid-latitudes is the ionospheric electric field that promptly penetrates from the poler region to the equator associated with storms and substorms. It is known that when the Region 1 field-aligned currents dominate as the substorm current wedge, a westward electric field penetrates to the mid-low latitudes on the night side. The oblique downward ExB drift associated with the westward electric field causes O^+ in the ionosphere to penetrate to lower altitudes, interacting with higher O_2 densities, and resulting in 630-nm airglow enhancement.

A strong substorm occurred at 1525 UT (0025 LT) on October 24, 2003, with a minimum AL index of ˜-1900 nT. Almost simultaneously with the substorm onset, we observed a 630-nm airglow enhancement without time delay at three Japanese stations (Rikubetsu (43.5^{o}N, 143.8^{o}E), Shigaraki (34.9^{o}N, 136.1^{o}E) and Sata (31.0^{o}N, 130.7^{o}E)). This event occurred during the main phase of a storm with a minimum Dst index of -44 nT. A Sudden Commencement (SC) associated with a solar wind increase was observed at the same time. From ground observations by ionosondes and a Fabry-Perot interferometer, we observed a downward motion of the ionosphere, while no change was observed in the ionospheric electron density and neutral winds. Then, we used the Multiscale Atmosphere-Geospace Environment (MAGE) model to simulate the penetrating electric field and neutral winds during this event on global scale.

With the substorm onset, the MAGE model shows that the vertical component of the ExB drift velocity decreased by ˜30-35 m/s without time delay in the latitudes over Japan, corresponding to an electric field of ˜2.0-3.2 mV/m. From the measurement of nighttime medium-scale traveling ionospheric disturbances, it has been reported that an electric field oscillation of ˜1.2 mV/m was sufficient to reproduce the 630-nm airglow amplitudes of ˜20%. However, in this event, electric field changes were estimated to be ˜2.0-3.2 mV/m in the MAGE model, while the 630-nm airglow enhancement was ˜250-500%. Thus, the model possibly underestimates the intensity of penetrating electric field. The westward electric field in the model extended from 75^{o}E to 150^{o}W (2100-0600 LT), which is comparable to the result of global modeling of substorm electric field by Ebihara et al. [2014]. The neutral wind was not changed in the MAGE model. Therefore, the simultaneous 630-nm airglow enhancement observed over Japan was confirmed to be caused by the westward electric field penetration associated with the strong substorm onset. We will also investigate changes in 630-nm airglow intensity based on the ionospheric plasma density and neutral atmosphere density in the MAGE model to clarify the relationship between the penetrating electric field and the 630-nm airglow enhancement.

中緯度で電離圏や熱圏の変動を引き起こす要因の 1 つとして、磁気嵐やサブストームに伴う極域から赤道まで瞬時に侵入する電離圏電場が挙げられる。これは、サブストームの開始に伴ってカレントウェッジ電流系が発達することで Region 1 電流が卓越し、夜側の中低緯度では西向き電場が侵入すると考えられている。この西向き電場に伴う ExB ドリフトが斜め下向きにかかることで、電離圏プラズマの O^+ がより O_2 の密度が高い低高度に侵入し、630-nm 夜間大気光が増光する。

2003 年 10 月 24 日の 15:25 UT (00:25 LT) に AL 指数の最小値が約-1900 nT で急速に発達した強いサブストームが発生した。これとほぼ同時に日本の 3 観測点（陸別（43.5° N, 143.8° E)、信楽（34.9° N, 136.1° E)、佐多（31.0° N, 130.7° E)）で南北方向に時間遅延のない 630-nm 大気光の増光を観測した。このイベントは、Dst 指数の最小値が-44 nT であった弱い磁気嵐の主相に発生し、同時に太陽風の急激な増強に伴う Sudden commencement (SC) が観測された。日本のイオノゾンデによる観測から、電離圏の下降運動が観測されたが、電離圏のピーク電子密度やファブリ・ペロー干渉計による中性風にはこのイベントに伴う変化が見られなかった。そこで本研究では、Multiscale Atmosphere-Geospace Environment (MAGE) モデルを使用して、このイベントにおける全球スケールでの侵入電場と中性風のシミュレーションを行った。

このモデル計算では、サブストーム開始に伴い、ExB ドリフト速度の鉛直成分は、日本上空で緯度方向に時間遅延なく約 30-35 m/s 減少した。これは、約 2.0-3.2 mV/m の電場に相当する。夜間の中規模伝搬性電離圏擾乱の観測では、1.2

mV/m の電場変動は約 20% の 630-nm 大気光変動を伴うことが報告されている。しかし今回のイベントでは、モデルから得られた電場変化は約 2.0-3.2 mV/m に対し、観測された 630-nm 大気光強度の増光は約 250-500% であった。電場変化に対して大気光強度の増加が異常に大きいため、モデルが侵入電場の強度を過小評価している可能性が考えられる。モデル計算の中では西向き電場は 75° E から 150° W（地方時 21:00-06:00 LT）まで広がっており、この結果は、Ebihara et al. [2014] によるサブストームに伴う侵入電場のグローバルモデリングによる先行研究と同程度であった。また、モデル計算では中性風は変化しなかった。したがって、日本上空で観測された南北方向に時間遅延のない 630-nm 大気光の増光は、強いサブストームの開始に伴う西向きの侵入電場によって引き起こされたと考えられる。講演では、モデルから得られる電子密度、帯域密度の高度分布に基づいて 630-nm 大気光強度の変化を調べ、侵入電場と 630-nm 大気光強度の関係を明らかにし、報告する予定である。

R005-15
A 会場 ：11/24　PM2 （15:30-18:15）
17:15〜17:30

#惣宇利 卓弥 [1)], 新堀 淳樹 [2)], 垰 千尋 [3)], 陣 英克 [3)], 大塚 雄一 [4)], 西岡 未知 [3,5)], PERWITASARI SEPTI[5)], 山本 衛 [6)]
([1 京大　RISH, [2 名古屋大学宇宙地球環境研究所, [3 情報通信研究機構, [4 名大・宇地研, [5NICT, [6 京大・生存圏研

North－ south asymmetry during the decay phase of mid-latitude plasma bubbles during a geomagnetic storm in March 2013

#Takuya Sori[1)], Atsuki Shinbori[2)], Chihiro Tao[3)], Hidekatsu Jin[3)], Yuichi Otsuka[4)], Michi Nishioka[3,5)], SEPTI PERWITASARI[5)], Mamoru Yamamoto[6)]
([1Research Institute for Sustainable Humanosphere, Kyoto University, [2Institute for Space-Earth Environmental Research, Nagoya University, [3National Institute of Information and Communications Technology, [4Institute for Space-Earth Environmental Research, Nagoya University, [5National Institute of Information and Communications Technology, [6Research Institute for Sustainable Humanosphere, Kyoto University

During a geomagnetic storm on 1 March 2013, an equatorial plasma bubble was generated over the magnetic equator after sunset in the Japanese－ Australian longitude sector. The plasma bubble extended to the mid-latitudes in both hemispheres with a geomagnetic conjugacy. On the other hand, the plasma bubbles were decayed during the recovery phase of the geomagnetic storm. The plasma density irregularity at the mid-latitudes related to the plasma bubble decayed earlier in the northern hemisphere than in the southern hemisphere. A background ionospheric plasma density in total electron content data was much smaller in the northern hemisphere than in the southern hemisphere. In this study, we clarify the cause of the north-south asymmetry of the mid-latitude plasma bubble decay during the geomagnetic storm using the Ground-to-topside model of Atmosphere and Ionosphere for Aeronomy (GAIA) model.

An ionospheric virtual height (h'F) at 3 MHz over Wakkanai (45.16° N, 141.75° E) estimated by the GAIA model declined by a few ten kilometers during 12:30－ 14:00 UT and rapidly increased during 14:00－ 17:00 UT. This resembled the temporal variation of h'F obtained from the ionosonde at Wakkanai. A meridional neutral wind at 142° E calculated by the GAIA model blew northward at 20－ 70 m/s in the northern hemisphere during 12:00－ 14:00 UT (21:00－ 23:00 LT) while it blew southward during the geomagnetically quiet day on 8 March. From these results, the ionospheric plasmas in the northern hemisphere were carried downward along magnetic field lines due to the enhanced northward neutral wind. At night, the ionospheric plasmas decreased at lower altitudes due to the increase in the recombination rate at lower altitudes, resulting in the rapid rise in h'F after 14:00 UT. On the other hand, the meridional neutral wind in the southern hemisphere blew northward during 10:00－ 12:30 UT and 15:00－ 20:00 UT although it was almost zero during 12:30－ 15:00 UT. This suggests that the mid-latitude ionospheric plasmas in the southern hemisphere were higher than those in the northern hemisphere. The mid-latitude plasma bubbles during geomagnetic storms can be asymmetric between northern and southern hemispheres because the background ionospheric plasmas in the northern hemisphere decreased due to the disturbed neutral wind.

R005-16
A 会場 ：11/24　PM2 （15:30-18:15）
17:30〜17:45

アメリカ経度域における GNSS およびイオノゾンデ観測による中緯度プラズマバブルの統計的研究

#加藤 颯太 [1)], 大塚 雄一 [1)], 野澤 悟徳 [1)], 新堀 淳樹 [1)], 惣宇利 卓弥 [2)], 西岡 未知 [3)], PERWITASARI SEPTI[3)]
([1] 名大 ISEE, [2] 京大 RISH, [3] 情報通信研究機構

Statistical study of mid-latitude plasma bubbles based on GNSS and ionosonde observation at the American longitudinal sector

#Sota Kato[1)], Yuichi Otsuka[1)], Satonori Nozawa[1)], Atsuki Shinbori[1)], Takuya Sori[2)], Michi Nishioka[3)], SEPTI PERWITASARI[3)]
([1]Institute for Space-Earth Environmental Research, Nagoya University, [2]Research Institute for Sustainable Humanosphere, Kyoto University, [3]National Institute of Information and Communications Technology

Radio waves used by Global Navigation Satellite System (GNSS) and satellite broadcasting and communications pass through the Earth's ionosphere. Plasma bubble, which is a localized plasma density depletion in the ionosphere and contains plasma density irregularities, affects radio waves passing through itself. Although the plasma bubbles are initiated at magnetic equator, recent GNSS observations have revealed the existence of a small number of plasma bubbles that reach mid or high latitudes. However, the conditions in which plasma bubbles extend to mid or high latitudes has not been clarified. In this study, we investigate relationship between poleward extension velocity of plasma bubble and ionospheric upward velocity at magnetic equator to clarify in which conditions, plasma bubbles reach mid-latitudes.

In this study, Total Electron Content (TEC) data obtained from GNSS receivers during the 11-year period from 2012 to 2022 in the American longitudinal sector (230° to 330° longitude), where many GNSS receivers are installed widely from the equator to high latitudes were analyzed. Virtual height of the F layer (h'F) from an ionosonde at Jicamarca (12° S, 283.2° E) were also used. From the GNSS-TEC data, two-dimensional map of Rate of TEC index (ROTI) representing ionospheric electron density irregularities are obtained. Mid-latitude plasma bubble is defined as an event in which a region of ROTI exceeding 0.5 TECU/min (1 TECU=10^16 m^(-2)) extends from the vicinity of the magnetic equator to more than 30° magnetic latitude. In this study 48 mid-latitude plasma bubbles are found. To derive poleward extension velocity of plasma bubbles, the following procedures are carried out. The maximum ROTI is determined for each latitude in the longitudinal range from 230° to 330°. The poleward extension velocity of plasma bubble is derived from the slope of the enhanced ROTI region in the time-latitude cross-section of the maximum ROTI. The average value was about 500 m/s. Ionospheric upward velocity over the magnetic equator was also derived from the rate of increase in h'F data from an ionosonde at Jicamarca. The average value was about 18 m/s. Comparing the poleward extension velocity in the enhanced ROTI region with the ionospheric upward velocity, we find that the poleward extension velocity in the enhanced ROTI region increases with increasing ionospheric upward velocity. This result indicates poleward extension velocity of plasma bubble increases with the increase in the eastward electric field at the magnetic equator through the Rayleigh-Taylor instability. We also find that relationship between the maximum arrival magnetic latitude of the enhanced ROTI region and the ionospheric upward velocity is not discernible. We speculate that the maximum latitude of mid-latitude plasma bubbles depends on not only the eastward electric field at the magnetic equator but also the condition of the ionosphere where the plasma bubbles extend.

全地球測位衛星システム (Global Navigation Satellite System ; GNSS) や衛星放送・通信で使われている電波は、電離圏を通過する。赤道域電離圏に発生するプラズマバブルは、電離圏の中で最も激しい擾乱現象のひとつであり、 プラズマバブルの中を通る電波に障害をもたらす。プラズマバブルは、磁気赤道で発生するが、近年の GNSS 観測から、中緯度さらには高緯度まで達するプラズマバブルが少なからず存在することが明らかになった。しかし、どのような条件においてプラズマバブルが中・高緯度まで発達するかは明らかにされていない。そこで、本研究では、中緯度まで到達するプラズマバブルが極域方向に拡大する速度及び、赤道における F 層の上昇速度を導出し、中緯度まで到達するプラズマバブルの発生条件を明らかにする。

本研究では、赤道から高緯度まで GNSS 受信機が広く設置されているアメリカ域（経度 230° から 330° ）において、2012 年から 2022 年の 11 年間に GNSS 受信機データから得られた全電子数 (Total Electron Content; TEC) データ、及び Jicamarca（12° S, 283.2° E）に設置されているイオノゾンデから得られた F 層の見掛け高度 (h'F) のデータを解析した。GNSS-TEC データから、電離圏電子密度擾乱を表す指数である Rate of TEC index (ROTI) を求め、ROTI の増大領域 (0.5 TECU/min 以上 (1 TECU=10^16 m^(-2)) が磁気赤道付近から磁気緯度 30° 以上にのびる事例を中緯度プラズマバブルとした。本研究では、48 例の中緯度プラズマバブルを検出した。これらの中緯度プラズマバブルの各事例について、経度 230° から 330° における ROTI の最大値を緯度ごとに抽出し、ROTI 最大値の時間-緯度断面図を作成した。図中における ROTI 最大値の傾きから、プラズマバブルが極域方向に発達する速度を導出した。平均値は約 500 m/s であった。また、Jicamarca のイオノゾンデで得られた h'F の時間変化から、磁気赤道における F 層の上昇速度を求めた。平均値は約 18 m/s であった。ROTI 増大領域の極方向への拡大速度と磁気赤道付近における F 層の上昇速度を比較すると、F 層

の上昇速度が大きいほど ROTI の増大領域の極域方向速度が大きくなる関係があった。この結果は、磁気赤道における東向き電場が増加すると、プラズマバブルの生成機構である Rayleigh-Taylor 不安定の成長率が大きくなり、プラズマバブルの発達速度が大きくなるためと考えられる。さらに、ROTI 増大領域の最大到達磁気緯度を F 層上昇速度と比較したところ、両者に明瞭な相関は見られなかった。この結果は、プラズマバブルの最大到達磁気緯度は、磁気赤道における東西電場だけでなく、プラズマバブルが発達する過程の電離圏の状態にも依存するためと考えられる。

R005-17
A 会場 ：11/24　PM2 （15:30-18:15）
17:45〜18:00

#木暮 優 [1,2,3], Jia Yue[2,3], Min-Yang Chou[2,3], Huixin Liu[1], Yuichi Otsuka[4]
[1 九大・理・地惑, [2NASA/GSFC, [3The Cathoric University of America, [4 名古屋大学宇宙環境研究所

Observations of Stratospheric Concentric Gravity Waves and Concentric Traveling Ionospheric Disturbances over the U.S.

#Masaru Kogure[1,2,3], Yue Jia[2,3], Chou Min-Yang[2,3], Liu Huixin[1], Otsuka Yuichi[4]
[1Department of Earth and Planetary Sciences , Kyushu University, [2NASA/GSFC, [3The Cathoric University of America, [4Institute for Space-Earth Environmental Research, Nagoya University

This work investigates the distributions of coincident stratospheric concentric gravity waves (GWs) observed by AIRS and concentric traveling ionospheric disturbances (TIDs) detected by GNSS-TEC during the four seasons of 2022 to illustrate the mesoscale vertical coupling between the lower atmosphere and ionosphere. We compared these disturbances in the stratosphere and ionosphere with tropospheric weather conditions, including convective available potential energy (CAPE) and locations of extratropical cyclone's centers, as well as background winds in the thermosphere. Epicenters of the concentric TIDs associated with stratospheric concentric GWs correspond to areas with high CAPE over the central-to-east U.S. (~60-110° W) in summer and over the southern U.S. (south of ~40° N) in spring and fall. On the other hand, in fall, winter, and spring, the epicenters over the northern U.S. (north of ~40° N) appeared in the south of high extratropical cyclone activity areas, corresponding to the centers of extratropical cyclones. These results suggest that the potential sources of concentric GWs driving TIDs over the continental U.S. were convection during the four seasons, although weather phenomena associated with the convection varied by season. Convection over the central-to-eastern U.S. in summer and the southern U.S. in spring could be linked to thunderstorms. On the other hand, convection over the northern U.S. from fall to spring could be induced by warm and wet air advection associated with extratropical cyclones. Over the North Atlantic Ocean in fall, hurricanes could induce convections. We also found that concentric TIDs are linked to 67% of the stratospheric concentric GW events, indicating that convection is a significant TID source in the lower atmosphere, contributing to the lower atmosphere-ionosphere vertical coupling. The thermospheric wind influences the local time and horizontal distribution of the concentric TIDs. Specifically, the thermospheric wind during daytime is weaker than that at nighttime, leading to a higher occurrence rate of concentric TIDs during daytime.

R005-18
A 会場 ：11/25　AM1 （9:00-10:15）
9:00〜9:15

半球間沿磁力線電流 (IHFACs) における準６日波の季節変動と緯度構造

#高山 久美 [1)], 吉川 顕正 [2)], 三好 勉信 [3)]
([1] 九大, [2] 九大/理学研究院, [3] 九大・理・地球惑星

Seasonal Variation and Latitudinal Structure of the Quasi-6-Day Wave on the Inter-Hemispheric Field Aligned Currents (IHFACs)

#Kumi Takayama[1)], Akimasa Yoshikawa[2)], Yasunobu Miyoshi[3)]
([1]Department of Earth and Planetary Sciences, Graduate School of Science, Kyushu University, [2]Department of Earth and Planetary Sciences, Kyushu University, [3]Department of Earth and Planetary Sciences, Faculty of Sciences, Kyushu University

The quasi-6-day wave is a type of atmospheric wave generated by the latent heat heating associated with the cumulus convection activity in the tropics [Miyoshi and Hirooka, 1999]. It propagates upward and affects the equatorial electrojet (EEJ) in the ionosphere, which has been confirmed from satellite observations [Yamazaki et al., 2018]. In addition, TIME-GCM calculations shows that the EEJ reaches its maximum intensity around the equinoxes [Liu et al., 2014]. Inter-hemispheric field-aligned currents (IHFACs) flow from the ionosphere of one hemisphere to the other through the magnetosphere, to resolve the non-uniformity of ionospheric currents with divergent spatial structure that occurs between hemispheres [Fukushima, 1979]. The direction of the IHFACs changes in the morning, noon, and evening, and its intensity is highest in February and August [S. Yamashita and T. Iyemori, 2002].

In this study, we used ground magnetic field data from MAGDAS and INTERMAGNET to clarify the effects of the quasi-6-day wave on the IHFACs. The ground magnetic field data used are the east-west (D) magnetic field components at 9 stations within the 210 geomagnetic longitude band and -35 to +35 geomagnetic latitude during the 2007-2011 magnetic quiet period. Principal component analysis is a statistical analysis method that can extract large components from any data and reveal its internal structure. We applied this method to the data to extract the IHFACs variation from the D components. The amplitude of the variation with a period of about 6 days was extracted, and this was taken to be the quasi-6-day wave. To show the latitudinal and seasonal structure of the quasi-6-day wave, the average amplitude for a given month over the 5-year timespan were calculated.

The results show that, the IHFACs are affected by the Q6DW. Also, the variation become stronger around the equinoxes, which is consistent with the seasonal dependence of the Q6DW. The latitudinal structure of the Q6DO appearing in the IHFACs has amplitudes from the equator to mid-latitudes, suggesting that the Q6DW may have been propagated between hemispheres via the IHFACs. More results and discussion will be presented in this presentation.

準 6 日波は大気波動の 1 つで、熱帯における積雲対流活動に伴う潜熱加熱によって発生し [Miyoshi and Hirooka, 1999]、上方に伝播、電離圏の赤道ジェット電流 (EEJ) に影響を与えることが衛星観測から確認されている [Yamazaki et al., 2018]。また TIME-GCM による計算から Equinox 前後で最大振幅となる [Liu et al., 2004] ことがわかっている。半球間沿磁力線電流（IHFAC）は、半球間で生じる発散的な空間構造を持つ電離層電流の非一様性を解消するために、片側半球の電離圏から磁気圏を通ってもう一方の半球に流れる電流である [Fukushima, 1979]。朝、昼、夜で向きが変化し、２月と８月に電流強度が最大となることが示されている [S. Yamashita and T. Iyemori, 2002]。

本研究では地上磁場観測データを用いて、IHFACs に現れる準 6 日波の影響を明らかにした。使用データは、九州大学磁場データ取得システム（MAGDAS）、国際リアルタイム磁場観測ネットワーク（INTERMAGNET）の 2007〜2011 年の磁気的静穏期における、地磁気経度 210° 帯、地磁気緯度-35° 〜＋ 35° 内 9 観測点の東西 (D) 成分である。解析手法として、データから大規模な成分を分離・抽出し、内部構造を明らかにすることができる主成分分析を各観測点に適用することにより、IHFACs による変動成分を抽出し、その変動成分から約６日周期の変動の振幅を取り出した。また、各月でその振幅を５年平均することで、準 6 日波による電離層電流変動の緯度構造と季節変動を示した。

その結果、春分/秋分前後に強くなる季節変動を示すことを明らかにした。これは準６日波の季節依存性と一致する。したがって、準６日波は IHFACs にも影響を与えたと考えられる。また、準６日波によると思われる 変動は赤道から中低緯度まで確認されたため、IHFACs を通して半球間を伝播したと考えられる。詳しい結果および考察は本発表で述べる予定である。

R005-19
A 会場 ：11/25　AM1 （9:00-10:15）
9:15〜9:30

津波で生成される大気波動と電離圏変動のグローバルシミュレーション

#品川 裕之 [1)], 三好 勉信 [2)]
([1] 九州大学国際宇宙惑星環境研究センター, [2] 九大・理・地球惑星

Global simulation of atmospheric waves and ionospheric variations generated by tsunamis

#Hiroyuki Shinagawa[1)], Yasunobu Miyoshi[2)]
([1]International Research Center for Space and Planetary Environmental Science, Kyushu University, [2]Department of Earth and Planetary Sciences, Faculty of Sciences, Kyushu University

It is widely recognized that tsunamis drive atmospheric waves and ionospheric variations. Various numerical simulations as well as observational studies have been made to understand the mechanisms of those variations. We also studied the atmospheric-ionospheric variations using two-dimensional atmosphere-ionosphere coupled models for the tsunami generated by the Sumatra earthquake on 26 December 2004 (Shinagawa et al., 2007) and the Tohoku-oki earthquake on 11 March 2011 (Shinagawa et al., 2013). However, past atmosphere-ionosphere simulations for tsunami-driven disturbances are based on regional models. Since regional models have some uncertainties about boundary conditions, it is difficult to self-consistently include the ionospheric dynamo processes and global neutral winds. To investigate the atmosphere-ionosphere variations driven by tsunamis, we have recently carried out global atmosphere-ionosphere simulations using the coupled model of axisymmetric three-dimensional non-hydrostatic atmosphere model (NHM) and the whole atmosphere-ionosphere coupled model (GAIA). The initial results of the simulations of atmospheric variations driven by tsunamis indicate: (1) acoustic waves, Lamb waves, and gravity waves are generated by initial uplift of the sea surface, (2) gravity waves are generated by propagating tsunamis, and (3) gravity waves are newly generated when propagating tsunamis are stopped by the land. Previous studies have suggested that if acoustic waves or Lamb waves are detected immediately after the generation of tsunamis, it may be possible to predict the arrival and the magnitude of tsunamis because the propagation speeds of acoustic waves and Lamb waves are faster than the propagation speed of tsunamis. Some studies have also indicated that the magnitude of tsunamis can be determined from the ionospheric/geomagnetic variations driven by the acoustic waves prior to the arrival of tsunamis. We have carried out the atmosphere-ionosphere simulations of the Tohoku-oki tsunami on 11 March 2011 using the new model, and we will report the atmospheric waves and ionospheric variations generated by the tsunami. We will also make some remarks on the possibility of the tsunami-arrival prediction using observations of atmospheric waves, ionospheric variations, geomagnetic variations.

References
Shinagawa, H., et al. (2007) A numerical simulation of ionospheric and atmospheric variations associated with the Sumatra earthquake on December 26, 2004. Earth Planets Space, 59. https://doi.org/10.1186/BF03352042
Shinagawa, H., et al. (2013) A simulation study of ionospheric variations in the vicinity of the epicenter of the Tohoku-oki earthquake on 11 March 2011, Geophys. Res. Lett., 40. https://doi.org/10.1002/2013GL057627

津波に伴って大気波動が発生し、電離圏の変動が起きることは良く知られており、さまざまな観測と数値シミュレーションによる研究が行われてきてきた。われわれのグループでも 2004 年 12 月 26 日のスマトラ地震による津波や (Shinagawa et al., 2007)、2011 年 3 月 11 日の東北沖地震の津波について (Shinagawa et al., 2013)、２次元の大気圏-電離圏シミュレーションによって大気圏-電離圏変動を調べてきた。しかしながら、これまでのシミュレーションでは、領域を限った大気圏-電離圏モデルしか使われてこなかった。領域モデルでは、境界条件の不確定さが入ってしまうため、電離圏ダイナモで生成される電離圏電場や、背景中性風の影響などを矛盾なく取り扱うことができないという問題がある。今回われわれは、軸対称３次元の非静力学大気圏モデル (NHM) と全領域大気圏-電離圏結合モデル (GAIA) を組み合わせることによって、津波による大気圏-電離圏変動のグローバルシミュレーションを行なった。初期計算の結果、津波に伴う大気波動に関しては、(1) 初期の急激な海面上昇による音波、ラム波、重力波などの生成、(2) 伝播する津波による重力波の生成、(3) 津波が陸地で堰き止められることによる新たな重力波の生成、の３つの過程があることがわかった。初期の海面上昇で発生する音波やラム波は津波の速度より速いため、津波発生直後に音波やラム波が検出できれば、津波の到来や規模が予測ができる可能性が過去の研究で示唆されている。また、津波で生成された音波による電離圏変動や地磁気変動を用いて津波の規模を予測する方法もいくつかのグループで検討されている。本発表では、新たなモデルを用いて 2011 年 3 月 11 日の東北沖津波に伴う大気圏-電離圏変動のシミュレーションを行い、津波で生成される大気波動とその電離圏への影響について報告する。さらに、大気波動、電離圏変動、地上磁場変動などの観測を用いた津波の到来／規模予測の可能性についても述べる予定である。

References
Shinagawa, H., et al. (2007) A numerical simulation of ionospheric and atmospheric variations associated with the Sumatra

earthquake on December 26, 2004. Earth Planets Space, 59. https://doi.org/10.1186/BF03352042

Shinagawa, H., et al. (2013) A simulation study of ionospheric variations in the vicinity of the epicenter of the Tohoku-oki earthquake on 11 March 2011, Geophys. Res. Lett., 40. https://doi.org/10.1002/2013GL057627

R005-20
A 会場 ：11/25　AM1 （9:00-10:15）
9:30〜9:45

Lamb 波とプラズマ圏空洞共鳴によって引き起こされた可能性のある短周期 Pc3 脈動

#家森 俊彦 [1)], 横山 佳弘 [2)], 青山 忠司 [3)]
([1] 京大, ([2]IRF, ([3] エフ・ファクトリー (株)

A short period Pc3 magnetic pulsation possibly caused by a Lamb wave and plasmaspheric cavity resonance

#Toshihiko Iyemori[1)], Yoshihiro Yokoyama[2)], Tadashi Aoyama[3)]
([1]Kyoto University, ([2]Swedish Institute for space physics, ([3]F-Factory Co. Ltd.

Low-altitude satellites such as Champ and Swarm and ground-based magnetic field observations often detect compressional Pc3 (period 10-45 sec) or Pc4 (45-150 sec) pulsations at mid- and low-latitudes during high-speed solar wind. These have been discussed in relation to a duct propagation between the magnetosphere and plasmasphere of magnetosonic waves generated by upstream waves or by changes in dynamic pressure of the solar wind, magnetospheric cavity resonance, and field-line resonance (Heilig et al., 2007; Sutcliffe et al., 2013; Balasis et al., 2015; et al.). Based on correlation analysis with solar wind parameters, it is believed that these originate from the solar wind, but we report that a peculiar Pc3 pulsation was observed by the Swarm satellites that may have been caused by the Lamb waves generated by the Tongan undersea volcanic eruption on January 15, 2022. The difference between this and the usual Pc3 pulsations observed at low and mid-latitudes is its spectral distribution, where the spectal density usually peaks between 20 and 30 sec, but in the example observed on the dayside orbit around the time when the Lamb waves are estimated to have passed, the spectral density peaks below 20 sec and is small in the periods of 20 sec or more. In order to confirm the existence of an event with a spectral density and distribution characteristic similar to this or more prominent than this, all orbits of Swarm-A, -B, and -C passing through the region of 10-14 MLT, ± 45 MLat from 2014 to April 2022 were searched, but no examples were found other than this event. The solar wind on January 15, 2022 was turbulent at high speed, so the possibility that this was the cause of the Pc3 cannot be completely denied, but the solar wind on this day was not particularly turbulent at high speed, and the timing coincides with the estimated time when the Lamb waves reached the longitude of the satellite orbit, so this phenomenon is likely to be related to Lamb waves. One possible explanation for the shift of the spectral peak toward the short period side is that the daytime plasmasphere may be trapping or resonating magnetosonic waves generated in the ionosphere. In other words, magnetosonic waves injected from the ionosphere may be reflected at the plasmapause, where the phase velocity is large, and waves with a period of about 10-20 seconds may be captured or resonate in the plasmasphere, resulting in large amplitude and short period Pc3 waves observed by the Swarm satellites. The cavity resonance in the plasmasphere has been investigated in detail, for example by Fujita and Itonaga (2003), to explain the characteristics of Pi2-type pulsations injected from nightside magnetosphere. Here, we also consider the injection of waves from the ionosphere, which originates from the daytime lower atmosphere.

Champ や Swarm などの低高度衛星や地上の磁場観測では高速太陽風などの時に中低緯度で圧縮性の Pc3(周期 10 - 45 秒) あるいは Pc4(45 − 150 秒) 脈動がしばしば検出される。これらは bow shock で生成され磁気圏に入射した upstream wave や太陽風の動圧変化等により生成された磁気音波の磁気圏とプラズマ圏との間のダクト伝播や磁気圏空洞共鳴、field-line resonance と関連付けて議論されてきた (Heilig et al., 2007; Sutcliffe et al., 2013; Balasis et al., 2015; 他)。太陽風パラメータとの相関解析から、これらの起源は太陽風にあると考えられているが、2022 年 1 月 15 日のトンガ海底火山噴火によって生じた Lamb 波が原因となり発生した可能性のある特異な Pc3 脈動が Swarm 衛星により観測されたので報告する。中低緯度で観測される通常の Pc3 脈動との違いはそのスペクトル分布にあり、通常は 20 − 30 秒 (あるいはそれ以上) の間にスペクトル密度のピークがあるが、Lamb 波が通過したと推定される時刻付近の昼間側軌道で観測された例では、スペクトル密度のピークが 20 秒以下にあり、20 秒以上の周期帯では小さい。これと同等あるいはそれ以上にきわだったスペクトル密度と分布の特徴をもつイベントの有無を確認するために 2014 年から 2022 年 4 月までの期間について 10 − 14MLT, ± 45MLat の領域を通る Swarm-A, -B,- C の全軌道を探索したが、このイベント以外では一例も見つからなかった。2022 年 1 月 15 日の太陽風は高速で乱れていたので、それによる Pc3 である可能性も完全には否定できないが、この日の太陽風が特別に高速で乱れていたというわけではなく、また、Lamb 波が衛星軌道の経度に到達した推定時刻とタイミングもよく一致するので、この現象は Lamb 波と関連している可能性が高い。周期が短周期側に偏っていることの説明としては、昼間側のプラズマ圏が電離圏で作られた磁気音波の閉じ込めあるいは共鳴を引き起こしている可能性が考えられる。すなわち、電離圏側から注入された磁気音波が、位相速度が大きくなるプラズマ圏界面で反射され、周期 10 − 20 秒程度の波がプラズマ圏で補足あるいは共鳴をして大振幅の Pc3 として Swarm 衛星で観測された可能性が考えられる。プラズマ圏の空洞共鳴については、夜側磁気圏に起因すると考えられている Pi2 型脈動の特性を説明するために、例えば Fujita and Itonaga(2003) などで詳しく調べられてきたが、ここでは昼間側でかつ下層大気に起因する電離圏側からの波の注入についても検討する。

R005-21
A 会場 ：11/25　AM1 （9:00-10:15）
9:45〜10:00

地上磁場データを用いた台風がもたらす電離圏擾乱の解析

#西村 美紀 [1)], 吉川 顕正 [2)], 魚住 禎司 [3)]
([1] 九州大学大学院理学府, [2] 九大/理学研究院, [3] 九州大学国際宇宙惑星環境研究センター

Analysis of Ionospheric Disturbances Caused by Typhoons Using Ground Magnetic Field Data

#Miki Nishimura[1)], Akimasa Yoshikawa[2)], Teiji Uozumi[3)]
([1]Department of Earth and Planetary Sciences, Graduate School of Science, Kyushu University, [2]Department of Earth and Planetary Sciences, Kyushu University, [3]International Research Center for Space and Planetary Environmental Science,Kyushu University

In recent years, it has become increasingly evident that intense convection activities, such as typhoons occurring in the troposphere, can have various impacts on the ionosphere. The SWARM satellite, orbiting at an altitude of about 500 km, observed small-scale geomagnetic fluctuations when passing over a typhoon [Aoyama et al., 2017]. These fluctuations might also influence the dynamics of the F-layer plasma [Du, X., 2023].

Typhoon VONGFONG, which formed in October 2014, intensified into a powerful storm with a minimum pressure of 900 hPa around 3:00 JST on October 8th, and later made landfall near Makurazaki City in Kagoshima Prefecture around 8:30 JST on the 13th. When two SWARM satellites passed over the typhoon around 10:00 JST on the 8th, magnetic field fluctuations with an amplitude of approximately 1.5 nT in the x-component (directed toward Earth along the geomagnetic meridian) and about 0.5 nT in the y-component (perpendicular to the geomagnetic meridian) were observed. These fluctuations suggest the presence of field-aligned currents, which may have been generated by a dynamo excited by acoustic waves propagating from the lower atmosphere to the ionosphere [V.A. Martines-Vedenko et al., 2019].

However, there are no reported cases of direct geomagnetic fluctuations caused by typhoons, and reports of magnetic field fluctuations observed by the SWARM satellite are still scarce. Therefore, further research is needed to establish the morphology of typhoon-induced magnetic field fluctuations. Our investigation focuses on whether geomagnetic fluctuations observed before and after the passage of a typhoon are caused by fluctuations in ionospheric currents.

The data used in this study comes from the ground-based geomagnetic observation network MAGDAS (Magnetic Data Acquisition System), which is globally deployed by Kyushu University's International Research Center for Space and Planetary Environmental Science (i-SPES), and from geomagnetic data provided by the Japan Meteorological Agency (JMA) geomagnetic observatories. Both datasets have a time resolution of one second. We analyzed the raw H and D component data, their time derivatives, and the five-minute standard deviation of the derivatives. The five-minute standard deviation of the time derivatives indicates the degree of data dispersion within each five-minute period.

We conducted a detailed analysis of data from Kanoya in Kagoshima Prefecture and Kakioka in Ibaraki Prefecture (provided by the JMA), as well as Kuju in Oita Prefecture and Ashibetsu in Hokkaido (MAGDAS), focusing on October 12th and 13th, 2014, around the time when Typhoon VONGFONG, previously confirmed to have caused magnetic fluctuations observed by the SWARM satellite, made landfall in Kagoshima Prefecture around 8:30 JST on October 13th. Our analysis revealed that in Kanoya, the time derivative of the H component increased by approximately 1.5 times between 11:30 and 12:30 JST on October 13th compared to other days without the typhoon. In Kuju, we observed that the time derivatives of both the H and D components and their five-minute standard deviations increased by about 2 to 3 times between 15:00 and 18:30 JST on October 13th, compared to other days without the typhoon.

Additionally, frequency analysis revealed that, particularly in Kuju, a spectral peak appeared in the 0.5 − 1 mHz range, which corresponds to the frequency band of atmospheric gravity waves, during the time period when fluctuations were observed. Such fluctuations were not observed at the observation points in Kakioka or Ashibetsu, which are located farther from the typhoon's center. Moreover, the minimum Dst index value during the period from 9:00 to 21:00 JST on October 13, 2014, was − 3 nT, indicating that no geomagnetic storm occurred. To further investigate whether these ground magnetic field fluctuations were caused by the typhoon, we analyzed approximately one year's worth of raw data, time derivatives, and their five-minute standard deviations from Kuju, covering the period from October 1, 2013, to the end of September 2014. We found no similar changes on days without typhoons.

In this presentation, we will discuss the mechanisms of typhoon-induced ground magnetic field fluctuations, focusing on this event and several other events currently under analysis.

近年、対流圏で発生する台風等の激しい対流活動が電離圏にさまざまな影響を及ぼしていることが明らかになりつつある。高度約 500km の軌道を飛行する SWARM 衛星が台風上空を通過時に、小規模な地磁気変動を観測し [Aoyama et al.,2017]、その影響は F 層プラズマダイナミクスにも及んでいる可能性がある [Du,X.,2023]。

2014 年 10 月に発生した台風 VONGFONG は、10 月 8 日 3 時 JST 頃に最低気圧 900hPa の猛烈な勢力に発達し、その後、13 日 8 時半 JST 頃に鹿児島県枕崎市付近に上陸した。8 日 10 時 JST 頃に 2 機の SWARM 衛星が台風の上空を通過

した際には、地球に向かう方向（地磁気子午面内）の x 成分でおよそ 1.5 nT、地磁気子午面に垂直な y 成分でおよそ 0.5 nT の振幅の磁場変動が観測された。この変動は、下層大気から電離圏へ伝播する音響波によって励起されるダイナモによって生成された沿磁力線電流の空間構造を反映している可能性を示唆している [V.A.Martines-Vedenko et al.,2019]。

しかし、台風を起因とする直接的な地上磁場変動の報告例はまだなく、SWARM 衛星による磁場変動の報告も少ないため、台風起源の磁場変動に関するモルフォロジーを確立するためには、更なる研究を積み重ねる必要がある。そこで、我々はまず台風通過前後における地上磁場の変動が、電離圏電流の変動に起因するかどうかという観点から調査を進めている。

使用データは、九州大学際宇宙惑星環境研究センターがグローバルに展開している地上磁場観測網 MAGDAS(Magnetic Acquisition System) および気象庁地磁気観測所が提供している地上磁場データである。データはいずれも 1 秒の時間分解能であり、H 成分と D 成分の生データとその時間微分値、微分値の５分間標準偏差を調べた。時間微分値の５分間標準偏差は、５分間のなかでデータの散らばりがどの程度あるのかを表すものである。

我々は、先述した既に SWARM 衛星で磁場変動が確認されている 2014 年の台風 VONGFONG が 10 月 13 日 8 時半 JST 頃に鹿児島県に上陸する前後の 12 日と 13 日の鹿児島県鹿屋と茨城県柿岡 (気象庁)、大分県久住と北海道芦別 (MAGDAS) のデータを詳細に解析した。その結果、鹿屋では H 成分の時間微分値が 13 日 11 時半から 12 時半 JST 頃に台風が来ていない他の日と比べて 1.5 倍程度大きくなることを、久住では H 成分・D 成分ともに時間微分値とその５分間標準偏差が 13 日 15 時から 18 時半 JST 頃に、同様に２～３倍程度、大きくなることを確認した。

また、周波数解析の結果から、特に久住では変動が見られた時間帯に大気重力波の周波数帯域である 0.5～1mHz でスペクトルのピークが現れた。このような変動は、台風の中心から離れた柿岡や芦別の観測点では見られないものだった。なお、2014 年 10 月 13 日の 9 時から 21 時 JST の時間帯における Dst 指数の最小値は－ 3nT であり、磁気嵐は発生していない。この地上磁場変動が台風の影響によるものなのかをさらに精査するため、2013 年 10 月 1 日から 2014 年 9 月末までのおよそ 1 年分の久住の生データ、時間微分値とその５分間標準偏差を調べたが、台風が来ていない日に同様の変化は見られなかった。

本講演は、このイベントと現在、解析を進めている複数のイベントに対して、台風を起因とする地上磁場変動の発生機構に関して議論を行う。

R005-22
A 会場 ：11/25　AM1 （9:00-10:15）
10:00〜10:15

#大矢 浩代 [1)], 土屋 史紀 [2)]
[(1] 千葉大・工・電気, [(2] 東北大・理・惑星プラズマ大気

D-region ionospheric response to the 2024 Noto Peninsula earthquake using OCTAVE LF transmitter signals

#Hiroyo Ohya[1)], Fuminori Tsuchiya[2)]
[(1]Graduate School of Engineering, Chiba University, [(2]Planetary Plasma and Atmospheric Research Center, Graduate School of Science, Tohoku University

In the D-region ionosphere, oscillations of LF (low frequency, 30-300 kHz) transmitter signals with a period of 100 s were reported about five minutes after mainshock of the 2011 Tohoku earthquake (Ohya et al., 2018). During the 2015 Nepal earthquake, variations in LF amplitudes with a period of 100-200 s were reported (Akashi et al., 2021). These variations were caused by acoustic waves excited by Rayleigh waves. However, detailed coupling between earthquakes and the D-region ionosphere has not been revealed. In this study, we investigate the D-region ionospheric variations associated with the 2024 Noto earthquake using OCTAVE (Observation of CondiTion of ionized Atmosphere by VLF Experiment) LF transmitter signals. We have built the OCTAVE observation network in Asia, Europe, and America for monitoring the ionosphere and magnetosphere. Intensity and phase were observed with a sampling time of 0.1 s. The mainshock of the Noto earthquake (Mw 7.5) occurred at 07:10 UT on 1 January, 2024. When the propagation velocity of the Rayleigh wave was assumed to be ˜3.5 km/s, we calculated the propagation time of acoustic wave between the Earth's surface and reflection height of the LF waves (about ˜90 km height). Variations in LF amplitudes and phase were seen in JJY40kHz-RKB and JJY60kHz-RKB paths. The amplitude and phase variations were 0.6-1.8 dB and 1.8 degrees, respectively. There was no change in JJI-RKB amplitude. The period of the LF variations was 60 − 300 s. The longer period of vertical seismic velocity observed at Wajima (WJM) was similar to that of the LF amplitudes (10 − 300 s). Acoustic waves with the similar periods of the seismic waves might propagated from the closest path point to the D-region height vertically. In this presentation, we will show the detailed phenomena in detail.

R005-P01
ポスター 3 ：11/25　PM1/PM2 （13:15-18:15）

３次元多成分イオン磁気流体力学シミュレーションによる初期地球における膨張水素大気の非熱的散逸モデリング

#草野 百合 [1)], 木村 智樹 [1)], 堺 正太朗 [2)], 吉田 辰哉 [2)], 前田 優樹 [3)], 中田 英太朗 [4)], 高田 亮馬 [1)], 寺田 直樹 [2)]
([1 理科大, [2 東北大, [3 東大, [4 北大

Non-thermal escape of expanded hydrogen atmosphere on early Earth modeled by a 3D multispecies magnetohydrodynamic simulation

#Yuri Kusano[1)], Tomoki Kimura[1)], Shotaro Sakai[2)], Tatsuya Yoshida[2)], Yuki Maeda[3)], Eitaro Nakada[4)], Ryoma Takada[1)], Naoki Terada[2)]
([1Tokyo University of Science, [2Tohoku University, [3The University of Tokyo, [4Hokkaido University

The most important element for Earth and other planets to hold oceans on the surface is the atmosphere. The atmospheric evolution has been controlled by the supply of gas from Earth's crust and its escape into space. Non-thermal atmospheric escape, such as ion pickup, which is one of the major processes of atmospheric escape, depends on the planet's intrinsic magnetic field, the solar wind, and solar XUV flux. Quantitative evaluation and long-term variability of each process are important for understanding the atmospheric evolution, but there is a lack of in-situ observations of the escape regions of each planet, which is a major unsolved problem. Previous studies have estimated the non-thermal escape rates from the planetary atmospheres such as Mars and Venus, using the global numerical simulations. For example, the atmospheric escape simulation of past Mars have shown that when the XUV flux increases 100 times compared to the present day, the atmospheric temperature (Kulikov et al., 2007) and ion production rate increase, and the escape rate increases by 10^{4-5} times (Terada et al., 2009). However, these studies are based on estimates of the composition of the present neutral atmosphere and are based on the assumption that the early Martian atmosphere was CO_2-rich and dry with a low greenhouse effect as well as the present Mars. On the other hand, the early atmosphere likely had a hydrogen-dominant atmosphere (Yoshida and Kuramoto., 2021), which is different from the present. A similar problem remains unresolved on Earth.

Here we hypothesized a hydrogen atmosphere of the early Earth (Yoshida and Kuramoto., 2021, altitude range of 1000~185000km, the maximum density of 3×10^{12}/cm^3), assuming an XUV flux 100 times larger than present, and investigated the non-thermal escape rate of atmospheric ions using a 3D multispecies magnetohydrodynamic (MHD) model (Terada et al., 2009). We assume that the early earth was in a non-magnetized period, when the influence of the solar wind would be large, such as during geomagnetic reversals. We set the solar wind speed to 1800 km/s , density to 2100/cc, and IMF absolute value to 7nT. As a result, the atmospheric escape rate at 200 R_p on the night side is found to be 4.0×10^{28}/s for $H_2{}^+$ and 5.0×10^{33}/s for H^+.(R_p is the radius of the Earth 6380 km.) A bow shock was formed at about 60 R_p on the dayside, and inside it, an expanded ionosphere was formed with the maximum plasma density of 5.4×10^6/cc due to the expanded atmosphere. The altitudes where the escape rates are large corresponds to the expanded ionosphere. The solar wind magnetic field penetrated into the expanding ionosphere on the dayside, and the magnetic flux density of the IMF was amplified by a factor of 300 to form an induced magnetosphere with a maximum magnetic flux density of 2000 nT. In addition, we estimated that the early hydrogen atmosphere (Yoshida and Kuramoto., 2021) depletes in 8.5 million years by this non-thermal escape rate. This results suggests that not only thermal escape but also nonthermal escape is significant for the early Earth atmospheric escape. We plan to investigate the dependence of atmospheric escape rate on the IMF, the solar XUV flux and solar wind dynamic pressure. We report the current status of our study in the presentation.

地球その他の惑星が表層に海洋を保持するために最も重要な要素は大気である。大気は、地殻からのガス供給と、宇宙空間への散逸にその収支を制御されながら進化してきた。宇宙空間への大気散逸の中でも主要なプロセスの１つである、イオンピックアップ等の非熱的散逸は、惑星の固有磁場、太陽風、太陽からの XUV フラックスに依存する。各過程の定量評価や長期変動の理解は進化の解明の上で重要だが、各惑星ともに散逸領域のその場観測等が不足しており、未解決の大問題である。先行研究では火星、金星などの惑星大気からの非熱的散逸率を、数値シミュレーションを使って全球的に推定している。例えば過去の火星を想定した大気のシミュレーションでは、XUV フラックスが現代と比較して 100 倍になると、大気の温度 (Kulikov et al., 2007) とイオン生成率が上昇し、散逸率も 10^{4-5} 倍増加する (Terada et al., 2009) ことが明らかになっている。しかしこれらの研究では現在の中性大気の組成をもとに推定されており、過去の火星大気も CO_2 主体で温室効果が低く乾燥していたという仮定の元で成り立っている。一方、実際の過去の大気は現代と異なり水素が有意に含まれている組成であった可能性がある (Yoshida and Kuramoto., 2021)。地球においても同様の点が未解決のままである。そこで本研究は、現代の 100 倍の XUV フラックスを想定し、過去の地球における組成を反映した水素大気 (Yoshida and Kuramoto., 2021, 高度 1000~185000km、最大密度 3×10^{12}/cm^3) を仮定し、多成分イオン MHD モデル (Terada et al., 2009) を使って大気起源イオンの非熱的散逸率を調べた。原始地球は地磁気反転時等で太陽風の影響が大きいと思われる非磁化の時代を仮定し、太陽風は速度 1800km/s, 密度 2100/cc, IMF 絶対値を 7nT に設定した。その結果夜側 200R_p（R_p は地球の半径、地表を R_p とする。）での大気散逸率は $H_2{}^+$ が 4.0×10^{28}/s、H^+ が 5.0×10^{33}/s という

結果が得られた。また昼側約 $60R_p$ でバウショックが形成され、その内側で高密度の（最大プラズマ密度〜5.4×10^6/cc）膨張した電離圏が形成された。散逸の大きい高度は膨張した電離圏に対応している。太陽風磁場が昼側の膨張電離圏に浸透・堆積し、IMF の磁束密度が 300 倍に増幅されて最大磁束密度 2000nT の誘導磁気圏が形成された。またこの非熱的な散逸率によって、初期の水素大気 (Yoshida and Kuramoto., 2021) は 850 万年で枯渇すると見積もられた。これは過去有意であると考えられていた熱的散逸 (Yoshida and Kuramoto., 2021) による枯渇時間の 50 分の 1 の時間である。つまり、過去の水素大気について、熱的散逸だけではなく非熱的散逸も無視できない可能性が示唆された。今後は、IMF の影響と XUV フラックス、太陽風動圧による変化を調べる予定である。発表では、本研究の現状を報告する。

R005-P02
ポスター 3 ：11/25　PM1/PM2 （13:15-18:15）

北極海の海氷減少が中層大気に与える影響

#森 祥輔 [1)], 三好 勉信 [2)]
[(1] 九大・理・地球惑星, [(2] 九大・理・地球惑星

The impact of Arctic Sea ice loss on the middle atmosphere

#Shosuke Mori[1)], Yasunobu Miyoshi[2)]
[(1]Department of Earth and Planetary Sciences, Graduate School of Science, Kyushu University, [(2]Department of Earth and Planetary Sciences, Faculty of Sciences, Kyushu University

Sea ice in the Arctic has been decreasing in recent decades. It has been reported that the Arctic Sea ice loss affects the planetary wave activity propagating from the troposphere to the stratosphere, thereby influencing the general circulation in the stratosphere. In this study, we examined the impact of sea ice loss on the middle atmosphere. The long-term GAIA simulation data (1989-2021) are used in this study. In GAIA simulation data, the meteorological reanalysis data (JRA-55) are included in the troposphere and lower stratosphere. Our analyses indicated that the Arctic Sea ice loss affects the Arctic temperature not only in the stratosphere but also in the mesosphere and lower thermosphere. For example, the Arctic temperature in the mesosphere (lower thermosphere) with the Arctic Sea ice loss is lower (higher) than that without the Arctic Sea ice loss. However, our analyses include influences of other boundary conditions such as sea surface temperature and atmospheric internal variability. In order to examine the effect of the Arctic Sea ice loss more precisely, numerical experiments with and without the Arctic Sea ice loss should be conducted. By analyzing these numerical experiment results, we will investigate the impact of the Arctic Sea ice loss on the general circulation in the middle atmosphere.

ここ数十年で北極海の海氷が減少してきている。その結果、対流圏から成層圏へ伝播するプラネタリー波の活動度が大きくなることで、北半球の成層圏での大気循環の変化や高温偏差などの影響を及ぼすことが報告されている。本研究では、成層圏に加え、中間圏・下部熱圏まで含めた中層大気全体に及ぼす影響を調べてみた。用いたのは、下部成層圏まで気象の再解析データ (JRA-55) を組み込んだ、全大気圏ー電離圏結合モデル（GAIA モデル）によりシミュレートされたデータである。方法としては、1989~2021 年冬季について、少氷年での大気循環の平均から多氷年での大気循環の平均を引くことで、海氷による影響を調べた。本解析により、北半球高緯度帯において、先行研究と同様に対流圏から成層圏に伝播するプラネタリー波活動度の増大や、極域成層圏の高温偏差が見られた。加えて、これらとほぼ同時に、極域中間圏では低温偏差、下部熱圏では高温偏差が見られた。しかし、これらの解析結果には海氷による影響に加え、例えば海面水温変動といった他の境界条件や、大気のもつ内部変動などの影響も含んでいると考えられる。海氷による影響をより正確に評価するためには、海氷減少の影響以外を排除した条件で、十分なサンプル数の数値シミュレーションが必要となる。そこで、1980 年代初頭と 2010 年代後半の北極海の海氷分布を与えた数値シミュレーションを実行し、どのような影響が現れるかを明らかにすることとした。詳細な結果は当日発表する予定である。

R005-P03
ポスター 3 ：11/25　PM1/PM2 （13:15-18:15）

ひまわり 8 号/9 号によって観測された 2015—2024 年の極中間圏雲の変動

#森山 陽介 [1)], 津田 卓雄 [1)], 安藤 芳晃 [1)], 村田 健史 [2)]
[(1] 電気通信大学, [(2] 情報通信研究機構

Polar mesospheric cloud variations from 2015 to 2024 observed by Himawari-8/9

#Yosuke Moriyama[1)], Takuo Tsuda[1)], Yoshiaki Ando[1)], Ken T. Murata[2)]
[(1]University of Electro-Communications, [(2]National Institute of Information and Communications Technology

Polar Mesospheric Clouds (PMCs), also known as Noctilucent Clouds (NLCs), are the highest clouds on Earth. The PMC consists of water-ice particles that can be formed under extremely low-temperature conditions around the mesopause region at high latitudes in summer, and thus their formation and loss are thought to be sensitive to atmospheric temperature, the mixing ratio of water vapor, and mesospheric dust as a condensation nucleus. Therefore, the variability of PMCs could be used as a valuable indicator to understand the variation of the high-latitude mesosphere. As for the long-term PMC variations, some previous studies mentioned that PMCs may be a possible indicator of global change (i.e., a miner's canary of global warming), and it has been considered to be an important topic. On the other hand, long-term PMC variations can be affected by various factors, such as the solar cycle of an approximately 11-year period and large-scale volcanic eruptions. In addition, short-term scale effects, such as effects due to Stratospheric Sudden Warming (SSW) in the winter hemisphere, may play important roles in the PMC variations. To observe these variations and understand their mechanisms, long-term PMC observations are needed, and comprehensive investigations on PMC variations are important.

Himawari-8 is the Japanese geostationary-Earth-orbit (GEO) meteorological satellite that started operation in 2015, and a PMC detection method was developed for the full-disk image captured by the Advanced Himawari Imager (AHI) onboard Himawari-8. As a result, the performance of the Himawari-8 PMC observation was comparable to that of the Cloud Image and Particle Size (CIPS) onboard the Aeronomy of Ice in the Mesosphere (AIM) satellite. Himawari-8/AHI ended its operation in December 2022, and Himawari-9/AHI took over its operation. To continue PMC observations, the PMC detection method developed for the Himawari-8/AHI was applied to the Himawari-9/AHI. Analysing simultaneous PMC observation data in early summer in the Southern Hemisphere (1-13 December 2022) by both satellites, comparisons were made between the PMC data from Himawari-8/AHI and Himawari-9/AHI. The results showed that 99.8% of the PMC detection results from Himawari-9/AHI agreed with those from Himawari-8/AHI. As for the PMC height data, 98.3% of the data showed agreement within ± 1 km. These results indicate that the Himawari-9/AHI PMC observations have the same performance as the Himawari-8/AHI PMC observations.

In this study, we are working on data analysis of about nine-year PMC data acquired by the Himawari-8/9 during 2015-2024 to investigate long-term PMC variations. To perform comprehensive investigations, we also analyse the solar activity index data, atmospheric temperature data, and water vapor data. In the presentation, we will show these results and discuss importance of several factors affecting observed PMC variations.

極中間圏雲（Polar Mesospheric Cloud: PMC）は、夜光雲（Noctilucent Cloud: NLC）としても知られ、地球上で最も高い雲である。PMC の実態は、夏の高緯度中間圏界面付近の極低温環境で凝結する水氷粒子であることから、その消長は、大気温度や水蒸気量、凝結核としての役割を果たす中間圏ダスト量などに敏感に反応すると考えられている。したがって、PMC の消長は、高緯度中間圏領域の大気の変動を知るための貴重な指標として用いることができると考えられている。特に、長期スケールの大気環境変動に関して、PMC は地球気候変動を把握する為の有効な指標となりえる (地球温暖化現象のカナリアとなりえる) と主張する先行研究もあり、重要な研究対象とされてきている。一方で、長期スケールの PMC 変動は、約 11 年周期の太陽活動、大規模な火山噴火など、様々な要因によって影響を受けて変動すると考えられている。加えて、冬半球の成層圏突然昇温（Stratospheric Sudden Warming: SSW）に伴う影響など、短期スケールの PMC への影響も考えられている。これらの PMC 変動を捉え、そのメカニズムを解明するためには、長期的な観測と包括的な調査が不可欠である。

ひまわり 8 号は 2015 年 7 月に運用を開始した日本の静止軌道衛星で、Advanced Himawari Imager (AHI) で取得される全球画像を用いた PMC 観測手法が開発された。その観測性能は、Aeronomy of Ice in the Mesosphere (AIM) 衛星搭載 Cloud Image and Particle Size (CIPS) の PMC 観測性能と同程度であると報告されている。ひまわり 8 号/AHI は 2022 年 12 月に運用を終了し、ひまわり 9 号/AHI に交替している。PMC 観測を継続するために、ひまわり 8 号/AHI で開発された判定手法をひまわり 9 号/AHI に適用した。両衛星が同時に PMC を観測した南半球の初夏（2022 年 12 月 1 日から 13 日）のデータを用いて観測性能を比較したところ、PMC 検出判定の結果について 99.8% の一致率を示した。PMC 上端高度については、高度分解能が 1 km であることから± 1 km の誤差を許容すると、98.3% が一致した。以上の結果より、ひまわり 9 号/AHI による PMC 観測は、ひまわり 8 号/AHI と同等の性能を有することを確認した。

本研究では、ひまわり 8 号/9 号によって 2015-2024 年に取得された約 9 年分の PMC データを解析し、その変動について調査する。太陽活動指数のデータや Aura 衛星搭載の Microwave Limb Sounder（MLS）によって観測された大気温度データと水蒸気量データを併用することで、PMC の長期変動について包括的に調査し、その要因について考察を行う。

R005-P04
ポスター 3 ：11/25　PM1/PM2 （13:15-18:15）

A method for atmospheric temperature profile estimation by Himawari-8/AHI limb-sounding

#津田 卓雄 [1)], 安藤 芳晃 [1)], 中川 広務 [2)], Ward William[3)], 堤 雅基 [4,5)], 穂積 裕太 [6,7)], 細川 敬祐 [1)], 村田 健史 [8)]
([1] 電通大, [2] 東北大, [3]University of New Brunswick（UNB), [4] 極地研, [5] 総研大, [6]National Aeronautics and Space Administration（NASA), [7]Catholic University of America（CUA), [8] 情報通信研究機構

A method for atmospheric temperature profile estimation by Himawari-8/AHI limb-sounding

#Takuo Tsuda[1)], Yoshiaki Ando[1)], Hiromu Nakagawa[2)], William Ward[3)], Masaki Tsutsumi[4,5)], Yuta Hozumi[6,7)], Keisuke Hosokawa[1)], Takeshi Murata[8)]
([1]University of Electro-Communications（UEC), [2]Tohoku University, [3]University of New Brunswick（UNB), [4]National Institute of Polar Research（NIPR), [5]Graduate University for Advanced Studies（SOKENDAI), [6]National Aeronautics and Space Administration（NASA), [7]Catholic University of America（CUA), [8]National Institute of Information and Communications Technology（NICT)

Himawari-8 is the Japanese Geostationary Earth Orbit (GEO) meteorological satellite, that is equipped with Advanced Himawari Imager (AHI). Himawari-8/AHI provides full disk images every 10 min in 16 observation bands, including three visible bands: blue (0.47 μ m), green (0.51 μ m), and red (0.64 μ m). These full disk images are normally used as nadir observations mainly for meteorological purposes. On the other hand, the full disk images by Himawari-8/AHI can also provide near-global limb-sounding data as the edges of images. As an example, there are a couple of reports on polar mesospheric cloud (PMC) observations by Himawari-8/AHI limb-sounding.

In the present work, we consider temperature estimations in the middle atmosphere as a further application using Himawari-8/AHI limb-sounding data. In the limb-sounding, Rayleigh scattering of the sunlight can be observed, and thus we can obtain height profiles of line-of-sight (LOS) integrated Rayleigh scattering signals. Extinction effects in the signals can be corrected based on a simulation in the Rayleigh scattering. After that, by inversion methods, such as the Abel transforms, the LOS-integrated signals can be converted into local signals, which could be considered to be proportional to the local number densities of the atmospheric molecules. Then, applying the Rayleigh scattering temperature lidar technique, height profiles of temperature can be derived from height profiles of the local signals under an assumption of the hydrostatic equilibrium. There are a couple of previous works demonstrating this kind of temperature estimation using limb-sounding data from low-Earth-orbit (LEO) satellites. On the other hand, there is no previous example of GEO satellites, which have an advantage in providing continuous observations from a fixed point in space. In the presentation, we will show our results for temperature estimations by Himawari-8/AHI limb-sounding, and discuss the potential of the estimated temperature data.

R005-P05
ポスター 3 ：11/25　PM1/PM2 （13:15-18:15）

高緯度帯観測に特化した夜光雲観測カメラの開発―キルナでの試験観測結果報告

#遠藤 哲歩 [1)], 川上 莉奈 [1)], 増田 歩音 [1)], Peter Dalin[2)], 津田 卓雄 [3)], 鈴木 秀彦 [1)]
([1] 明治大, [2]The Swedish Institute of Space physics, [3] 電通大

Development of NLC Imager for observation in the high latitude region. -The test observation in Kiruna, Sweden

#Akiho Endo[1)], Rina Kawakami[1)], Ayune Masuda[1)], Dalin Peter[2)], Takuo Tsuda[3)], Hidehiko Suzuki[1)]
([1]Meiji university, [2]The Swedish Institute of Space physics, [3]University of Electro-Communications

Noctilucent cloud (NLC) images often contain fine wavy structures ranging from several kilometers to several tens of kilometers. These are thought to reflect local small-scale atmospheric disturbances in the upper mesosphere. Satellite imaging data cannot resolve these fine structures, and thus, ground-based imaging of the NLC is the effective method to study the small-scale disturbances in the upper mesosphere.

NLCs are mainly observed by satellite (e.g. AIM satellite) in the high latitude regions. However, this area is under the influence of the midnight sun, which makes it difficult to detect NLCs from the ground because of the bright background sky condition. Therefore, opportunities for NLC observations from ground in the high latitude regions are limited. On the other hand, there is an opportunity for NLC observation during the period of decline for NLC occurrence even in the high latitude region. In addition, slow variation in the solar elevation angle enables continuous observation of NLCs with similar geometric conditions throughout the night. Thus, there is evident merit in studying the NLC morphology if the opportunity for NLC observation increases in the high-latitude regions.

We have examined the feasibility to overcome this “bright background problem” by developing an optical imager specialized for noctilucent cloud observations [Nakamura et al.,2021]. Noctilucent clouds are known to have a spectral peak at 400-500 nm in their radiance [Lange et al.,2022]. On the other hand, the background spectrum in twilight sky attenuates in wavelengths shorter than 680nm. Therefore, there should be the optimum wavelength band for noctilucent cloud observation which gives a better signal-to-noise ratio (SNR) in shorter wavelength regions. In this study, the most suitable bandpass for NLC observations is proposed based on the ground spectra of the twilight background sky obtained in the polar region. We proposed that an imaging observation by using a cooled CMOS camera equipped with the bandpass filter which has the center wavelength at 371 nm and 40nm bandwidth can give effective SNR (SNR$>$1.80) for NLC even under a bright sky condition which corresponds to a local solar zenith angle ˜91° .

We carried out the test observation of the developed imager in Kiruna, Sweden (N 67.8, E20.4) in August, 2024. As a result, we succeeded in capturing the NLC with the NLC imager, the digital camera and the small spectrometer between 23:00 on 19 August and 1:00 on 20 August (LST). We present the prompt result of this test observation and discuss the performance of the new camera.

R005-P06
ポスター 3 ：11/25　PM1/PM2 （13:15-18:15）

極域中間圏界面領域への高エネルギー粒子降込みに伴う OH 大気光強度変動

#石井 智士 [1)], 鈴木 秀彦 [2)], 田中 良昌 [3,4,5)], 田口 真 [1)], 堤 雅基 [4,5)], 江尻 省 [4,5)], 西山 尚典 [4,5)], 門倉 昭 [3,4,5)]
([1] 立教大, [2] 明治大, [3]ROIS-DS, [4] 国立極地研究所, [5] 総研大

Variation of OH Airglow Intensity Associated with Energetic Particle Precipitation in the Polar Mesopause Region

#Satoshi Ishii[1)], Hidehiko Suzuki[2)], Yoshimasa Tanaka[3,4,5)], Makoto Taguchi[1)], Masaki Tsutsumi[4,5)], Mitsumu K Ejiri[4,5)], Takanori Nishiyama[4,5)], Akira Kadokura[3,4,5)]
([1]Rikkyo University, [2]Meiji university, [3]ROIS-DS, [4]National Institute of Polar Research, [5]SOKENDAI

We conducted ground-based spectral observations of OH (8-4) airglow emitted from the mesopause region at Syowa Station during the winter seasons from February 2008 to October 2019. These observations have been carried out again since 2021. We derived the rotational line intensities of the OH (8-4) band (OH intensity) and the corresponding rotational temperatures. We observed distinct intensity variations occurring over periods ranging from several tens of minutes to several hours. These variations differed from the sinusoidal patterns typically caused by atmospheric gravity waves, which are commonly observed in the mid-latitude regions. Instead, they exhibited sharp peaks. The OH molecule becomes excited through an exothermic reaction between an ozone molecule and atomic hydrogen. It is believed that energetic particle precipitation (EPP) into the upper atmosphere produces NOx and HOx, which subsequently lead to the destruction of ozone molecules. Therefore, the OH intensity is believed to fluctuate due to changes in the atmospheric composition of the polar mesopause associated with EPP. We extracted EPP events from cosmic radio noise absorption data obtained through the imaging riometer observations at Syowa Station. Image data captured by the color digital cameras at Syowa Station were used to check auroral activities. Analysis of these data suggests that some events of the OH intensity variations occurring within a few hours appear to be correlated with the temporal development of auroral substorms. The OH intensity increases before EPP events, decreases afterward, and also decreases when the aurora becomes active.

In this presentation, we will illustrate the temporal variations in OH intensity correlated with the auroral activities detected over Syowa Station from 2016 to 2022. Additionally, we will discuss the effects of EPP in the polar mesopause regions.

R005-P07
ポスター 3 ：11/25　PM1/PM2 （13:15-18:15）

大気光イメージング観測による大気重力波構造を利用した新たな風速決定

#鈴木 臣 [1)], 塩川 和夫 [2)]
([1] 愛知大学, [2] 名大宇地研

A New Approach to Measuring Wind Speed with Airglow Imaging of Atmospheric Gravity Waves

#Shin Suzuki[1)], Kazuo Shiokawa[2)]
([1]Faculty of Regional Policy, Aichi University, [2]Institute for Space-Earth Environmental Research, Nagoya University

In this study, we estimated wind speed near the mesopause by observing atmospheric gravity waves using airglow imaging. According to the linear dispersion relation for gravity waves, the vertical wavelength can be derived from the intrinsic velocity (the difference between the horizontal phase velocity and the background wind) and the horizontal wavelength. In airglow imaging, the horizontal phase velocity and horizontal wavelength of the waves can be directly obtained from the images. Assuming that the same wave structure is observed in airglow emissions at different altitudes, the ratio of horizontal to vertical wavelength can be calculated from the phase difference between the wavefronts observed in two airglow images and the altitude difference of the airglow layers. This allows for the determination of the background wind solely from airglow observations.

On May 2, 2010, clear gravity wave structures were observed with the Shigaraki airglow camera (OMTI: Optical Mesosphere Thermosphere Imager) in OI airglow (altitude: 95 km) and OH airglow (altitude: 85 km). The gravity waves had a horizontal wavelength of 28.6 km and a horizontal phase velocity of 33.9 m/s, propagating northeastward (about 52.4° from north). The calculated tilt of the vertical wavefront, based on the phase difference of the gravity waves observed between the OI and OH airglow images, was about 20.4° , corresponding to an estimated background wind speed of 1.3 m/s in the direction of gravity wave propagation. Simultaneous wind measurements at the OI airglow altitude using a Fabry-Perot interferometer (FPI) indicated a wind speed of 75.5 m/s towards the southeast. When projected along the direction of gravity wave propagation, the FPI wind speed was 1.5 m/s, consistent with the estimated wind speed of 1.3 m/s obtained in this study, thus validating both the results and the estimation algorithm. These findings suggest that airglow imaging is a viable method for estimating winds in the mesopause region, offering a cost-effective alternative to significantly more expensive FPI or meteor radar systems.

R005-P08
ポスター 3 ：11/25　PM1/PM2 （13:15-18:15）

#佐藤 洸太 [1)], 津田 卓雄 [1)], 雁金 沙弥香 [1)], 青木 猛 [1)], 斎藤 徳人 [2)], 野澤 悟徳 [3)], 川端 哲也 [3)], 川原 琢也 [4)], 高橋 透 [5)]
([1] 電通大, [2] 理化学研究所, [3] 名大・宇地研, [4] 信州大・工, [5] 電子航法研

Development of a the time-delayed multi-beam observation method applied to the Tromsoe Na lidar

#Kota Sato[1)], Takuo Tsuda[1)], Sayaka Karigane[1)], Takeshi Aoki[1)], Norihito Saito[2)], Satonori Nozawa[3)], Tetsuya Kawabata[3)], Takuya Kawahara[4)], Toru Takahashi[5)]
([1]The University of Electro-Communications, [2]RIKEN, [3]Institute for Space-Earth Environment Research, Nagoya University, [4]Faculty of Engineering, Shinshu University, [5]Electronic Navigation Research Institute

The sodium (Na) layers are normally distributed at 80-110 km altitudes in the merosphere and lower thermosphere (MLT) region. The Na resonance scattering lidar is a laser remote sensing system that can observe Na layers, which is one of the most powerful tools for measurements for the MLT region. In recent lidar observations, low-density Na layer events have been found at higher altitudes (up to 170 km), which are so-called thermospheric Na. These high-altitude Na evens have the potential to extend the lidar observation to higher altitudes.

The Tromsoe Na lidar was developed in 2009-2010 and is equipped with a laser diode (LD) pumped laser system, which has advantages in stability and lifetime. The Tromsoe Na lidar is capable of simultaneous multi-beam observation in 5 directions by splitting the 4-W power laser into 5 beams. The Inter-Pulse-Period (IPP) of the pulsed laser is 1 msec, and thus the corresponding observation range is 0-150 km. In other words, the Tromsoe Na lidar was originally designed for 80-110 km of Na layers, and it is not enough for observations for thermospheric Na events. To overcome this subject, we propose the time-delayed multi-beam observation method. In this method, we perform a pulse-to-pulse switching in the direction of the laser beam in the multi-beam lidar observations. If we apply this method to the two-direction observations of the Tromsoe Na lidar, the IPP in each direction becomes 2 msec, which corresponds to the range coverage of 0-300 km. To implement this method, we have been working on developments in a system for the pulse-to-pulse switching in the direction of the laser beam, and a data acquisition system, which fits the time-delayed multibeam laser sensing.

In this study, we focus on the feasibility of this pulse-to-pulse switching through fundamental experiments using a commercial galvanometer scanner. In the experiments, the galvanometer scanner was operated at every 1 msec, which is the same as the laser repetition period of the Tromsoe Na lidar system, and the laser beam line was switched in two directions. The two beam-lines were measured by photodetectors and beam profilers. Based on these experiments and the data analysis of experimental results, the switching time and beam pointing accuracy were evaluated. As a result, the switching time was 0.90 msec, which was found to be fast enough for the Tromsoe Na lidar system. The beam pointing accuracy was evaluated by simulations of transmitting beam size and receiving field-of-view (FOV) using geometric calculations. The simulation results indicate that the experimental results of the pointing accuracy are good enough for the Tromsoe Na lidar system. These results suggest that the time-delayed multi-beam method can be applied to the Tromsoe Na lidar using our experimental system equipped with the commercial galvanometer scanner.

In the presentation, we will show the details of the feasibility of the pulse-to-pulse switching, described above. The current status of development in the FPGA-based data acquisition system for the time-delayed multibeam laser sensing will be also reported.

R005-P09
ポスター 3 ：11/25　PM1/PM2 （13:15-18:15）

中間圏・下部熱圏のダイナミクスを高い時間・空間分解能で計測する共鳴散乱 Ca/Ca+ ライダー

#橋本 彩香 [1)], 小林 蒼汰 [1)], 三好 咲也子 [1)], 大鐘 千彰 [1,2)], 桂川 眞幸 [1,2,3)], 江尻 省 [3,4)], 中村 卓司 [3,4)]
([1] 電通大基盤理工, [2] 電通大量子センター, [3] 極地研, [4] 総研大

Ca/Ca+ resonance-scattering lidar for measuring a variety of dynamics in MLT region with a high temporal and spatial resolution

#Ayaka Hashimoto[1)], Sota Kobayashi[1)], Sayako Miyoshi[1)], Chiaki Ohae[1,2)], Masayuki Katsuragawa[1,2,3)], Mitsumu K. Ejiri[3,4)], Takuji Nakamura[3,4)]
([1]Univ. of Electro-Comms. Dep. of Sci., [2]Univ. of Electro-Comms. IAS, [3]Natl. Inst. of Polar Res., [4]The Grad. Univ. for Advanced Studies

Meteoric origin metal atoms and ions which are distributed in the mesosphere and lower thermosphere, are important tracers for understanding the Earth's entire atmosphere, from the surface to the upper thermosphere and ionosphere. We have developed a resonance scattering lidar targeting calcium, which uniquely allows the detection of both neutral atoms and ions from ground-based lidar observations. The laser source of the developed lidar system is based on the injection-locked method, combining high frequency purity (tens of MHz) with high output (>10 mJ). A major feature of this system is its ability to simultaneously oscillate at the resonant wavelengths of calcium atoms (Ca: 422.7918 nm) and calcium ions (Ca^+: 399.4777 nm) using a single laser resonator. Although Ti:sapphire, the laser medium, has a broad wavelength range (660-1100 nm), it is practically limited to about plus/minus 30 nm around specific wavelengths. However, by incorporating precise wavelength dependency into the output mirror of the laser resonator, simultaneous oscillation was achieved at the gain center (786.9554 nm) and at wavelengths more than 50 nm away (845.5836 nm). During test observations with this lidar system, we were able to capture clear signals over an entire night while maintaining high temporal and spatial resolution. This presentation will report on the details of the laser system and the progress of the test observations.

中間圏と下部熱圏に分布する流星起源の金属原子やイオンは、地表から超高層の熱圏・電離圏までを含めた地球大気全体を一つの大気として捉える上で重要なトレーサーである。我々は地上からのライダー観測において唯一、中性原子とイオンの双方を捉えることができるカルシウムをターゲットとする共鳴散乱ライダーを開発した。開発したライダーシステムのレーザー光源は、注入同期法をベースとしているため、高周波数純度（数十 MHz）と高出力（>10 mJ）を兼ね備えている。最大の特徴として、単一のレーザー共振器でカルシウム原子（Ca）とカルシウムイオン（Ca^+）の共鳴波長（Ca：422.7918 nm、Ca^+：399.4777 nm）を同時に発振できることが挙げられる。レーザー媒質であるチタンサファイアは広い波長帯域（660-1100 nm）をもつが、実際には特定の波長を中心とした± 30 nm 程度に制限される。しかしながら、レーザー共振器の出力鏡に正確な波長依存性を持たせることで利得中心（786.9554 nm）とそこから 50 nm 以上も離れた波長域（845.5836 nm）での同時発振を実現した。このライダーシステムを稼働させて行った試験観測では、高い時間分解能と空間分解能を保ちつつ、一晩にわたって明瞭な信号を捉えることができた。本発表では、レーザーシステムの詳細と試験観測の進歩状況について報告する。

R005-P10
ポスター 3 ：11/25　PM1/PM2 （13:15-18:15）

#堤 雅基 [1)], Renkwitz Toralf[2)], Chau Jorge L.[2)], Vierinen Juha[3)]
[(1] 極地研, [(2]Leibniz Institute of Atmospheric Physics, [(3] ノルウェー北極大学

High resolution wind observations based on network MF radar meteor echo measurements

#Masaki Tsutsumi[1)], Toralf Renkwitz[2)], Jorge L. Chau[2)], Juha Vierinen[3)]
[(1]National Institute of Polar Research, [(2]Leibniz Institute of Atmospheric Physics, [(3]The Arctic University of Norway

We have recently redeveloped MF radar meteor wind measurements technique by Tsutsumi and Aso [2005], and have significantly improved its time/spatial resolutions by using the MF system at Syowa Station (69S, 39E), Antarctic. Because the duration of meteor echoes is proportional to the square of the radio wavelength, the duration for MF (2-3 MHz) meteor echoes is more than 100 times longer than that of usual VHF (~30 MHz) meteor echoes, indicating that the actual observation time of MF radar meteor measurement is significantly longer and that a more continuous and dense measurement is possible under a geomagnetically quiet condition where MF radio wave can travel without significant absorption or retardation. The redeveloped technique shows that horizontal wind velocities can be estimated with a highly improved time resolution of about 10 minutes in the height region of 80-115 km, and can even be resolved horizontally every 50 km or so within the 10 minutes at around 90 km, the centroid height of meteor echo distribution. Such resolutions are unprecedentedly high as meteor wind measurements [Tsutsumi et al., JPGU 2023].

This technique is being applied to MF radars at the northern hemisphere, Saura (69N, 16E) and Juliusruh (54N, 13E), routinely operated by Leibniz Institute of Atmospheric Physics. These radars are well equipped with an interferometer capability with 9 and 6 receiver channels, respectively. We have found that existing archived data of these radar systems can be applicable to the meteor echo analyses as those we have done with the Syowa system.

However, one radar measurement can provide only radial wind component, not the tangential component. This means that the vorticity is hard to estimate with one radar system, hindering further statistical analyses of the wind field.

To overcome this limitation we are now trying to conduct common volume meteor measurements using two MF radar systems in the northern high latitude, that is, the Saura system mentioned above and the Tromsoe system (70N, 19E) operated by Arctic University of Norway. Because the Tromsoe system has currently only limited number of receiving antennas and channels, we are planning to add a digital receiver and antenna system to enable all-sky interferometer capability. The Saura and Tromsoe systems are ideally separated to share a common illuminating volume, and are expected to resolve fine time and spatial structures of wind fields, even with much better resolutions than those of recent VHF meteor radar based network measurements.

References

Tsutsumi, M. and Aso, T. MF radar observations of meteors and meteor-derived winds at Syowa (69S, 39E), Antarctica: A comparison with simultaneous spaced antenna winds, Journal of Geophyiscal Research-Atmospheres, 110, doi:10.1029/2005JD005849, 2005.

Tsutsumi, M., Renkwitz, T., and Chau, J. L., High resolution wind observations based on MF radar meteor echo measurements in the northern and southern mid-to-high latitudes, Japanese Geoscience Union Meeting, Makuhari, May 2023.

R005-P11
ポスター 3 ：11/25　PM1/PM2 （13:15-18:15）

#横山 佳弘 [1)], Sergienko Tima[1)], Brändstöm Urban[1)]
[(1] スウェーデン宇宙物理学研究所

ARTIFICIAL BARIUM CLOUDS MOTION AT THREE DIFFERENT ALTITUDES: RESULTS OF THE BROR EXPERIMENT

#Yoshihiro Yokoyama[1)], Tima Sergienko[1)], Urban Brändstöm[1)]
[(1]Swedish Institute for space physics

The Barium Release Optical Rocket (BROR) mission conducted at Esrange, Sweden, on 23rd March 2023, performed barium releases into the earth's atmosphere at eight different altitudes between 130 and 245 km to investigate small-scale electromagnetic phenomena in the auroral ionosphere. In the initial three releases, which were performed at 132 km, 160 km, and 193 km, the motions of both neutral and ionized barium clouds were clearly and distinctively observed by the ground-based optical camera network for as long as a few tens of minutes. The neutral cloud motion represents the thermospheric convection, and the ionized cloud motion is predominantly controlled by the ExB drift motion. In horizontal plain, all neutral clouds resulting from the initial three releases had a strong westward component in their motion with almost constant velocity, while the ionized clouds behaved quite differently from each other; the first ionized cloud moved southwest with a relatively slow speed, the second cloud moved southeast, and the third first directed southwest but afterward changed its direction to southeast, almost parallel to the path of second ionized cloud. In addition, in the second and third cloud motion, several accelerations and declamations were observed.

Although it is said that no large parallel electric field to the magnetic field line exists at the altitude of the aurora ionosphere, the ionized barium cloud resulting from the second release showed considerable difference in vertical motion from the theoretical estimated value considering the contribution of the ExB drift, which implies that there should be some mechanism that make ionized cloud accelerate in the vertical direction.

In this presentation, we will show the detailed motion of clouds resulting from the initial three releases of BROR in relation to the aurora activity and discuss the plausible mechanism that explains the vertical motions of ionized clouds.

R005-P12
ポスター 3 ：11/25　PM1/PM2 （13:15-18:15）

昭和基地におけるミリ波多周波数分光放射計を用いた中間圏/下部熱圏一酸化窒素の時間変動の研究

#水野 亮 [1)], 後藤 宏文 [1)], 長濱 智生 [1)], 中島 拓 [1)], 片岡 龍峰 [2)], 田中 良昌 [2)], 江尻 省 [2)], 冨川 喜弘 [2)], 鈴木 ひかる [3)], 土屋 史紀 [3)], 村田 功 [3)], 笠羽 康正 [3)]
([1] 名大・宇地研, [2] 極地研, [3] 東北大学

A study on temporal variation of NO in the MLT region using a multi-frequencymm-wave spectroradiometer at Syowa Station

#Akira Mizuno[1)], Hirofumi Goto[1)], Tomoo Nagahama[1)], Taku Nakajima[1)], Ryuho Kataoka[2)], Yoshimasa Tanaka[2)], Mitsumu K Ejiri[2)], Yoshihiro Tomikawa[2)], Hikaru Suzuki[3)], Fuminori Tsuchiya[3)], Isao Murata[3)], Yasumasa Kasaba[3)]
([1]Institute for Space-Earth Environmental Research, Nagoya University, [2]National Institute of Polar Research, [3]Tohoku university

Energetic particle precipitation (EPP) onto the polar regions induced by the solar activity ionizes atmospheric molecules, and the subsequent ion chemistry produces NO_x and HO_x, leading to depletion of ozone.

We developed a new multi-frequency spectroradiometer using a waveguide-type frequency multiplexer and broad-band FFT spectrometer to make simultaneous observations of multi-spectral lines including NO and O_3, and we started the routine observation at Syowa Station in July 2022.

Frequency switching method was used for the observations, which is less sensitive to sky inhomogeneities due to cloudlets and able to reduce dead time caused by rotational motion of the switching mirror to change the elevation angles. CO in the 230 GHz band, two ozone spectra (J=$7_{1,7}$-$6_{0,6}$ and J=$10_{2,8}$-$10_{1,9}$) and six NO spectra (F=7/2-5/2, 5/2-3/2, 3/2-1/2 with J=5/2-3/2 for each p_{ul}=-→ + and + → -) in the 250 GHz band have been observing routinely.

In this presentation, we report the data analysis results on temporal variations of NO.

From July 2022 to the end of 2023, there were five geomagnetic storms with Dst indices exceeding -100 nT, and significant increases in NO were observed in four of them. Among these geomagnetic storms, those on March 24 and April 24, 2023, NO increments in the recovery phase were observed in addition to the ordinary increases in the main phase of geomagnetic storms. The increment of NO in the March recovery phase showed good correlation with the arrival of the fast solar wind; in the April case, NO slightly increased for 9 days after the main phase keeping high column density level, but the relationship with fast solar wind was not as clear as in the March case because of the lack of NO data due to bad weather during the arrival of the fast solar wind. For small geomagnetic storms with Dst indices between -50 nT and -100 nT, there are signatures of increase in NO corresponding to geomagnetic storms, but some of them are not clearly significant. Drawing an appropriate baseline for long-term variability is an important issue to assess small NO enhancements related to the small geomagnetic storms.

During a large magnetic storm on May 11, 2024, with Dst index exceeding -400 nT, a large increase of NO by about 1.5 $\times$ 10^{15} cm^{-2} was observed, and this NO level continued for about four days.

In this presentation, we will report the results of detailed analyses of individual case studies including comparisons with satellite data of precipitating flux of energetic particles, and also report the correlation between geomagnetic storms of about -50 nT and NO temporal variation in more detail.

太陽活動に伴い極域に降り込んだ高エネルギー粒子が、大気分子を電離しイオン反応を介して NO_x, HO_x などを生成しオゾンを破壊することが知られている。

我々は、高エネルギー粒子が降り込んだ際の大気側の応答を明らかにするため、2012 年よりミリ波分光放射計を用い、昭和基地上空の一酸化窒素およびオゾンを周波数設定を切り替えながら交互に観測を行ってきた。この状況を打開し複数の分子を同時に観測するために、導波菅型周波数マルチプレクサと広帯域 FFT 分光計を用いた多周波ミリ波分光放射計システムを開発し、2022 年の 7 月から定常観測を開始した。観測には、雲などの空の非一様性の影響を受けにくく高度角の切り替えに伴うデッドタイムの少ない周波数スイッチングを用い、230GHz 帯の CO、250GHz 帯の 2 本のオゾン（J=$7_{1,7}$-$6_{0,6}$ と J=$10_{2,8}$-$10_{1,9}$）および 6 本の NO のスペクトル (J=5/2-3/2 の F=7/2-5/2, 5/2-3/2, 3/2-1/2 の 3 本が p_{ul}=－→＋と＋→－ 2 組で計 6 本) を観測している。2023 年 12 月末までについてはしらせで日本に持ち帰った全観測データをもとに、2024 年については大きな磁気嵐発生時のデータを昭和基地で 1 時間ごとに束ねて日本に転送して解析を進めている。

本発表では 12 時間平均 6 時間観測グリッドの NO 柱密度データを用いて、その時間変動についての解析結果を報告する。

2022 年 7 月から 2023 年末まで Dst 指数が-100nT を超える磁気嵐が 5 回あったが、そのうち 4 回に NO の柱密度に有意な増加が見られた。そのうち、2023 年 3 月 24 日、4 月 24 日の磁気嵐では主相直後の NO の増加に加えて回復相でも NO の増加が見られた。3 月の回復相での NO の増加は高速太陽風の到来と良い対応を示し、4 月の事例では途中悪天候による NO のデータ欠損があるため高速太陽風との関係は明瞭ではないが、高レベルの NO の緩やかな増加が 9 日程度

継続する傾向が見られた。Dst 指数が-50nT から-100nT の間の磁気嵐に対しては、対応する NO 増加の兆候が見られるもののそれらの有意性を議論する上で、長期変動のベースラインをどのように適切に引くかが課題である。

また、2024 年 5 月 11 日の Dst 指数が-400nT を超える大きな磁気嵐の際には $1.5 \times 10^{15}\mathrm{cm}^{-2}$ ほどの NO の大きな増加が確認され、高い NO 柱密度の状態が 4 日間程度継続した。

発表では、これらの個々の事例について降り込み粒子のフラックスの時間変動との比較なども含めた詳細な解析結果を報告するとともに、-50nT 程度の比較的小さい磁気嵐と NO との相関をさらに詳しく調べて報告したい。

R005-P13
ポスター 3 ：11/25　PM1/PM2 （13:15-18:15）

ファブリ・ペロー干渉計による波長 427.8nm のオーロラを通した N2+ アップフローの計測：測定誤差のモデル計算

#菊池 大希 [1)], 塩川 和夫 [1)], 大山 伸一郎 [1)], 小川 泰信 [2)], 栗原 純一 [3)]
([1] 名大 ISEE, [2] 極地研, [3] 情報大

N2+ upflow measurement through auroral 427.8-nm emission by a Fabry-Perot interferometer: Model calculation for measurement errors

#Taiki Kikuchi[1)], Kazuo Shiokawa[1)], Shin ichiro Oyama[1)], Yasunobu Ogawa[2)], Junichi Kurihara[3)]
([1]Institute for Space-Earth Environmental Research, Nagoya University, [2]National Institute of Polar Research, [3]Hokkaido Information Univeristy

Several satellite missions have reported the existence of ionosphere-origin ions in the magnetosphere. The AKEBONO satellite observed that heavy ions, such as nitrogen molecular ions ($N_2{}^+$), were transported to high altitudes in addition to $H^+$and O^+, which are the dominant ions for the upflow (Yau et al., 1993). It is pointed out that $N_2{}^+$ in the polar upper atmosphere are transported upward along the magnetic field line in association with auroral heating. Frictional heating between molecular ions and neutral particles and resonant wave-particle interactions have been considered as possible heating mechanisms. However, obtaining sufficient energy for ion outflow to the magnetosphere solely by the ion frictional heating or resonance heating process, it takes at least 10 times longer than the lifetime of the molecular ions (Peterson et al., 1994). Therefore, the heating mechanisms responsible for transporting these ions into the magnetosphere remain unclear. The Fabry-Perot interferometer (FPI) can be utilized to measure the velocity of a specific ion or neutrals in the lower ionosphere. Then, we tried to measure the upward velocity of the $N_2{}^+$ along the magnetic field line from the observations of auroral 427.8-nm emission using the FPI. This work holds the potential to improve our understanding of ion dynamics in the Earth's upper atmosphere and magnetosphere.

We conducted a campaign observation by an FPI on March 8-14, 2024, at Skibotn, Norway (69.3° N, 20.4° E). By fitting the Gaussian distribution independently to the 14 fringes in the interference images obtained by the FPI, we obtained 14 independent values of the ion velocity and estimated the measurement error from their variation. In general, this variation is considered to be a statistical error due to random measurement noise because we are measuring very weak light. This measurement error decreases when the auroral emission intensity is stronger to produce larger fringe counts. However, even when the same peak counts of fringes were obtained as the FPI measurements at 557.7 nm and 630 nm reported by Shiokawa et al. (2012), we found that the measurement error of 427.8 nm measurement was more than five times larger than those for 557.7 nm and 630.0 nm. One possible cause is that multiple wavelengths of $N_2{}^+$ (1NG) band emission are transmitted through the bandpass filter, resulting in multiple fringes that overlap to form one large fringe. This suggests that (1) errors can occur by fitting the Gaussian function to the overlapped fringes, which have a shape different from that of the Gaussian function, and that (2) differences in the $N_2{}^+$ temperature between the two (north and south) observation points could cause systematic errors because the intensity ratio of the band emission lines (and thus, the fringe shape) varies depending on the $N_2{}^+$ temperature. Therefore, we estimated the magnitude of these measurement errors by performing model calculations for possibilities (1) and (2). In this presentation, we will report the results of the model calculations. We will also report the latest results of the campaign observations at Skibotn, Norway, to be conducted in Sep. - Oct. 2024.

地球磁気圏では電離圏由来のイオンが多くの人工衛星により観測されている。電離圏イオンの主要素であるプロトンや酸素イオンに加えて、窒素分子イオン ($N_2{}^+$) のような比較的重い分子イオンも高高度に輸送されていることが、あけぼの衛星による観測によって報告された (Yau et al., 1993)。窒素分子はオーロラ粒子の降り込みによってイオン化および加熱されて磁力線に沿って上昇することで、磁気圏への流出が発生している可能性が指摘されている。加熱機構としてイオン－中性大気間の摩擦加熱や、電磁波による共振加熱が考えられているが、これらだけでは電離圏を脱出するのに必要なエネルギーを得るための加熱継続時間が、窒素分子イオンの平均寿命より一桁以上長くなってしまい、有効な加熱過程はよくわかっていない。(Peterson et al., 1994)。 ファブリ・ペロー干渉計 (FPI) は、観測対象を限定して低高度電離圏を定常的に観測できる強力な観測装置である。そこで本研究で窒素分子イオンがオーロラ光や太陽光の共鳴散乱として発する波長 427.8 nm 付近の $N_2{}^+$(1NG) の発光を FPI を用いて観測することで、その発光波長のドップラーシフトから、窒素分子イオンの磁力線に沿った上向き速度の計測に挑戦した。この研究は MTI 領域のイオンダイナミクスの理解を前進させる大きなポテンシャルを持っている。

2024 年 3 月 8 日から 14 日にノルウェー・シーボトン (69.3° N,20.4° E) で集中観測を行った。この観測では、FPI で観測された干渉画像にみられる 14 本のフリンジにそれぞれ独立にガウス分布をフィッティングすることにより、14 個の独立な測定量を求めるとともに、それらのばらつきから測定誤差を見積もった。一般的にこのばらつきは、非常に暗い光を計測していることによるランダムな計測ノイズに基づく統計誤差と考えられ、オーロラ発光が強くてフリンジのカウント量が大きいときにはこの測定誤差は小さくなることがわかっている。しかし、同じ装置で波長 557.7 nm、630 nm を観測した Shiokawa et al.,(2012) と同じカウント量のフリンジが得られた時でも、427.8 nm の観測では 5 倍以上の測定誤

差が生まれてしまった。この原因として、N_2^+ (1NG) のバンド発光の複数波長がバンドパスフィルターを透過しており、複数のフリンジが生じ、それらが重なりあって大きな一つのフリンジを形成していることが考えられる。これにより、①ガウス分布と異なる形状のフリンジにガウス分布をフィッティングしていることによる誤差や、②バンド発光の強度比が N_2^+ の温度に依存するため、観測地点の N_2^+ の温度の違いが系統誤差を引き起こす可能性が示唆される。そこで、これら①、②の可能性についてモデル計算を実施することによりこれらの測定誤差の大きさを推定した。本発表ではこのモデル計算の結果について報告する。また、2024 年 9-10 月に計画しているノルウェー・シーボトンでの集中観測の結果についても報告予定である。

R005-P14
ポスター 3 ：11/25　PM1/PM2 （13:15-18:15）

トーチ極側境界と内部で発生する非伝播型・極方向伝播型脈動オーロラの時空間変動

#吹澤 瑞貴 [1)], 小川 泰信 [1)], 田中 良昌 [1)]
[(1] 国立極地研究所

Spatio-temporal variability of non-propagating and poleward propagating pulsating aurora in the torch

#Mizuki Fukizawa[1)], Yasunobu Ogawa[1)], Yoshimasa Tanaka[1)]
[(1]National Institute of Polar Research

Pulsating auroras are quasi-periodic blinking auroras with intervals of a few seconds to a few tens of seconds and occur over a wide area from just after auroral break-up to the day side. Recently, they have been the focus of interest as it has been suggested that relativistic electrons precipitating in the pulsating aurora contribute to the destruction of the mesospheric ozone. Magnetospheric satellites have revealed that the precipitating electrons that generate the pulsating aurora are driven by pitch-angle scattering due to wave-particle interactions near the magnetic equatorial plane. However, satellite observations are unable to separate spatio-temporal variations, and it has not been clarified what produces the difference between pulsating auroras that pulsate with and without propagation. In this study, we aim to identify the type of pulsating auroras and their spatio-temporal variability through cooperative observations by an all-sky camera and the European Incoherent Scattering (EISCAT) radar in the northern part of the Scandinavian Peninsula.

We conducted cooperative observations with the EISCAT VHF radar at Tromso (69.58 degrees N, 19.23 degrees E) and all-sky cameras at Tromso, Skibotn (69.35 degrees N, 18.82 degrees E) and Kilpisjarvi (69.05 degrees N, 20.36 degrees E) on 25-26 March 2023. A non-propagating pulsating aurora was observed when the polar boundary of the torch passed over the EISCAT radar observation point from 01:00-01:10 UT on 26 March 2023. The torch structure then moved to the north, and the interior of the torch passed over the EISCAT radar observation point from 01:30-01:40 UT, and a poleward propagating pulsating aurora was detected. The peak height of the observed electron density was 94-102 km for the non-propagating pulsating aurora and 101-105 km for the propagating pulsating aurora. This suggests that the non-propagating pulsating aurora at the polar boundary of the torch has a higher mean energy of precipitating electrons than the poleward propagating pulsating aurora inside the torch.

The precipitating electrons that cause the pulsating aurora precipitate into the ionosphere due to pitch angle scattering caused by cyclotron resonance with the chorus waves generated near the magnetic equatorial plane. The resonance energy increases as the chorus waves propagate along the magnetic field lines from the magnetic equatorial plane. It has been proposed that a duct structure is necessary for the high magnetic latitude propagation of the chorus wave. In other words, the existence of a duct structure at the polar boundary of the torch is thought to allow chorus waves to propagate along the magnetic field lines and generate non-propagating pulsating auroras in the ionosphere. On the other hand, inside the torch, there is no duct structure, and the chorus waves propagate off the magnetic field lines to the outer L-shell. This results in causing electrons to precipitate into the ionosphere from the inner to the outer L-shell in turn, which may generate a poleward propagating pulsating aurora in the ionosphere. To confirm this hypothesis, we compared the propagation time of the pulsating aurora in the ionosphere with the propagation time of the chorus wave in the magnetosphere and the electron precipitating time. All-sky images showed that it took about 10 seconds for the pulsating aurora to propagate from 67.0 degrees magnetic latitude to 68.3 degrees magnetic latitude. On the other hand, using the Tsyganenko magnetic field model TS05, the time taken for an electron to precipitate from the magnetosphere to the ionosphere was calculated to be t1 = 0.79 s for a 30 keV electron from the magnetic equatorial plane at L = 6.6 to an altitude of 100 km. The time taken for the chorus wave to propagate obliquely from the magnetic equatorial plane at L = 6.6 to L = 7.3, corresponding to a magnetic latitude of 68.3 degrees, was t2 = 0.2 s. The time taken for the electron to precipitate from that point to an altitude of 100 km was t3 = 1.3 s. Therefore, it is difficult to explain the poleward propagation of the pulsating aurora by the oblique propagation of chorus waves since the time difference between the electrons' precipitation at magnetic latitude 67.0 degrees and their precipitation at magnetic latitude 68.3 degrees is t2 + t3 - t1 = 0.64 s, which is much shorter than the propagation time of the pulsating aurora of about 10 s.

Another possible mechanism for the poleward propagation of pulsating auroras is the radial outward propagation of chorus wave excitation regions in the magnetospheric equatorial plane. The geomagnetic data observed by the magnetometer at Tromso with a time resolution of 10 s confirmed geomagnetic pulsations with a period of about 60 s and 100 s. As the period of the geomagnetic pulsation is longer than the propagation period of the pulsating aurora, geomagnetic data with a higher temporal resolution will be analysed to discuss the relationship between the geomagnetic pulsation and the outward propagation of the chorus wave excitation region.

Generalized-Auroral Computer Tomography will also be conducted using auroral images at wavelengths of 427.8 nm and 557.7 nm observed by all-sky cameras at Tromso, Skibotn and Kilpisjarvi to investigate spatiotemporal variations in the 3D

emission intensity and mean energy of the precipitating electrons of the poleward propagating pulsating aurora.

脈動オーロラは数秒から数十秒の間隔で準周期的に点滅するオーロラであり、オーロラブレイクアップ直後から昼間側にかけて広い範囲で発生する。近年、脈動オーロラ中に降下する相対論的電子が中間圏オゾンの破壊に寄与していることが示唆されており注目を集めている。脈動オーロラを発生させる降下電子は磁気赤道面付近の波動-粒子相互作用によるピッチ角散乱によって駆動されることが磁気圏観測衛星により解明されている。しかし、衛星観測では時空間変動の分離が不可能であり、その場で点滅する脈動オーロラと伝搬を繰り返す脈動オーロラの違いが何によって生み出されるかについては解明されていない。そこで本研究では、スカンジナビア半島北部に設置された全天カメラと欧州非干渉散乱(EISCAT) レーダーの協同観測によって脈動オーロラの種類を同定しながらその時空間変動を明らかにすることを目的とする。

我々は、2023 年 3 月 25 – 26 日に Tromsø (69.58° N, 19.23° E) に設置された EISCAT VHF レーダーと Tromsø、Skibotn (69.35° N、18.82° E)、Kilpisjärvi (69.05° N、20.36° E) の 3 地点に設置された全天カメラの協同観測を実施した。そして、2023 年 3 月 26 日 01:00 – 01:10 UT に EISCAT レーダー観測点上をトーチの極側境界が通過し、非伝搬型の脈動オーロラが観測された。その後トーチ構造が北側に移動し、01:30 – 01:40 UT には EISCAT レーダー観測点上をトーチの内部が通過し、極方向伝搬型の脈動オーロラが観測された。このときに観測された電子密度のピーク高度は非伝播型脈動オーロラが 94 – 102 km、伝播型脈動オーロラが 101 – 105 km であった。これはトーチの極側境界の非伝搬型脈動オーロラの方が、トーチの内部の極方向伝搬方脈動オーロラよりも降下電子の平均エネルギーが高いことを示唆する。

脈動オーロラを引き起こす降下電子は磁気赤道面付近で発生したコーラス波とのサイクロトロン共鳴によるピッチ角散乱により電離圏に降下する。そしてその共鳴エネルギーはコーラス波が磁気赤道面から磁力線に沿って伝搬するに従って増加する。コーラス波の高磁気緯度伝搬にはダクト構造が必要であると提案されている。すなわち、トーチの極側境界ではダクト構造が存在してコーラス波が磁力線に沿って伝搬することで電離圏で非伝搬型の脈動オーロラが発生すると考えられる。一方で、トーチの内部ではダクト構造が存在せず、コーラス波が磁力線を外れて外側の L シェルに伝搬することで、電子が内側から外側の L シェルに向かって順番に電離圏に降下することで、電離圏では極方向伝搬する脈動オーロラが発生するのではないか考えられる。この仮説を確かめるために電離圏における脈動オーロラの伝搬時間と磁気圏でのコーラス波の伝搬時間と電子の降下時間を比較した。全天画像を確認したところ脈動オーロラが磁気緯度 67.0 度から 68.3 度まで伝搬にするのにかかる時間は約 10 秒であった。一方で Tsyganenko 磁場モデル TS05 を使用して磁気圏から電離圏までの電子の降下時間を計算したところ、L = 6.6 の磁気赤道面から 30 keV の電子が高度 100 km まで降下するのにかかる時間は t1 = 0.79 秒であった。また、コーラス波が L = 6.6 の磁気赤道面から磁気緯度 68.3 度に対応する L = 7.3 まで斜め伝搬するのにかかる時間 は t2 = 0.2 秒であり、その地点から高度 100 km まで電子が降下するのにかかる時間は t3 = 1.3 秒であった。そのため、磁気緯度 67.0 度に電子が降下してから磁気緯度 68.3 度に電子が降下するまでの時間差は t2 + t3 - t1 = 約 0.6 秒であり、脈動オーロラの伝搬時間約 10 秒に比べて非常に短いため、コーラス波の斜め伝搬で脈動オーロラの極方向伝搬を説明するのは難しい。

その他の脈動オーロラの極方向伝搬メカニズムとして磁気圏赤道面内でのコーラス波励起領域の動径方向外向きの伝搬が考えられる。Tromsøに設置された磁力計により観測された時間分解能 10 秒の地磁気データを確認したところ、約 60 秒周期と約 100 秒周期の地磁気脈動が確認された。この地磁気脈動の周期は脈動オーロラの伝搬周期と比べて長いため、さらに時間分解能の高い地磁気データを解析し、地磁気脈動とコーラス波励起領域の外向き伝搬との関係について議論する予定である。

また、Tromsø, Skibotn, Kilpisjarvi に設置された全天カメラによって観測された波長 427.8 nm、557.7 nm のオーロラ画像を用いて一般化オーロラコンピュータトモグラフィを実施し、極方向伝播型脈動オーロラの 3 次元発光強度や降下電子の平均エネルギーの時空間変動についても調査する予定である。

R005-P15
ポスター 3 ：11/25　PM1/PM2 （13:15-18:15）

STARLINK 衛星を使って超高層大気の変動をどこまで検出できるか

#山本 衛 [1)], 惣宇利 卓弥 [1)]
(1 京大・生存圏研

How are STARLINK satellites useful for monitoring variations in the upper atmosphere?

#Mamoru Yamamoto[1)], Takuya Sori[1)]
(1Research Institute for Sustainable Humanosphere, Kyoto University

The upper atmosphere is located at the top of the Earth's atmosphere, approximately 100 to 1000 km above sea level. It can be considered a transitional region where the Earth's atmosphere changes into the solar-terrestrial system. Part of the atmosphere is ionized by ultraviolet and X-ray radiation from the sun, resulting in weakly ionized plasma, which is why it is also called the ionosphere, but the degree of ionization is only about 0.1 percent at most. Most of the upper atmosphere comprises extremely thin but electrically neutral components. Difficulties in studying the upper atmosphere are often due to a lack of knowledge about this neutral part of the atmosphere. On the other hand, the upper atmosphere is also a region where satellites fly. With the recent progress in space development, the number of artificial satellites launched has drastically increased. In particular, the US company SpaceX has launched many STARLINK satellites for Internet communication. We can find over 6,000 orbital objects named "STARLINK" in the database. This time, we focused on the STARLINK satellite and tried to detect variations in the upper atmosphere from the time variations in the satellite's orbital elements. We are finding variations owing to the increase of the neutral atmosphere in response to recent geomagnetic storms (or, in some cases, not in response to geomagnetic storms). Attempts to detect neutral atmospheric density from satellite orbital variations are not very new. However, we believe that by utilizing a large number of highly homogeneous satellites, we would be able to improve the accuracy and time resolution. In the presentation, we will discuss what can be seen from the data and the possibility of this study.

超高層大気は地球大気の最上部に位置する、おおよそ高度 100〜1000km の範囲であり、地球大気が太陽系空間に変化していく遷移領域ともいえる。太陽からの放射に含まれる紫外線や X 線によって大気の一部が電離した弱電離プラズマとなっており、そのため電離圏とも呼ばれるが、電離度は最大でも 0.1 パーセント程度でしかない。超高層大気の大部分は、超希薄だが電気的に中性な成分である。超高層大気の研究における困難は、この中性大気部分の知識不足に起因することが少なくない。我々の研究分野をさらに発展させるため、中性大気の振る舞いの解明を進める必要性については、異論は少ないと思う。超高層大気は、一方で人工衛星が飛び交う空間でもある。特に最近の宇宙開発の進展にともなって、人工衛星の打ち上げ数はここ 10 年ほどで数十倍に増加してきた。特に、米国の Space X 社がインターネット通信のために多数の STARLINK 衛星を打上げている。今では"STARLINK"と名付けられた軌道物体は 6000 個を超えている。今回、我々は STARLINK 衛星を取り上げて、衛星の軌道要素の時間変動から、超高層大気の変動の検出を試みた。解析を始めたところではあるが、最近の磁気嵐などに呼応した（あるいは、一部では磁気嵐に対応しない）中性大気の増加とみられる変動が見つかっている。衛星軌道の変動から中性大気密度を検出する試みは決して新しいものではないが、同質性の高い多数の衛星を活用することで、その精度や時間分解能を向上させられるのではないだろうか。発表ではデータから何がどう見えるのか、研究対象としての可能性はどうか、などについて議論をする。

R005-P16
ポスター 3 ：11/25　PM1/PM2 （13:15-18:15）

科学衛星あらせによって観測された広帯域静電ノイズ低周波数成分の解析

#伴 太智 [1)], 三宅 壮聡 [1)], 笠原 禎也 [2)]
([1] 富山県大, [2] 金沢大学

Analysis of the Low-Frequency Components of Broadband Electrostatic Noise observed by ARASE

#Ban Taichi[1)], Miyake Taketoshi[1)], Kasahara Yoshiya[2)]
([1]Toyama Prefectural University, [2]Kanazawa University

Various types of low frequency waves are observed by Electric Field Detector (EFD) onboard Arase satellite.In this study, we aimed to extract broadband, noise-like, low-frequency waves, potentially representing the BEN (Broadband Electrostatic Noise) low-frequency component, from the electric field data collected by the Arase scientific satellite's Electric Field Detector (EFD). To address the challenge of large data volumes and avoid subjective bias from manual identification, we employed machine learning to classify the low-frequency waves. Using EFD observation data from a five-year period between 2017 and 2022, we applied the R-CNN method to detect low-frequency wave signals. This approach successfully identified 286 instances of low-frequency wave data, presumed to be BEN, and automatically retrieved their occurrence times, frequency bands, and central frequencies. We then utilized k-means clustering on the obtained spectral image data to classify the waves, resulting in three distinct categories, out of which 204 instances were identified as likely BEN low-frequency wave data. Further analysis was conducted on the extracted data to examine the frequency bands and explore the correlation between BEN low-frequency waves and magnetic fields, aiming to definitively identify the BEN's low-frequency component.

本研究では、科学衛星あらせの電場観測器（EFD）の観測データから BEN 低周波成分と思われる広帯域でノイズ状の低周波波動を抽出し，詳しい発生条件などの解析を行う。抽出にはデータ数の量の問題、また目視による個人の先入観を排除するために、機械学習を利用して低周波波動の分類を行った。2017 年から 2022 年にかけて 5 年間の EFD 観測データから、R-CNN 法を用いて低周波波動の検出を行う。その結果、286 個の BEN と思われる低周波波動データを検出し、それぞれの発生時間と周波数帯、中心周波数を自動的に取得した。次に、得られたスペクトル画像データに k-means 法によるクラスタリングを用いて波動の分類を行った。その結果、低周波波動を 3 種類に分類することができ、その中の 2 種類 204 個が BEN と思われる低周波波動データの取得に成功した。今後は取得したデータから周波数帯域や、BEN 低周波波動と磁場との相関関係について解析を行い、BEN 低周波成分を特定を検討する．

R005-P17
ポスター 3 ：11/25　PM1/PM2 （13:15-18:15）

#木之下 隆弘 [1)], 田口 聡 [1)], 小池 春人 [1)]
([1] 京大理

Spatial-scale dependence of temporal variability in the mesoscale plasma flow in the high-latitude ionosphere

#Takahiro Kinoshita[1)], Satoshi Taguchi[1)], Haruto Koike[1)]
([1]Department of Geophysics, Graduate School of Science, Kyoto University

Plasma convection occurring in the high-latitude ionosphere is thought to be largely determined by the solar wind and magnetospheric conditions for large-scale structures with latitudinal spatial scales exceeding a few hundred kilometers. It is also widely accepted that for small-scale structures, such as those below about 10 km, the variability in the plasma flow is associated with Alfven waves propagating along the magnetic field line. The motivation for this study is to understand what unique properties exist in the mesoscale plasma convection, which is an intermediate scale between the two above-mentioned scales, independent of control by external variables such as IMF and of occurrence of the Alfven wave variations. In this study we focus on mesoscale plasma flow structures with latitudinal spatial scales from 20 km to 250 km, and identify the spatial scale dependent properties in the temporal variability of the mesoscale plasma flow. We analyzed ion drift data from the SWARM satellites, and examined in detail the data obtained during the period when the two of the SWARM satellites were flying in nearly identical orbits with a time difference ranging from about 20 s to 100 s. The mesoscale plasma flow with spatial scales from 20 km to 250 km were classified into three groups depending on the spatial scale. The results obtained for the mesoscale plasma flow in dayside local time are presented to clarify how the characteristic quantities of the time variability of the plasma flow differ between the three mesoscales.

R005-P18
ポスター 3 ：11/25　PM1/PM2 （13:15-18:15）

南極昭和基地大型大気レーダーによる電離圏沿磁力線不規則構造の観測

#香川 大輔 [1)], 橋本 大志 [2)], 西村 耕司 [3)], 齊藤 昭則 [4)]
([1] 京大・理, [2] 極地研, [3] 京大・生存研, [4] 京都大・理・地球物理

Imaging Observation of Ionospheric Field Aligned Irregularities by the PANSY radar at Antarctic Syowa Station

#Daisuke Kagawa[1)], Taishi Hashimoto[2)], Koji Nishimura[3)], Akinori Saito[4)]
([1]Kyoto University Graduate School of Science, [2]National Institute of Polar Research, [3]Kyoto University, RISH, [4]Department of Geophysics, Graduate School of Science, Kyoto University

Program of Antarctic Syowa MST/IS radar (PANSY radar) is the large atmospheric and VHF-band radar located at the Antarctic Syowa Station. This radar has the capability of observing plasma quantities at altitudes of 100-500km using the ionospheric incoherent scatter (IS). In 2015, the PANSY radar performed the first ionospheric IS observation in the Antarctica.This radar also has a frequency of 47MHz, so it can observe the echoes of field aligned irregularities (FAIs) in E-region. If FAIs have a space scale of half wavelength of radio waves, they are coherently backscattered, so the PANSY radar observes the coherent echoes from 3-meter-scale FAIs in E-region. In order to suppress contamination from the FAI echoes during the IS observation, Hashimoto et al.(2019) separated the FAI echoes from IS echoes by the multichannel signal processing technique using the antenna array for observing FAIs (”FAI array”). On the other hand, if we utilize this method to observe FAIs, we can resolve E-region FAIs in detail and measure their motion.

PANSY radar has the array for observing meteors (Meteor array) as well as the FAI array. The FAI array has the degree of freedom only of azimuth angles because its antennas are positioned linearly, whereas the Meteor array can observe FAIs three-dimensionally because the five antennas of the Meteor array are positioned areally. Therefore, we expect that we transmit the radio waves using the FAI array and receive the FAI echoes using the Meteor array.

However, it is expected that the Fourier imaging or the Capon imaging cannot accurately measure the spatial structures caused by the antenna pattern. FAI echoes are generally observed if the conditions that radio waves are perpendicular to FAI are satisfied. The grating lobes, however, are generated because the distance of adjacent antenna are wide, so it is considered that the ”ghosts” are also mistakenly generated in the non-echoing region. Therefore, due to remove their effects and provide the accurate spatial structure, we conducted deconvolution based on Alternating Direction Method of Multipliers; ADMM (Boyd et al.(2011)). This algorithm sequentially estimates the three-dimensional position of FAI which is the local solution in the Convex Optimization Problem, observation of the FAI by the PANSY radar. We can conduct high-resolution FAI imaging observation because the algorithm makes the smaller responses of the non-mainlobe region, such as grating lobes and sidelobes, by conducting iteration process until the estimate converges.

In this presentation, we will introduce the result of the application of imaging method based on the ADMM which can remove the effects of the antenna pattern and conduct accurate and high-resolution FAI observation.

南極昭和基地大型大気レーダー (PANSY レーダー) は、南極の昭和基地に設置されている大型 VHF 帯大気レーダーである。本レーダーは電離圏非干渉性散乱 (IS) を用いて地表 100km から 500km におけるプラズマ物理量を観測することが可能であり、2015 年には南極で初となる電離圏 IS 観測が開始された。また、47MHz の周波数を用いているため、E 領域における沿磁力線不規則構造 (Field Aligned Irregularity; FAI) エコーの観測も可能である。FAI がレーダー電波の半波長の空間スケールを持つとき、電波をコヒーレントに散乱するため、PANSY レーダーでは約 3m スケールの E 領域 FAI からのコヒーレント・エコーを観測できる。Hashimoto et al.(2019) では、この FAI エコーの混入による IS 観測への干渉を除去するため、PANSY レーダーに備えられた FAI 観測用アンテナアレイ（以下、FAI アレイ）を用いた多チャンネル信号処理技術により、異なる角度からの信号（IS エコーと FAI エコー）を分離した。一方、FAI の観測に主眼を置いて同様の手法を用いれば、E 領域 FAI を詳細に解像し、その運動を観測することが可能である。

PANSY レーダーには FAI アレイのほか、流星観測用アレイ（以下、流星アレイ）も備えられている。FAI アレイは直線状に配置されているため自由度は方位角方向にしか持たないのに対し、流星アレイは 5 本のアンテナが面的に配置されているため、流星アレイを用いることで FAI の立体的な位置情報を得ることができる。そのため、本研究では FAI アレイを用いて電波の送信を行い、流星アレイを用いて FAI からの反射波の受信を行うことを想定する。

しかし、観測された FAI に対して Fourier 法や Capon 法等でエコー到来方向を推定すると、アンテナパターンに起因した空間構造の不確定性が発生することが想定される。本来、FAI はレーダー電波と地磁気の磁力線が直交するところで観測されるはずであるが、流星アレイのアンテナ間隔が大きいためにグレーティングローブを生じ、これによってそれ

以外の方位にも偽像が生じると考えられる。そこで、その影響を除去し真の空間構造を推定するために、本研究では交互方向乗数法（Alternating Direction Method of Multipliers; ADMM）（Boyd et al.(2011)）に基づいた処理を行った。本アルゴリズムでは、PANSY レーダーによる FAI 位置推定という凸最適化問題において FAI 位置、つまり局所解を逐次的に推定する。イタレーション処理を収束するまで行うことにより、グレーティングローブやサイドローブといったメインローブ以外の領域における応答値を抑えつつ高分解能な FAI のイメージング観測が可能となる。

本発表では、アンテナの放射パターンの影響を抑圧し FAI の正確かつ高分解能に観測できる、ADMM に基づいたイメージング手法の適用について、シミュレーション結果及び実データに対する初期結果を紹介する。

R005-P19
ポスター 3 ：11/25　PM1/PM2 （13:15-18:15）

#エマヤ ヨナ [1)], 冨川 喜弘 [2)], 西山 尚典 [2)]
([1] 総研大, [2] 極地研

Large amplitude perturbations in equatorward wind surges during the intense geomagnetic storm on 3-4 November 2021

#Jonna Wehmeyer[1)], Yoshihiro Tomikawa[2)], Takanori Nishiyama[2)]
([1]The Graduate University for Advanced Studies, [2]National Institute of Polar Research

During geomagnetic storms energy is injected into the high latitude atmosphere via precipitating particles and strong electric fields that map down from the magnetosphere to the ionosphere. The acceleration of the ionospheric plasma leads to joule heating of the thermosphere producing a steep latitudinal pressure gradient. The resulting strong equatorward winds are important to the middle and low latitude ionospheric response to magnetic storms by driving the ionospheric disturbance dynamo whose effects last on even after the high latitude ionosphere already recovered [Blanc and Richmond, 1980]. Disturbances of those equatorward winds might have a significant impact on the evolution of the disturbance dynamo, but scale and occurrence rate of strong disturbances are poorly understood [e.g. Shiokawa et al., 2003; Zhang et al., 2015; Guo et al., 2018]. In this study we searched for variations in the equatorward surge at mid-latitudes and especially focused on disturbances at which the thermospheric wind reverses and turns northward.

To investigate thermospheric winds we used data from ICON MIGHTI observations, and data from Fabry – Pérot interferometers (FPIs) distributed over north and middle America. For ICON MIGHTI observations we focused on simultaneous observations with FPIs characterized by a radial distance of less than 500 km at 250 km altitude, which is the approximate altitude of red line (630.0 nm) observations made by both instruments. ICON MIGHTI observations are limb observations, which means that the observed winds are integrated over a horizontal line of sight, which makes it difficult to identify local perturbations. Simultaneous observations enable us to combine information about averaged background winds with information about local wind changes, so we can gain a more holistic image of local conditions at FPI observatories. To search for travelling ionospheric disturbances that originate from thermospheric winds we used the GNSS TEC data binned 1 degree longitude by 1 degree latitude at a 5-minute interval.

This poster focuses on a strong geomagnetic event from November 3^{rd} to November 4^{th}, 2021, with a peak Kp index of 8^{-} and a SYM-H low-peak of -118nT on November 4^{th}. The strong storm was preceded by several moderate geomagnetic disturbances beginning on October 27^{th} [Geleta and Mengistu Tsidu, 2024]. Previous studies have analyzed the intensity and effect of the storm induced equatorward surge with wind speeds up to 250 m/s [e.g. Regi et al., 2022; Gan et al., 2024], but FPI observations also show significant perturbations, some with rapid changes in wind speed of over 300 m/s. In this poster we present a detailed analysis of the characteristics of such disturbances.

R005-P20
ポスター 3 ：11/25　PM1/PM2 （13:15-18:15）

日本 3 地点及び TIMED 衛星での長期観測に基づく中間圏・熱圏夜間大気光の磁気嵐に対する応答の研究

#堀田 雄斗 [1)], 塩川 和夫 [1)], 大塚 雄一 [1)], ユエ ジア [2)]
([1] 名大宇地研, [2] ゴダード宇宙飛行センター

Study of the airglow responses to geomagnetic storms based on long-term observations in Japan and by the TIMED satellite

#Yuto Hotta[1)], Kazuo Shiokawa[1)], Yuichi Otsuka[1)], Jia Yue[2)]
([1]Institute for Space-Earth Environmental Research, Nagoya University, [2]NASA Goddard Space Flight Center

We investigated responses of six mesospheric and thermospheric nocturnal airglow intensities (OH, O2, O(557.7nm), Na(589.3nm), O(630.0nm), O(777.4nm)) and OH and O2 rotational temperatures to geomagnetic storms based on superposed epoch analysis using long-term data obtained over Japan. We used airglow data obtained by the Airglow Temperature Photometers (ATPs) of Optical Mesosphere Thermosphere Imagers (OMTIs) at Rikubetsu (RIK) (43.5° N, 143.8° E, 2004.3.15-2023.10.31), Shigaraki (SGK) (34.8° N, 136.1° E, 2010.7.5-2023.10.31), and Sata (STA) (31.0° N, 130.7° E, 2004.1.1-2023.10.31). The responses to 46 storms with minimum Dst values below -100 nT were investigated. We found that the intensity of O2 and O(557.7nm) in the mesosphere and O(630.0nm) and O(777.4nm) in the thermosphere increased within a few days after the start of the storms. No noticeable variations were seen for the OH and O2 rotational temperatures in the mesopause region. One possible reason for the increase of the mesospheric airglow intensity is that the atomic oxygen produced by the dissociation of O2 molecules at high latitude auroral zone are transported to lower latitudes. To confirm this hypothesis, we analyzed data from the Sounding of the Atmosphere using Broadband Emission Radiometry (SABER) for the TIMED satellite and investigated changes in O mixing ratios before and after these storms. As a result, the increase in O mixing ratio was partially observed by the satellite. However, we could not identify propagation of the oxygen atom from high latitudes. We also investigated the OH and O2 volume emission rates and temperature variations obtained from SABER. The lack of noticeable response in OH volume emission rate and temperature in the Japanese latitudes was consistent with the ground-based observations, but the volume emission rate of O2 showed a decreasing trend after storms, which was the opposite of the ground-based observation.

私たちは 6 種類 (OH, O2, O(557.7nm), Na(589.3nm), O(630.0nm), O(777.4nm)) の中間圏、熱圏夜間大気光の強度および、中間圏の OH, O2 の回転温度の磁気嵐に対する応答を、日本で得られた長期データの重ね合わせエポック解析により調べた。大気光データとしては、陸別 (43.5° N, 143.8° E, 2004.3.15-2023.10.31)、信楽 (34.8° N, 136.1° E, 2010.7.5-2023.10.31)、佐多 (31.0° N, 130.7° E, 2004.1.1-2023.10.31) に設置された OMTIs の分光温度フォトメータのデータを用いた。Dst 指数の最小値が-100 nT を下回る 46 例の磁気嵐に対する応答を調べた。主な結果として、中間圏の O2, O(557.7nm) および熱圏の O(630.0nm), O(777.4nm) の強度が磁気嵐開始の数日後に増加した。中間圏の OH と O2 の回転温度については、顕著な変化は見られなかった。中間圏の大気光強度増加の考えられる原因の一つは、高緯度オーロラ帯で O2 の解離により生成された O 原子が低緯度まで伝搬されたということである。この仮説を確かめるために、TIMED 衛星の SABER のデータを解析し、磁気嵐前後の O 混合比の変化を調査した。結果として、O 混合比の部分的な増加は見られたが、高緯度帯からの伝搬は確認できなかった。私たちは SABER から得られる OH, O2 の体積発光率および温度の変化についても調査した。OH の体積発光率および日本付近の緯度帯での温度に顕著な応答がないという結果は地上観測の結果と一致したが、O2 の体積発光率は磁気嵐後に減少を見せる傾向があり、この結果は地上観測の結果に反していた。

R005-P21
ポスター 3 ：11/25　PM1/PM2 （13:15-18:15）

電離圏における HF 帯電波の正常波と異常波の伝搬経路と減衰計算

#阿部 祥大 [1)], 中田 裕之 [1)], 細川 敬祐 [2)], 大矢 浩代 [1)]
([1] 千葉大学大学院融合理工学府, [2] 電気通信大学大学院

Calculation of propagation paths and attenuation of the ordinary and extraordinary modes for HF radio waves in the ionosphere

#Shota Abe[1)], Hiroyuki Nakata[1)], Keisuke Hosokawa[2)], Hiroyo Ohya[1)]
([1]Graduate School of Science and Engineering, Chiba University, [2]Graduate School of Informatics and Engineering, University of Electro-Communications

When radio waves propagate through the ionosphere, the propagation path of the radio wave varies with time since the refractive index is determined by the distribution of electron density. Additionally, the radio waves propagating through the ionosphere are attenuated by collisions between particles. This attenuation arises from the movement of electrons in the plasma, driven by the radio wave's electric field, leading to collisions with neutral particles and ions in the ionosphere. In this study, we have calculated the attenuation of High Frequency (HF) radio waves, considering the effect of the geomagnetic field.

In calculating the propagation paths of radio waves, the ray-tracing method was employed. Considering the effect of geomagnetic field, radio waves in the ionosphere propagate in two modes: Ordinary mode (O-mode) and Extraordinary mode (X-mode). We conducted calculations of attenuation of radio waves propagating through the ionosphere. The primary factor of this attenuation is collisions between particles and can be calculated by integrating the absorption coefficient κ, which is determined by the imaginary part of refractive index, along the propagation path. Assuming the comparison with HF Doppler observations, we calculated the attenuation in the propagation between Chofu(transmitter) and Sugadaira(receiver). The calculation results showed that the attenuation in the ionosphere during the daytime in equinoctial seasons is significant, with the values of about 10 dB for O-mode and 30 dB for the X-mode. The received signal strength was estimated by superimposing the O-mode and X-mode and then compared with that obtained by HF Doppler observations. As a result, a similar trend was obtained between the calculated and observed values with an error of about 8 dB .

In the presentation, detailed examinations of propagation characteristics for each mode and the received signal strength considering ionospheric attenuation, will be discussed.

電波が電離圏中を伝搬する際、電離圏の屈折率は時々刻々と変化する電子密度分布により決まるため、電波の伝搬経路も時刻によって異なる。また、電離圏中を伝搬する電波は粒子同士の衝突により減衰が生じる。これは、電波の電場によってプラズマ中の電子が動き、この電子が電離圏中の中性粒子やイオンに衝突することによって生じる。本研究では地磁気を考慮した HF 帯電波の減衰の計算を行った。

電波の伝搬経路の計算にはレイトレーシング法を使用した。地磁気の影響を考慮すると、電離圏中の電波は 2 つのモード（正常波・異常波、以下それぞれ、O-mode・X-mode）で伝搬する。本研究では電離圏中を伝搬する 2 つのモードの電波の減衰についてそれぞれ計算を行った。この減衰の主な要因は粒子同士の衝突であり、屈折率の虚数部から求められる吸収係数 κ を伝搬経路に沿って積分することによって計算できる。HF ドップラー観測との比較を想定し、送信点を調布、受信点を菅平として送受信点間での電波伝搬の際に生じる減衰の計算を行った。その結果、春秋の昼に減衰が大きく、その減衰量は正常波では約 10dB、異常波では約 30 dB という結果を得た。また、計算により得られた正常波・異常波を合成した際の受信強度を算出し、HF ドップラー観測により得られた受信強度と比較をした。その結果、計算と観測で似た結果が見られ、その差は約 8 dB であった。

発表では、各伝搬モードの伝搬特性を詳細に調べることと電離圏での減衰量から受信強度を算出し、実際に観測された電波の受信強度との比較を行い、その結果について紹介する。

R005-P22
ポスター 3 ：11/25　PM1/PM2 （13:15-18:15）

トモグラフィ手法の改良と準リアルタイム・サービスの開始

#野﨑 太成 [1)], 斎藤 享 [2)], 山本 衛 [3)]
([1 京大 RISH, ([2 電子航法研, ([3 京大・生存圏研

Improvement of GNSS-based Ionospheric Tomography algorithm and the Launch of Near-Real-Time Services

#Taisei Nozaki[1)], Susumu Saito[2)], Mamoru Yamamoto[3)]
([1Research Institute for Sustainable Humanosphere, Kyoto University, ([2Electronic Navigation Research Institute,National Institute of Maritime,Port,and Aviation Technology, ([3Research Institute for Sustainable Humanosphere, Kyoto University

The ionosphere is constantly undergoing variations influenced by solar activity and the lower layers of the atmosphere. The distribution of electron density in the ionosphere leads to phenomena such as reflection, absorption, and delay of radio waves. Particularly, radio waves in the L-band, commonly used in GPS satellite positioning, experience delays in the ionosphere, contributing to positioning errors. Therefore, for the advanced utilization of satellite positioning, it is essential to investigate the effects of the ionosphere.

Ssessanga et al. (2021) developed 3-D ionospheric tomography based on GNSS-TEC observation with ionosonde data assimilation, which can analyze 3-D ionospheric electron density distributions. This analysis realizes near-real time monitoring of the ionosphere and is expected to improve performance in satellite positioning or other applications.

In this study, we improved the observation matrix used in ionosonde data assimilation to make it more physically accurate, and examined how these changes affect distribution of the electron density. Additionally, as a consideration for further improvement, we investigated changes in analysis accuracy when using the previous time step's solution as the background model in a three-dimensional variational method. We discuss performances of the improved ionospheric tomography analysis. Finally, we start operating this tomography in near real-time base within the ENRI system. An overview of the system will be provided in the presentation.

R005-P23
ポスター 3 ：11/25　PM1/PM2 （13:15-18:15）

#PERWITASARI SEPTI[1,2)], 西岡 未知 [1,2)], Hozumi Kornyanat[1,2)]
([1 情報通信研究機構, ([2 情報通信研究機構

Development of SEALION Equatorial Plasma Bubble Alert and Data Portal

#SEPTI PERWITASARI[1,2)], Michi Nishioka[1,2)], Kornyanat Hozumi[1,2)]
([1National Institute of Information and Communications Technology, ([2National Institute of Information and Communications Technology

The equatorial plasma bubble (EPB) is one of the most important features in space weather because of its significant effect on communication and navigation. Therefore, real-time information on the EPB occurrence will be useful in detecting the degradation of radio propagation conditions. SEALION is an ionospheric observation network in Southeast Asia that has been on operation since 2003. SEALION various ionospheric observation (ionosonde, VHF radar, GNSS-receivers) installed across the Southeast Asia; Chiang Mai (18.76° N, 98.93° E), Chumphon (10.72° N, 99.37° E), Phuket (7.90° N, 98.39 ° E), Bac Liu (9.30° N, 105.71° E), Cebu (10.35° N, 123.91° E) and Kototabang (0.20° S, 100.32° E). The real-time alert is currently based on the auto-detection of spread-F from SEALION FMCW ionosonde. The validation has been carried out with the manual scaling data and found to have $>$80% match. Statistical studies of the seasonal and local time variation have also been carried out and compared to previous studies, which have a good agreement. To accommodate data sharing among the ionospheric community, especially in Southeast Asia, we have also developed a data portal to access and download SEALION and ASEAN-IVO data. This portal provides ready-to-use ASCII data as well as data plots. The is planned to provide auto-scaled ionogram parameters (h'Es, h'F, foEs, and foF2), GTEX, ROTI, and S4 data. This system is planned to be open in the 2025 fiscal year. We will discuss the auto-detection development, validation, and future improvement during the presentation.

R005-P24
ポスター 3 ：11/25　PM1/PM2 （13:15-18:15）

CEJ 発生日のプラズマバブル成長イベント検証

#加藤 彰紘 [1)], 吉川 顕正 [2)], 藤本 晶子 [3)]
([1] 九大/理学府/地球惑星科学専攻, [2] 九大/理学研究院, [3] 九工大

An investigation into Plasma Bubble events on CEJ occurrence days in South America

#Akihiro Kato[1)], Akimasa Yoshikawa[2)], Akiko Fujimoto[3)]
([1]Department of Earth and Planetary Sciences, Kyushu University, [2]Department of Earth and Planetary Sciences, Kyushu University, [3]Kyushu Institute of Technology

Plasma bubbles (bubbles) are ionospheric disturbance phenomena that occur in the magnetic equatorial and due to Rayleigh-Taylor instability, so the generation of an

eastward electric field is necessary for their development. In the ionospheric E region, current systems include the Eastward Equatorial electroJet (EEJ) and the westward Counter-ElectroJet (CEJ), which contribute to bubbles through their interaction with the E-F region. Therefore, bubbles occurrence is supposed to be suppressed during counter electrojet (CEJ) events, due to its accompanying westward electric field. However, in South America, bubbles have been observed even during CEJ events, and the relationship between the equatorial jet current structure and plasma bubbles is not yet fully understood.

This study investigates CEJ and bubbles occurrence events in Brazil and Peru using EE-index (EEJ monitoring index), ROTI, Ionosonde data, and the Jicamarca IS radar. Since EEJ/CEJ and bubbles strongly depend on solar activity and seasonal variations, the analysis focuses on equinox when bubbles occurrence frequency is high and is limited to events where bubbles occur continuously for three days. This allows for the examination of CEJ's effects on days with high bubble occurrence rates.

The results show that during solar minimum periods (2008, 2009) and solar maximum periods (2014, 2015), the suppression effect of CEJ is checked, as observed in previous studies. However, during the transition from solar maximum to minimum (2016, 2017), there were unusual events where CEJ and bubbles occurred. Particularly in Peru, after CEJ events, bubbles were observed when the F-layer height (h'F) was below 300 km after a CEJ (EUEL<-20nT), with bubbles in pockets near the magnetic equator (± 10°). This suggests that CEJ influences the growth process of bubbles in terms of latitude/altitude direction rather than their occurrence.

This presentation will discuss the effects of CEJ on plasma bubble , comparing Brazil and Peru on the above results.

プラズマバブル（以下、バブル）は磁気赤道域で発生する電離圏擾乱現象の一つであり、レイリー・テイラー不安定性によって引き起こされ、東西方向の電場が重要な役割を果たす。電離圏 E 領域を流れる電流系として、東向きの赤道ジェット電流（EEJ）と西向きのカウンタージェット電流（CEJ）があり、これらが E-F 領域との相互作用を通じてバブルの発生に寄与している。通常、EEJ の東向き電場はバブルの発生を促進し、CEJ の西向き電場はその発生を抑制する。しかし、南米域において、CEJ 発生時でもバブルが確認されており、赤道ジェット電流構造とプラズマバブルの発生の関係性はまだ十分に理解されていない。

本研究では、ブラジルとペルーにおける CEJ およびバブル発生イベントを、EE-index（EEJ モニタリング指数）、ROTI、イオノゾンデ、ヒカマルカ IS レーダを用いて調査した。EEJ/CEJ およびバブルは太陽活動や季節変動に依存性を持つため、解析期間を磁気圏静穏時・バブル発生頻度が高い春分・秋分に絞り、バブルが連続して 3 日間発生するイベントに限定した。これにより、バブル発生率が高い日の CEJ の影響を調査することができる。

結果として、太陽活動の極小期（2008,2009 年）および極大期（2014,2015 年）には、CEJ による抑制効果が十分に働くことが確認されたが、極大から極小への移行期間である 2012, 2016,2017 年には CEJ とバブルが発生する特異なイベントが見られた。特にペルーでは、CEJ(EUEL<-20nT) 発生後の F 層高度が 300km 未満で、プラズマバブルが磁気赤道近傍（± 10° ）にポケットされるようなイベントが確認され、CEJ がバブルの発生有無ではなく、緯度/高度方向の成長過程に与える影響が考えられる。

本発表では、上記の結果に基づき、ブラジルとペルー域を比較しプラズマバブル発生に関する CEJ の影響について議論する。

R005-P25
ポスター 3 ：11/25　PM1/PM2 （13:15-18:15）

#Topacio Xzann Garry Vincent Miranda[1)], 吉川 顕正 [2)]
(1 九州大学大学院理学府地球惑星科学専攻, (2 九大/理学研究院

An analysis of EEJ meridional currents from ground magnetic data using principal component analysis

#Xzann Topacio[1)], Akimasa Yoshikawa[2)]
(1Department of Earth and Planetary Sciences, Graduate School of Sciences, Kyushu University, (2Department of Earth and Planetary Sciences, Kyushu University

The equatorial electrojet (EEJ) is a prominent eastward geomagnetic current flowing at the magnetic dip equator, primarily recognized through its significant influence on the H (northward) magnetic component as observed from the ground. Besides its main eastward flow, the EEJ encompasses meridional currents flowing perpendicular to the main current, whose effect on the main eastward current is less understood. This study aims to investigate the effects of the meridional currents of the EEJ on the main EEJ itself by employing principal component analysis (PCA) on ground magnetic data, particularly focusing on isolating these effects from other concurrent geomagnetic influences such as the inter-hemispheric field-aligned currents (IHFACs).

Data from several ground magnetic stations near the dip equator was analyzed, revealing that the first principal component of the D (eastward) component predominantly corresponded to the IHFACs and their seasonal variations. The second principal component was preliminarily associated with the meridional currents and the intensification of the EEJ, as well as the global Sq currents. This implies that the meridional currents might be related to the intensification and decay of the EEJ. The longitudinal variation of the second principal component further supports this identification.

These initial findings demonstrate the potential of PCA in distinguishing EEJ-related magnetic signatures from other geomagnetic phenomena in ground-based observation data, offering insights into the three-dimensional structure of the EEJ. Future efforts will aim at validating these results through methodological refinement and comparative analyses with models, satellite data, and other resources.

R005-P26
ポスター 3 ：11/25　PM1/PM2 （13:15-18:15）

HF ドップラー観測と TEC データを用いた 2022 年台風 14 号（NANMADOL）接近・通過に伴う電離圏擾乱の解析

#榎本 陸登 [1)], 中田 裕之 [2)], 細川 敬祐 [3)], 大矢 浩代 [4)]
([1] 千葉大, [2] 千葉大・工, [3] 電通大, [4] 千葉大・工・電気

Analysis of Ionospheric Disturbances Associated with Typhoon NANMADOL Using HF Doppler Observations and TEC Data

#Rikuto Enomoto[1)], Hiroyuki Nakata[2)], Keisuke Hosokawa[3)], Hiroyo Ohya[4)]
([1]Graduate School of Science and Engineering, Chiba University, [2]Graduate School of Science and Engineering, Chiba University, [3]Graduate School of Communication Engineering and Informatics, University of Electro-Communications, [4]Graduate School of Science and Engineering, Chiba University

In recent years, the analysis of ionospheric disturbances associated with typhoons has been advanced by the use of TEC data, and large-scale variations with a period of several ten minutes have been reported (Chou et al., 2017: Song et al., 2019: Wen et al., 2020: Song et al., 2022). However, the ionospheric disturbances of a few seconds to a few minutes have not yet been sufficiently reported. Further analysis of these disturbances would be very important for quantifying the coupling between the ionosphere and the lower atmosphere. In this study, we have analyzed ionospheric disturbances associated with the approaching and passage of Typhoon NANMADOL in 2022 using the HF Doppler sounding system and TEC provided by Softbank Corporation. HF radio waves are usually reflected in the F region of the ionosphere. The reflection height of the radio waves is determined by the vertical profiles of ionospheric electron density. HF Doppler (HFD) sounding system can capture the temporal variations of reflected altitudes as Doppler frequency (Nakata et al., 2021). The temporal resolution of the HFD soundings is 5-10 seconds, which is relatively high compared to other ionospheric observation systems. Ionospheric disturbances associated with typhoons with a period of a few minutes to several tens of minutes have been reported in several cases by this system (Okuzawa et al.,1986: Chum et al., 2018). In addition to the HFD soundings, we used GNSS-TEC data every second obtained by the base stations of Softbank. This makes it possible to observe variations in several tens mHz. There are many reports related to ionospheric disturbances associated with typhoons due to gravity wave modes, whose frequencies correspond to a few mHz. In this study, we analyzed not only the ionospheric disturbances due to the gravity wave mode but those due to the acoustic wave mode, whose frequencies correspond to several tens mHz. Typhoon Nanmadol in 2022 made landfall in Kagoshima Prefecture on September 18, 2022. In this study, we analyzed Doppler shifts acquired at Sugadaira and Iitate observatories using 6055 kHz radio waves transmitted from the Nagara Transmitter operated by the Nikkei Radio. The data period was from 0:00 to 9:00 UT (9:00 to 18:00 JST) from September 17 to 21. Typhoon Nanmadol was closest to the observatories on September 19 to 20. On both days, the Doppler shift variations were more intense than the often days. Then, frequency analysis of the HFD data was utilized, and the intensity of variations for gravity wave mode and acoustic wave mode was analyzed. The intensity of the variation in each mode reached its maximum on different days. As for the gravity wave mode, the intensity mainly depends on the typhoon's power. On the other hand, as for the acoustic wave mode, the distance from the typhoon was also effective. The HFD soundings observe ionospheric variations at an altitude of about 200 km during the daytime, while the TEC data can capture variations at higher altitudes. The dense TEC data provided by SOFTBANK Corp. is a high temporal resolution (1 second). Therefore, it is possible to quantitatively evaluate the ionospheric disturbances depending on typhoons' power and the distances from the observing points. In the presentation, we will report the analysis results of TEC variations associated with Typhoon Nanmadol.

The SoftBank's GNSS observation data used in this study was provided by SoftBank Corp. and ALES Corp. through the framework of the "Consortium to utilize the SoftBank original reference sites for Earth and Space Science".

台風に伴う電離圏擾乱の解析は近年、TEC データを用いることで約数 10 分周期の大きい変動が報告されるようになった (Chou et al., 2017: Song et al., 2019: Wen et al., 2020: Song et al., 2022)。しかし、時間分解能の高い観測が十分でなかったため、台風に伴って発生する数秒から数分周期の電離圏変動の解析は未だ十分に行われていない。これらの解析を進めることは、電離圏と下層大気のカップリングを定量化する上で非常に重要であると考えられる。本研究では、2022 年台風 14 号（アジア名：NANMADOL）接近から通過に伴う電離圏変動について HF ドップラー観測とソフトバンク株式会社の提供する TEC を用いて解析を行った。通常 HF 帯電波は、 F 領域電離圏で反射する。HF ドップラー（HFD）観測システムでは、この性質を利用することで反射高度の時間変化をドップラー周波数として捉えることが可能である (Nakata et al., 2021)。今回用いる観測システムの時間分解能は 5 − 10 秒程度であり、他の電離圏観測システムとしてもかなり高い。数分から数 10 分の台風に伴う電離圏擾乱は本システムでも過去に数例観測されている (Okuzawa et al.,1986: Chum et al., 2018)。今回、HFD 観測に加えて、ソフトバンク社の提供する 1 秒値 GNSS-TEC データを利用した。このことにより、数 10mHz の帯域の変動を観測することが可能となる。台風に伴う変動については、これまでにも大気重力波による変動が報告されてきているが、これは数 mHz の変動である。今回は HFD データおよび TEC データを用いて、大気重力波による変動だけでなく、数 10mHz に相当する音波モードの変動についても解析を進めた。2022 年

台風 14 号は、2022 年 9 月 14 日に日本の南海上で発生し、9 月 18 日に非常に強い勢力で鹿児島県に上陸した。 今回、菅平・飯舘の両観測点において、日経ラジオ社長柄送信所から送信された 6055kHz の電波により取得されたドップラーシフトの解析を行った。データの期間は、9 月 17 日〜21 日の 0:00〜9:00UT（9:00〜18:00JST）である。台風 14 号は、19〜20 日にかけて菅平・飯舘観測点に最も接近したが、この両日にドップラーシフトの変動が激しくなっており、変動強度の上昇がみられた。 そこで、HFD データに対して周波数解析を行い、大気重力波モードと音波モードについてそれぞれのモードの変動強度解析を行ったところ、 変動強度のピークには時間差が見られた。大気重力波モードは台風の発達に伴う変動強度の変化が見られたが、音波モードは台風との距離の影響が非常に強いことが明らかとなった。 HFD データでは、日中では高度約 200km での変動をとらえているが、TEC データでは、より高高度での変動をとらえることが可能である。ソフトバンク株式会社の提供する TEC データは、非常に稠密で 1 秒という高分解能のデータであることから、台風の発達や観測点との距離による電離圏擾乱の変動の特徴を定量的に評価できると考えている。本発表では、このデータを使用した台風 14 号に伴う TEC 変動の解析結果について報告をおこなう予定である。

本研究で使用したソフトバンクの独自基準点の後処理解析用データは、「ソフトバンク独自基準点データの宇宙地球科学用途利活用コンソーシアム」の枠組みを通じて、ソフトバンク株式会社および ALES 株式会社より提供を受けたものを使用しました。

R005-P27
ポスター 3 ：11/25　PM1/PM2 （13:15-18:15）

FMCW による測距機能を備えた HF ドップラー観測システムと、観測事例の紹介

#並木 紀子 [1)], 細川 敬祐 [1)], 野崎 憲朗 [1)], 中田 裕之 [2)], 坂井 純 [1)], 冨澤 一郎 [1)], 有澤 豊志 [1)]
([1] 電気通信大学, [2] 千葉大学, [3] 電通大, [4] 千葉大・工

An HF Doppler Observation System with FMCW-Based Ranging Capabilities: System Design and preliminary observations

#Noriko Namiki[1)], Keisuke Hosokawa[1)], Kenro Nozaki[1)], Hiroyuki Nakata[2)], Jun Sakai[1)], Ichiro Tomizawa[1)], Toyoshi Arisawa[1)]
([1]The University of Electro-Communications, [2]Chiba University, [3]The University of Electro-Communications, [4]Department of Electrical and Electronic Engineering, Graduate School of Engineering, Chiba University

The HF Doppler (HFD) observation system is one of the ionospheric remote sensing techniques that utilizes the reflection of HF radio waves at the ionospheric E and F regions. The ionosphere exhibits various kinds of variations due to energy inflows from the Sun, the Earth's magnetosphere, or from the ground, causing frequency changes, i.e., Doppler shifts, in the reflected waves. These Doppler shifts can be used to visualize the vertical/horizontal movements of the ionosphere phenomena. The HFD observation is considered to be suitable for remote sensing of the lower ionosphere.

One of the HFD observation systems in Japan is based on the experimental station JG2XA, operated by a group at the University of Electro-Communications since 2001. An overview of the HFD project and measurement data is available at "http://gwave.cei.uec.ac.jp/˜hfd/". This HFD observation system includes 11 receiving stations across Japan, and by combining data from multiple receiving stations and frequencies, the distribution and temporal variations of plasma in the lower ionosphere over Japan have been analyzed. For a long time, information from the conventional HFD system (i.e., the Doppler shift data) alone was insufficient to determine the altitude/location of the ionospheric phenomena. As a result, there has been a demand for a function to measure the distance to the reflection points. To fulfill the need for ionospheric distance observations, we have implemented an HFD observation system with ranging capability by transmitting a signal that combines an FMCW signal, which sweeps the frequency band centered on the single transmission frequencies of 5.006 MHz and 8.006 MHz, with the original single-frequency signal. Since 2024, we have been conducting continuous pilot observations in the Kanto area using this system. To achieve FMCW-based ranging at remote locations, we utilized synchronized signals based on 10 MHz and 1 pps from GNSS. Additionally, for heterodyne detection at receiving points, we adopted the same model of function generator as the transmitter and a physical mixer as the local signal source, confirming that the desired distance information can be obtained from the difference in frequency. Along with the development of the FMCW receiver, we also developed a plotting code. Although challenges remain in terms of data storage capacity and the processing load for plotting data due to the higher sampling rate compared to conventional HFD observation data, we successfully visualized high-resolution reflection altitude data using Python.

At the 2023 conference, since the FMCW transmission system was still under development, the demonstration was limited to the theoretical validation of distance measurement using the conventional system. The actual observation of radio wave propagation in physical space and the ability to measure real phenomena remained unknown. In this presentation, we will introduce the design of the FMCW ranging-enabled HFD transmission and reception system currently in operation, and show several characteristic observations of ionospheric E and F region reflections obtained with high spatial and temporal resolution, on the order of several kilometers.

短波ドップラー（HF Doppler: HFD）観測システムは、地上から送信された短波帯の電波が電離圏 E、F 領域反射される性質を利用して、電離圏の擾乱現象をリモートセンシングする手法である。電離圏には、太陽や地球磁気圏、または地上からのエネルギー流入によって、電子密度の変動が絶えず生じており、地上からの送信電波に周波数の変化、すなわちドップラーシフトを印可する。このドップラーシフトによって、電離圏擾乱現象の鉛直運動，水平運動などを観測することができる。HFD 観測システムは、特に、電離圏下部の遠隔観測に適しているとされている。

日本における HFD 観測システムの一つとして、電気通信大学のグループが 2001 年から運用を行っている実験局 JG2XA を用いたネットワーク観測がある。HFD プロジェクトの概要と測定データは" http://gwave.cei.uec.ac.jp/˜hfd/"において公開されている。この HFD 観測システムは、日本国内に受信点が 11 カ所設置されており、複数受信点、複数周波数のデータを組み合わせることによって、電離圏下部に発生する擾乱現象の時空間変動が解析されている。しかし、これまで観測してきたドップラーシフトの空間変化や時間変化のみでは、物理現象の発生高度・領域を特定するための情報が不足しているため、反射点の距離測定機能が求められてきた。電離圏距離観測の要望を実現するために、実験局で取り扱う単一の送信周波数 5.006 MHz および 8.006 MHz を中心とした周波数帯域を掃引する FMCW 方式の信号と、元の単一周波数信号を合成して送信する方法で、測距機能を備えた HFD 観測システムを実現し、2024 年から試験的に関東近隣で継続的な試験観測を続けている。遠隔地点での FMCW 方式による測距を実現させるために、GPS の 10 MHz と 1 pps による同期信号を利用している。加えて、受信点でのヘテロダイン検波のため、現段階ではローカル信号として送信機と同じ型番のファンクションジェネレータとダブルバランスドミキサーを採用し、差周波から目的とする距離情報を得

られることが確認できている。FMCW 方式受信機の開発と共に、データプロット用プログラムの開発にも取り組み、従来の HFD 観測データと比較してサンプリングレートが高いため、保存容量の圧迫やグラフ化処理の重さが課題であるものの、Python を利用して高精度データの可視化に成功した。

2023 年の講演会では、FMCW 方式の送信システムはまだ開発途中であったため、従来システムによる測距理論の実証までにとどまり、実空間を伝搬した電波がどのように観測できるかは確認できていなかった。今回の発表では、現在実際に稼働している FMCW 測距機能を備えた HFD 送受信システムの仕組みを紹介し、数 km の高い距離分解能および時間分解能によって得られた、実測による電離圏 E、F 領域反射のいくつかの特徴的な見え方を紹介する。

R005-P28
ポスター 3 ：11/25　PM1/PM2 （13:15-18:15）

NICT の国内定常観測で得られたイオノグラムの調整について

#西岡 未知 [1)], 津川 卓也 [1)]
[(1] 情報通信研究機構

Ionogram adjustment obtained by NICT's ionosonde observation

#Michi Nishioka[1)], Takuya Tsugawa[1)]
[(1]National Institute of Information and Communications Technology

Ionosonde observation system operated by National Institute of Information and Communications technology (NICT) was replaced to Vertical Incidence Pulsed Ionospheric Radar 2 (VIPIR2) in 2016 and 2017. At the beginning of the replacement, a calibration was done for the ionograms and range bias of 300 μ sec has been removed. NICT has been provided the range adjusted ionograms since then. On the other hand, Teraoka et al (2022 JpGU, 2023 SGEPSS) pointed out that virtual heights of sporadic E-lay (h'Es) decreased around 2017 when the new ionosonde was installed based on an analysis of the manual scaled parameters. The initial range calibration may not be sufficient. Therefore, adjustment was performed again, and the result will be reported in this presentation. We conducted an analysis of direct radio wave transmitted from the antenna and of the calibration signal. We also compared the virtual height with other observational data. It was found that the virtual height was lower by about 25 km. NICT plans to make these corrections and complete the adjustment of the published ionograms by the end of FY 2024.

2016-2017 年頃、NICT のイオノゾンデ観測は、従来の 10C 型から、米国で開発されてきた VIPIR 型にシステム移行した。導入当初、先行機との比較より高さ校正を行い 300 μ秒のバイアスを除去してイオノグラムを作成し、自動/手動読み取りおよびイオノグラムの公開を行ってきた。一方で、手動読取り h'Es の解析結果によると、10C から VIPIR に変わる 2017 年頃に h‘Es が明らかに小さくなっていることが指摘された [寺岡氏, 2022 JpGU]。そこで今回、VIPIR 導入時に行った高さ校正が十分でない可能性があるため、改めてイオノグラムの調整を行った。送信アンテナから送信された直達波の解析、キャリブレーション信号の解析、他観測との比較とを通じて、見かけ高度が約 25 ㎞低く出ていることが分かった。NICT では 2024 年度末までにこれらの補正を行い、公開しているイオノグラムの調整を完了させる予定である。本発表では本調整状況について報告する。

R005-P29
ポスター 3 ：11/25　PM1/PM2 （13:15-18:15）

イオノゾンデ受信機網によるスポラディック E 層の水平構造・水平移動の観測

#古城 侑季 [1)], 齊藤 昭則 [1)], 西岡 未知 [2)], 前野 英生 [2)], 近藤 巧 [2)]
([1] 京都大・理・地球物理, [2] 情報通信研究機構

Horizontal structures and movements of sporadic E layers observed with ionosonde receiver networks

#Yuki Kojo[1)], Akinori Saito[1)], Michi Nishioka[2)], Hideo Maeno[2)], Takumi Kondo[2)]
([1]Department of Geophysics, Graduate School of Science, Kyoto University, [2]National Institute of Information and Communications Technology

スポラディック E（Es）層は、電離圏 E 領域中の高度 100km 付近に突発的に現れるプラズマ密度の高い層である。Es 層の形成と移動には、潮汐風が大きな役割を果たしていることが知られている。この潮汐風の分布は高度に依存するため、Es 層の形成や移動についての物理過程を解明するためには高度の測定が重要である。Es 層の水平方向の運動については、様々な観測手法や数値シミュレーションによって研究がなされてきた。例えば、TEC 観測は観測地点が多いため、Es 層の水平構造や水平移動を捉えるのに優れている。しかし、水平方向と高度方向を合わせた 3 次元的な Es 層観測を定常的におこなうことのできる手法は無く、未だ Es 層の水平移動の物理過程の解明には至っていない。そこで、本研究では、高度の測定が可能なイオノゾンデ観測を用いて Es 層の水平移動を捉えることを試みている。NICT が運営しているイオノゾンデ観測施設は国内に 4 箇所あり、垂直観測と斜入射観測を行っている。しかし、イオノゾンデ同士の距離は一般的な Es 層の水平スケールよりも遠く、Es 層の水平方向の動きを調べるには観測点数が十分でない。そこで、本研究では新しく受信機を設置し、イオノゾンデと受信機による多点観測を行い、日本上空の Es 層の水平構造とその運動を調べた。

受信機は、2023 年 6 月に阿蘇と宮崎に 2 台、2024 年 7 月に別府に 1 台設置をおこなった。これらの受信機は、稚内、国分寺、山川、大宜味にある NICT 電波観測施設のイオノゾンデから送信された高周波の電波を受信する。イオノゾンデから送信された電波は、イオノゾンデと受信機の中間地点上空の Es 層で反射され、中間地点の Es 層の電子密度を測定する。Es 層の密度の相関から、複数の観測点で同じ Es 層が観測されているかどうかを判定し、Es 層の水平移動を計算することができる。新しい受信機は山川のイオノゾンデ周辺に設置されているため、山川イオノゾンデの垂直観測や受信機との斜入射観測を比較することにより、多点観測を行うことができる。本研究では、このイオノゾンデ観測網で取得した観測データを用いて、Es 層の水平構造と水平運動について議論する。

R005-P30
ポスター 3 ：11/25　PM1/PM2 （13:15-18:15）

短波ドップラー観測システムの距離測定機能による 2024 夏期 Es 高度変化の観測

#野崎 憲朗 [1)], 並木 紀子 [1)], 中田 裕之 [2)], 細川 敬祐 [1)]
([1 電通大, ([2 千葉大学

Observation of Ionospheric Es height variation in 2024 summer using range measurement function of HF Doppler observation system

#Kenro Nozaki[1)], Noriko Namiki[1)], Hiroyuki Nakata[2)], Keisuke Hosokawa[1)]
([1]The University of Electro-Communications, ([2]Chiba University

電気通信大学では JG2XA 局 5.006MHz と 8.006MHz の短波ドップラー観測 (HFD) に FMCW 距離測定機能を追加して 2024 年 3 月から調布 − 千葉回線 (大圏距離 50km) で反射高度の高精度、高密度連続観測を継続している。高度分解能は約 1km 時間分解能は 50ms が得られる。

FMCW 距離測定はドップラ観測では得られないゆっくりした高度変化が観測可能であり、夏期のスポラディック E(Es) 連続観測について報告する。中緯度の Es は主として東西風の上下方向のウィンドシアによって生成され、高度 110km 以上では大気潮汐の半日モード、110km〜100km では 1 日モードに乗って下降し、100km 以下に滞留する事がシミュレーションでわかっており、イオノゾンデや IS レーダによって観測されているが、日々の変動が大きい。

日本上空で Es 活動が強くなる 2024 年 5,6,7,8 月の 5.006MHz と 8.006MHz の E 領域反射高度の変化を追尾した。

短波ドップラーの FMCW 距離測定では東京上空の Es が概ね大気潮汐の半日モードに乗って高度 130km 付近から下降するのが観測される。日々変化が大きく、潮汐のモードに乗らないトレースの観現状の FMCW 距離測定機能は HFD に比べて感度が低く、弱い信号強度の Es を追尾しきれず、改良の余地がある。また、斜め反射は高度の増加として観測される。

発表ではイオノゾンデとの比較、ドップラ観測との対応、観測された Es の日々変化等について報告する。

R005-P31
ポスター 3 ：11/25　PM1/PM2 （13:15-18:15）

#細川 敬祐 [1)], 眞弓 奈菜子 [1)], 山本 淳 [2)], 斎藤 享 [3)], 坂井 純 [1)], 高橋 透 [4)], 冨澤 一郎 [1)], 中田 裕之 [5)], 齊藤 昭則 [6)], 篠原 学 [7)], 西岡 未知 [8)], 津川 卓也 [8)], 石井 守 [8,9)]
([1 電通大, [2 海上保安大学校, [3 電子航法研, [4 電子航法研, [5 千葉大・工, [6 京都大・理・地球物理, [7 鹿児島高専, [8 情報通信研究機構, [9 名古屋大学 ISEE

Observations of sporadic E using marine traffic radio waves

#Keisuke Hosokawa[1)], Nanako Mayumi[1)], Atsushi Yamamoto[2)], Susumu Saito[3)], Jun Sakai[1)], Toru Takahashi[4)], Ichiro Tomizawa[1)], Hiroyuki Nakata[5)], Akinori Saito[6)], Manabu Shinohara[7)], Michi Nishioka[8)], Takuya Tsugawa[8)], Mamoru Ishii[8,9)]
([1Graduate School of Informatics and Engineering, University of Electro-Communications, ([2Maritime Science and Technology, Japan Coast Guard Academy, ([3Electronic Navigation Research Institute, ([4Electronic Navigation Research Institute, ([5Chiba University, ([6Department of Geophysics, Graduate School of Science, Kyoto University, ([7National Institute of Technology, Kagoshima College, ([8National Institute of Information and Communications Technology, ([9Institute for Space-Earth Environmenal Research, Nagoya University

The sporadic E layer (Es) is recognized as one of the most outstanding phenomena in the E region. During Es events, the electron density at an altitude of around 100 km is significantly enhanced, often exceeding the maximum electron density in the F region. At mid-latitudes, Es typically occurs during the summer months, with two distinct peaks in occurrence: one during the day and another at night. The increase in critical frequency due to Es can reflect obliquely incident radio waves at frequencies up to 150 MHz. The impact of Es on analog television and FM radio signals within this frequency range has been well documented over the years. Our studies have shown that VHF radio waves used for aeronautical navigation (known as NAV signals in the 108 – 118 MHz range) are also affected by the presence of Es. In particular, it has been statistically confirmed that Es-related anomalous propagation of the NAV signals frequently occurs in Japan during the summer months. Following these findings, routine monitoring of anomalous propagation of NAV signals has been conducted at nine stations across Japan since 2019.

In this study, we propose utilizing another VHF radio wave used for maritime navigation, known as the Automatic Identification System (AIS), for wide-area observations of Es. The AIS operates at a frequency of 162 MHz, which is higher than that of aeronautical radio waves; therefore, only intense Es, with a critical frequency of around 30 MHz, would be detected. Our AIS signal monitoring has been carried out in Kure, Hiroshima. To assess the feasibility of using AIS for Es monitoring, we present two case studies of Es events detected simultaneously by the monitoring observations of NAV and AIS radio waves: one on May 30, 2023, and the other on June 5, 2023. Additionally, we leverage data from multi-constellation GNSS receivers across Japan, particularly the electron density disturbance index ROTI, to further infer the 2D structure and dynamic characteristics of Es over a wide area. In both intervals, the spatial structure of several Es traces, extending from east to west, was clearly visualized, and their speed and direction were estimated. Based on these findings, we discuss the factors that control the motion of Es, through comparison with recent numerical simulations.

R005-P32
ポスター 3 ：11/25　PM1/PM2 （13:15-18:15）

MSTID と Es 層の結合の地方時依存性の統計解析

#渡辺 一唯 [1)], 大塚 雄一 [1)], 新堀 淳樹 [1)], 惣宇利 卓弥 [2)], MAHESWARAN VEERA KUMAR[3)], 西岡 未知 [4)], PERWITASARI SEPTI[4)]
[(1] 名古屋大学宇宙地球環境研究所, [(2] 京大　RISH, [(3]SASTRA Deemed University, [(4] 情報通信研究機構

Statistical Analysis of the Local-time Dependence of the Coupling between MSTID and Es-layer

#Kazui Watanabe[1)], Yuichi Otsuka[1)], Atsuki Shinbori[1)], Takuya Sori[2)], Veera Kumar Maheswaran[3)], Michi Nishioka[4)], SEPTI PERWITASARI[4)]
[(1]Institute for Space-Earth Environmental Research, Nagoya University, [(2]Research Institute for Sustainable Humanosphere, Kyoto University, [(3]SASTRA Deemed University, [(4]National Institute of Information and Communications Technology

Previous studies have suggested that the E and F regions are coupled by electrodynamic forces. In this study, to study the local-time dependence of the coupling between the sporadic-E (Es) layer and Medium-Scale Traveling Ionospheric Disturbances (MSTIDs), ionosonde data obtained at Wakkanai, Kokubunji, Yamagawa, and Okinawa and Total Electron Content (TEC) data obtained from the Global Positioning System (GPS) receivers in Japan between May and August from 1997 to 2022 were examined.

The perturbation components of TEC due to MSTIDs were obtained by subtracting a one-hour moving average from the original TEC data for each pair of satellite and receiver. MSTID activity was defined as a ratio of delta-I / I-bar × 100%, where delta-I: is the standard deviation of TEC perturbations observed in specific regions ranging 4.05° × 4.05° over each ionosonde in one hour, I-bar is the background TEC observed in the same area and during the same period as delta-I.

MSTID activities are averaged between 19-02 LT. The correlation coefficients between the daily variations of nighttime MSTID activities and foEs (the critical frequencies of the Es-layer) at each local time for 1 day before and after the MSTID generations from May to August were calculated. The correlation coefficients between MSTID activities and foEs at a period of about 3 hours on 19-02 LT were highly positive. These correlation coefficients became higher with latitudes. This result indicates that the foEs (Es layer) at this period plays an important role in the strength of the coupling and the generation of MSTIDs, and the coupling is stronger with latitudes. The correlation coefficients between MSTID activities and foEs at 09-14 LT were also positive. This trend is evident in the Kokubunji in years of high solar activity. We can speculate that this result shows that the variation of the semidiurnal tides causing the Es-layer is strong in these conditions.

In the above, the correlation between nightly averaged MSTID activities and hourly foEs was examined. Additionally, the correlation between hourly MSTID activities and hourly foEs was also examined. We found that the correlation coefficients between MSTID activities for the period in which the MSTID occurs and foEs for about an hour before and after were highly positive. This finding indicates that One of the Es-layer or MSTID could affect one hour before and after the other. In addition, this time range tends to extend to two hours in years of high solar activity.

これまでの研究で、E 領域と F 領域は電気力学的な力によって結合していることが示唆されている。本研究では、スポラディック E 層 (Es 層) と中規模進行性電離層擾乱 (MSTID) の結合の地方時依存性を調べるために、1997 年から 2022 年までの 5 月から 8 月にかけて、稚内、国分寺、山川、沖縄で得られたイオノゾンデと、日本の全地球測位システム (GPS) 受信機から得られた全電子量 (TEC) のデータを調べた。

MSTID による TEC の擾乱成分は、衛星と受信機のペアごとに、元の TEC データから 1 時間の移動平均を差し引くことで求めた。MSTID 活動度を、δ I/I ☒× 100% の比として定義した。ここで、δ I は各イオンゾンデ上空で 1 時間に 4.05° × 4.05° の範囲で観測された TEC の摂動の標準偏差、I ☒はδ I と同じ領域で同じ期間に観測された背景 TEC である。

はじめに、MSTID 活動度を 19-02LT で平均した。5 月から 8 月にかけて、夜間の MSTID 活動度の日々変動と、MSTID 発生前後 1 日の各地方時における foEs(Es 層の臨界周波数) との相関係数を求めた。19-02LT の約 3 時間における MSTID 活動度と foEs の相関係数は高い正の値を示した。これらの相関係数は緯度が高いほど高くなった。この結果は、この時期の foEs（Es 層）が MSTID の発生と結合の強さに対して重要な役割を果たしていることと、緯度が高いほど結合が強いことを示している。また、09-14LT の MSTID 活動度と foEs の相関係数も正であった。この傾向は、太陽活動が高い年の国分寺で顕著である。この結果は、このような条件では Es 層を引き起こす半日潮汐の変動が強いことを示していると考えられる。

上記の研究では、夜間平均の MSTID 活動度と 1 時間毎の foEs の相関を調べた。さらに、1 時間毎の MSTID 活動と 1 時間毎の foEs の相関も調べた。その結果、MSTID が発生した時間帯の MSTID 活動度と、その前後約 1 時間の foEs との相関係数は高い正の値を示した。この結果は、Es 層と MSTID の一方が、もう一方の前後 1 時間に影響を及ぼす可能性があることを示している。また、この時間幅は太陽活動が高い年には 2 時間に及ぶ傾向がある。

R005-P33
ポスター 3 ：11/25　PM1/PM2 （13:15-18:15）

イオノゾンデ観測を用いた機械学習によるスポラディック E 層の統計解析と発生予測

#采山 裕紀 [1)], 横山 竜宏 [1)], 劉 鵬 [2)]
([1] 京大生存研, [2] 京大生存研

Statistical analysis and prediction of sporadic E layer by machine learning using ionosonde observation

#Yuki Uneyama[1)], Tatsuhiro Yokoyama[1)], Peng LIU[2)]
([1]Research Institute for Sustainable Humanosphere, Kyoto University, [2]Kyoto University Research Institute for Sustainable Humanosphere

The Sporadic E layer (hereinafter referred to as the Es layer) is a localized ionospheric layer that typically appears at an altitude of approximately 100 km, primarily during the early morning or daytime to evening in the summer. When the Es layer is significantly active, it can reflect VHF-band television and FM radio waves, causing them to unexpectedly reach distant locations. The objective of this research is to predict the occurrence of the Es layer to avoid such radio wave interference.

To observe the Es layer, the echoes of pulse waves emitted with sweeping frequencies are recorded. A graph that plots these echoes by frequency and apparent height is called an ionogram. However, due to the substantial noise contained in ionograms, simple algorithms for automatic detection have not provided sufficient accuracy, and parameter readings have long been conducted manually. Therefore, this study attempts to predict the occurrence of the Es layer by using a machine learning model that performs image analysis.

In this study, a model was used to predict ionogram images by following the sequence of steps described below. Instead of predicting images, the model predicts one-dimensional vectors, so the images are first converted into vectors. The vectors of the past hour (4 data points) are used as inputs to the model to predict the next vector, thereby obtaining the vector 15 minutes ahead. Finally, by reconverting the vector into an image, the image 15 minutes ahead is obtained. Here, it is necessary for the conversion between images and vectors to be reversible. The prediction model for continuous time series vectors utilized a Transformer, commonly used in natural language processing. The Transformer, with its self-attention mechanism, is a model that can prominently learn the impact of input vectors on the vectors to be predicted, and it has been shown to be useful not only in natural language processing but also in image processing and time series prediction. First, the two-dimensional vector of the image was smoothed into a one-dimensional vector. Learning was then conducted by inputting four of these vectors into the Transformer. A dataset of 512 sets of time series data was used, with 80% allocated for training data and the remaining for test data. The results of the trained model showed that the mean SSIM (Structural Similarity Index) between the output image and the correct image was 0.804, indicating that the generated images had a fairly high accuracy based on objective evaluation.

In this study, a model was developed to predict the occurrence of the Es layer using time series image data. While high-accuracy predictions were achieved for data with strong temporal continuity, it was found that predicting the sudden occurrence of the Es layer was difficult. Future considerations for predicting the occurrence of the Es layer include incorporating not only image information but also the probability of Es layer occurrence as input variables, or changing the output to a binary prediction of occurrence or non-occurrence, or to the probability of occurrence. Furthermore, this model could be developed into one that predicts changes in the F layer in ionograms.

スポラディック E 層 (以下, Es 層) とは, 主に夏季の早朝や日中〜夕方にかけて上空約 100km 付近に出現する局所的な電離層のことである. 発生が顕著な時には, VHF 帯を用いているテレビや FM ラジオ電波が反射され, 予想外に遠距離にまで電波が到達してしまうことがある. そのような電波障害を回避するために, Es 層の発生を予測することが本研究の目的である.

Es 層を観測するには, 周波数を掃引して発射したパルス電波のエコーを記録する. それを周波数と見かけの高さでグラフ化したものがイオノグラムである. しかし, イオノグラムに含まれる多数のノイズのため, 単純なアルゴリズムを用いた自動検出では十分な検出精度を出すことができず, 長らく人間の目によりパラメータ読取りが行われていた. そこで, 画像解析を行う機械学習モデルを用いることで, Es 層を学習し発生予測を試みた.

本研究では, 以下に記す一連の流れを行うモデルを用いて, イオノグラム画像の予測を行った. 画像の予測ではなく, 1 次元ベクトルを予測するモデルを利用するため, まず画像をベクトルに変換する. 過去 1 時間 (4 データ) のベクトルを, 次のベクトルを予測するモデルの入力とすることで 15 分後のベクトルが得られる. 最終的にベクトルを画像に加工しなおすことで 15 分後の画像が得られる. ここで, 画像とベクトルは可逆変換を行う必要がある. 時系列的に連続なベクトルの予測モデルは, 自然言語処理で用いられ Transformer を用いた. Transformer は self-Attention という機構により, 入力ベクトルが予測対象のベクトルに与える影響を顕著に学習 できるモデルであり, 自然言語処理だけでなく画像処理や時系列予測にも有用であることが示されている. まず, 2 次元のベクトルである画像に対し, 平滑化を行い 1 次元ベクトルとした. このベクトル 4 つを Transformer に入力して学習を行った. 512 セットの時系列データをデータセットとし, 80% を学習

用データ, 残りをテスト用データとした. 学習を行ったモデルの結果は, 出力画像と正解画像の平均 SSIM(画像類似性評価指数の 1 つ) を算出すると, 0.804 となり客観的評価でかなり良い精度の画像が生成されていることが分かった.

本研究では, 時系列画像データを用いて Es 層の発生予測を行うモデルを作成した. 時間的連続性の高いデータに対しては精度の高い予測が行えたが, 突発的に発生する Es 層の予測は難しいことが分かった. 今後は Es 層の発生を予測するために, 入力変数に画像情報だけでなく Es 層の発生確率を入れることや, 出力を画像ではなく発生の有無の二値とする, あるいは Es 層の発生確率とするなどの工夫が考えられる. また, このモデルはイオノグラムの F 層の変化を予測するモデルとして発展させることも考えられる.

R005-P34
ポスター 3 ：11/25　PM1/PM2 （13:15-18:15）

Es 層形成過程の解明のための観測ロケットによる中性大気・電離大気の同時観測:RIDE キャンペーン

#齊藤 昭則 [1)], 阿部 琢美 [2)], 松岡 彩子 [1)], 石坂 圭吾 [3)], 齋藤 義文 [2)], 田川 雅人 [4)], 熊本 篤志 [5)], 横田 久美子 [4)], 小嶋 浩嗣 [6)], 栗田 怜 [6)], 村田 直史 [7)], 斎藤 享 [8)], 高橋 透 [8)], 西岡 未知 [9)], 細川 敬祐 [10)], 中田 裕之 [11)], 横山 竜宏 [6)], Liu Huixin[12)], 安藤 慧 [9)], 木暮 優 [12)], 西山 尚典 [13)], 坂崎 貴俊 [1)], 江尻 省 [13)]
([1] 京都大学・理, [2]JAXA 宇宙科学研究所, [3] 富山県大学・工, [4] 神戸大学・工, [5] 東北大学・理, [6] 京都大学・生存圏研究所, [7]JAXA, [8] 電子航法研究所, [9] 情報通信研究機構, [10] 電気通信大学・情報理工, [11] 千葉大学・工, [12] 九州大学・理, [13] 国立極地研究所

Measurements of the neutral and ionized atmospheres by a sounding rocket to elucidate the generation process of Es: RIDE campaign

#Akinori Saito[1)], Takumi Abe[2)], Ayako Matsuoka[1)], Keigo Ishisaka[3)], Yoshifumi Saito[2)], Maasto Tagawa[4)], Atsushi Kumamoto[5)], Kumiko Yokota[4)], Hirotsugu Kojima[6)], Satoshi Kurita[6)], Naofumi Murata[7)], Susumu Saito[8)], Toru Takahashi[8)], Michi Nishioka[9)], Keisuke Hosokawa[10)], Hiroyuki Nakata[11)], Tatsuhiro Yokoyama[6)], Huixin Liu[12)], Satoshi Andoh[9)], Masaru Kogure[12)], Takanori Nishiyama[13)], Takatoshi Sakazaki[1)], Mitsumu K Ejiri[13)]
([1]Graduate School of Science, Kyoto University, [2]Institute of Space and Astronautical Science, Japan Aerospace Exploration Agency, [3]Faculty of Engineering, Toyama Prefectural University, [4]Graduate School of Engineering, Kobe University, [5]Graduate School of Science, Tohoku University, [6]Research Institute for Sustainable Humanosphere, Kyoto University, [7]Japan Aerospace Exploration Agency, [8]Electronic Navigation Research Institute, [9]National Institute of Information and Communications Technology, [10]Graduate School of Informatics and Engineering, University of Electro-Communications, [11]Graduate School of Engineering, Chiba University, [12]Graduate School of Science,Kyushu University, [13]National Institute of Polar Research

The Rocket Investigation of Daytime E-region (RIDE) campaign is a direct observation of the neutral and ionized atmospheres, electric field and magnetic field that form the sporadic E(Es) layer at an altitude of 90-130 km. This will be achieved by the S-310-46 rocket from Uchinoura in the summer of 2025. The project has three principal objectives: (1) To elucidate and predict phenomena in which the interaction between the neutral and ionized atmospheres is important by combining in-situ observations from rocket experiments with numerical models and ground-based observations, (2) to complete the in-situ measurement package of the neutral and ionized atmospheres and electromagnetic fields, and (3) to develop human resources for future missions. The target phenomenon is the Es layer, a region of high plasma density that appears at approximately 100 km altitude at mid-latitudes. In order to elucidate the formation and dissipation processes of the Es layer, comprehensive observations of the neutral and ionized atmospheres and electromagnetic field are essential. In this experiment, comprehensive in-situ measurements will be made at an altitude of 90 to 130 km during the ascent and descent of the S-310 rocket at 11:00 to 14:00 local time in summer over Japan. The S-310 rocket is equipped with seven instruments, each designed to measure a specific physical quantity as follows: Neutral mass spectrometer (neutral atmosphere composition), neutral atmosphere density and wind instrument (neutral atmosphere density and velocity), ion drift velocity instrument (ion composition, temperature, and velocity), impedance probe (plasma density), Langmuir probe (electron temperature and plasma density), electric field instrument (electric field), and magnetic field instrument (magnetic field). The data obtained from each instrument are linked by the equation of motion of ions and ionospheric currents, and then compared with the predictions derived from a numerical simulation of the ionosphere. The numerical simulations provide insight into the relationship between the formation of the Es layer and wind/electric field, as well as the relationship between wind and altitude for horizontal migration of the Es layer. In addition to the direct measurements obtained by rockets, ground-based observations will be conducted using an ionosonde receiver network and a GNSS receivers network. Wide-area multi-point observations of aviation VHF radio waves and ship VHF radio waves anomalously reflected by the Es layer will be conducted to elucidate the impact of the Es layer on social systems that utilise radio waves.

Rocket Investigation of Daytime E-region (RIDE) キャンペーンは、2025 年夏期に、内之浦から S-310-46 号機ロケットにより、高度 90-130km においてスポラディック E(Es) 層を形成する中性大気・プラズマ大気・電場・磁場の直接観測を行うものである。その目的は以下の 3 つである　(1) 中性粒子とプラズマの相互作用が重要な現象を、ロケット実験による直接観測と、数値モデル・地上観測との組み合わせで解明し、予測につなげる (2) 中性粒子、プラズマ、電磁場の直接計測パッケージを完成する (3) 将来の展開のための人材育成を行う。対象とする現象は中緯度域高度 100km 付近に出現する高プラズマ密度領域である Es 層である。Es 層の形成・消滅過程の解明にはプラズマと中性大気と電磁場の総合的な観測が不可欠であり、地上観測では両者の同時観測が困難なため、その解明は十分には進んでいない。本実験では、世界的にも Es 層の出現頻度の高い東アジア域に位置する日本南部において、Es 層の出現頻度の高い夏期の地方時 11〜14 時に、S-310 ロケットの上昇時・下降時の高度 90〜130km において、中性大気・プラズマ大気・電場・磁場の総合的な直接計測を行う。ロケット搭載測定器は 7 台であり、それぞれから計測される物理量は以下である：中性大気質量分析器（中

性大気組成)、中性大気密度・風計測装置（中性大気密度・速度)、イオンドリフト速度測定器（イオン組成・温度・速度)、インピーダンスプローブ（プラズマ密度)、ラングミュアプローブ（電子温度・プラズマ密度)、電場観測装置（電場)、磁場観測器（磁場)。これらの物理量の観測によって、電離圏におけるイオン速度を決める要素のほぼ全てが測定でき、Es 層形成に関わるプラズマの集積・発散を支配する物理過程を同定することができる。また、電離圏における電流を決める要素も測定される物理量から導出可能であり、風による電場と電離圏電流の形成の評価を行うこともできる。また、測定される物理量の相互の関係から計測の精度・信頼性の評価も可能である。各観測装置からのデータは、イオンの運動方程式と電離圏電流の関係式により、相互に結びつけられるが、さらに 3 次元電離圏数値シミュレーションによる予測と比較される。数値シミュレーションでは Es 層形成領域と風・電場の関係や Es 層水平移動の風と高度の関係などが予想されており、それらの数値モデルの予想と実際に観測される Es 層の物理量の整合性が議論される。この数値モデルの再現性の直接観測による検証は、数値モデルによる Es 層の発生予測へ発展する上で重要である。これらのロケットによる直接計測に加えて、多地点におけるイオノゾンデ受信機網と GNSS 受信機網による地上観測を実施し、ロケットで観測された Es 層の時間発展と空間的広がりを明らかにする。また、Es 層によって異常反射される航空機航法用 VHF 電波と船舶用 VHF 電波の広域多点観測を行うことで、電波を用いる社会システムに対して Es 層が与える影響の解明も行う。

R005-P35
ポスター 3 ：11/25　PM1/PM2 （13:15-18:15）

観測ロケット搭載ラングミュアプローブデータを用いたウエーク内電子温度分布について

#上田 遥介 [1)], 阿部 琢美 [2)], 齊藤 昭則 [1)]
(1 京都大・理・地球物理, (2 ＪＡＸＡ宇宙科学研究所

Estimation of Wake Effects in Observations Using a Langmuir Probe on a Sounding Rocket

#Yosuke Ueda[1)], Takumi Abe[2)], Akinori Saito[1)]
(1Department of Geophysics, Graduate School of Science, Kyoto University, (2Institute of Space and Astronautical Science, Japan Aerospace Exploration Agency

地球上空の大気や磁場の状態を把握するため、様々な観測ロケットが打ち上げられている。ラングミュアプローブは、数多くの観測ロケットに搭載されている電子温度・密度測定機器である。2024 年夏期の打ち上げが計画されている観測ロケット S-310-46 号機にも搭載される予定であり、スポラディック E 層の電子温度構造の解明などが期待されている。

観測ロケットはスピンしながら高速で移動するため、その移動が観測データに影響を与える。特に、プローブがロケット進行方向の後ろ側 (ウエーク)(図 2 参照) に入ると、観測・推定される電子温度・密度は大きく変化する。この影響を排除するため、プローブがウエークに入った時のデータを除くなどの手法がとられることが多い。そのため、ウエークの影響が及ぶ範囲を正確に決定するとともに、どのような物理過程を経て電子温度・密度推定が生じるのかを理解することが重要である。

2014 年 8 月に打ち上げられた観測ロケット S-520-29 号機搭載ラングミュアプローブの観測データ及び、計算されたロケットの姿勢データを用いて解析を行った。まずはウエークによる影響の発生条件、電子温度に対して与える影響の大きさを推定した。今回、ロケットのアタック角（ロケット機軸と速度ベクトルのなす角度）の大きさとウエークの影響の大きさが関連していると考え、アタック角とラングミュアプローブによる観測データを比較した。

ラングミュアプローブにより推定された電子温度・密度とロケットのスピン位相の関係を調べたところ、ウエークの中では他に比べ電子温度は高く、電子密度は低く推定された。また、電子密度とスピン位相、アタック角の関係を調べたところ、アタック角が大きいほどウエークの影響が大きくなることも読み取れた。

本解析により、アタック角の大きさとウエークによる影響には相関関係があることが示された。また、特定のアタック角において、電子密度が他より高く、電子温度が他より低く推定されるという結果も見られた。ウエークの周りにショックのような形で高電子密度のエリアが形成される現象は他の観測データから報告例があり（Ergun et al., 2021）、そのような構造ができている可能性がある。今後、シミュレーションなどの手法も含め、検討していく。

電離圏イオンドリフト速度測定器の性能評価について

#加藤 千晶 [1)], 阿部 琢美 [2)], 栗田 怜 [3)], 小嶋 浩嗣 [4)]
([1] 京大院工, [2]JAXA 宇宙科学研究所, [3] 京都大学　生存研, [4] 京大

On performance evaluation of ion drift velocity analyzer

#Chiaki Kato[1)], Takumi Abe[2)], Satoshi Kurita[3)], Hirotsugu Kojima[4)]
([1]Graduate School of Engineering, Kyoto University, [2]Institute of Space and Astronautical Science, Japan Aerospace Exploration Agency, [3]Research Institute for Sustainable Humanosphere, Kyoto University, [4]Kyoto university

Understanding of the atmosphere-ionosphere coupling is crucial to reveal ionospheric irregularity phenomena such as medium-scale traveling ionospheric disturbance (MS-TID) and equatorial spread-F. In contrast to many theoretical considerations, few simultaneous observations of plasma and neutrals in the lower ionosphere has been conducted, which results in insufficient demonstration of the ion-neutral　interaction. Rocket observations of the ionosphere is helpful, while it is difficult to directly observe ion-neutral interaction in weakly ionized plasma by ground-based instruments. Under such a background, we are developing ion drift velocity analyzer (IVA), which can measure ion drift velocity and density in the lower E region. IVA will be installed on the rocket so that it can make in-situ measurement of the ionospheric ions along with other scientific instruments for the upper atmosphere. This observation will provide an essential data set which is necessary for a quantitative discussion.

Specification of flight model IVA has been almost determined through performance evaluations of prototype IVA. In order to check the performance of flight model, we conducted laboratory experiments by using the large vacuum chamber at Institute of Space and Astronautical Science, Japan Aerospace Exploration Agency. Ultraviolet plasma source and ion accelerator are placed at the ends of the chamber, which can simulate not only the ionospheric plasma conditions but drifting ions with energy of 1-6 eV. In the experiment, IVA collector current was measured by sweeping the retarding voltage under two kinds of conditions; 1) changing ion energy and 2) changing the sensor's look angle with respect to the ion accelerator. The results clearly indicate the success of producing ions with a drift energy of 1-6 eV.

We can obtain physical quantities of the ions to be measured by evaluating differential value of the ion current with retarding voltage. In our data analysis, ion density and temperature are estimated by using the maximum differentiated current and a gradient of log differentiated current, respectively. In our presentation, we discuss ion drift energy, temperature and density estimated from the retarding potential profile of ion current and the current distribution for various incident angle.

電離圏に特徴的な現象である中規模移動性電離圏擾乱 (MS-TID)、赤道スプレッドＦ等の解明には中性大気とプラズマの相互作用の理解が重要な鍵となる。中性大気とプラズマは粒子衝突を介して相互に影響を及ぼしているが、理論的な予測に対し観測的な検証は不十分である。電離圏のような弱電離プラズマ中での両者の相互作用は地上実験での測定が困難で、宇宙空間で観測する以外に方法は無い。このような背景のもと、我々は電離圏下部においてイオンドリフト速度および密度の推定を可能にするイオンドリフト速度測定器の開発を進めている。中性大気観測の計測器とともに観測ロケットに搭載しデータを取得することで、両者の相互作用の直接同時観測を実現し、定量的議論に必要な数値データを提供することができる。

これまでプロトタイプモデルを使用して測定器の性能を評価してきたが、大半の仕様が固まったため、観測ロケットに搭載するフライトモデルを製作し、プラズマ環境下でデータを取得した。今回の性能評価試験では、真空チェンバー内に、イオン加速装置を用いて電離圏中に存在する低エネルギーの熱的プラズマ環境の生成を試みた。生成した低エネルギーイオンビームのバルクエネルギーは 1~6 eV 程度である。イオン加速装置、イオンドリフト速度測定器を宇宙科学研究所の大型スペースサイエンスチェンバー内に設置し、測定器のリターディング電圧を制御しながら、1. 生成するイオンのエネルギーを変化させた時、2. イオンの運動方向に対して測定器の角度を変化させた時、の条件下で電極により得られる電流値データを取得した。測定結果より、生成されるイオンのエネルギーに応じて電流値グラフから読み取れるイオンのエネルギーが変化していることを確認できた。

現在開発中の測定器は Retarding Potential Analyzer(RPA) と同様にエネルギー積分型であるため、コレクタで収集されるイオン電流値をリターディング電圧で微分することにより、そのエネルギーをもつイオンの数量に関係した物理量が得られる。ここでは微分電流の最大値を用いてイオンの数密度を、微分電流の対数値のリターディング電圧に対する勾配からイオン温度を推定した。本発表では、取得データから推定したイオンのバルクエネルギー、イオン温度、イオン密度と、電流分布の角度依存性について報告する。

R005-P37
ポスター 3 ：11/25　PM1/PM2 （13:15-18:15）

RIDE ロケットキャンペーンに向けた中性質量分析器 NMS の開発

#米田 匡宏 [1)], 齊藤 昭則 [1)], 齋藤 義文 [2)], 川島 桜也 [2)], 笠原 慧 [3)], 横田 勝一郎 [4)]
([1] 京都大学, [2] 宇宙科学研究所, [3] 東京大学, [4] 大阪大学

Development of a Neutral Mass Spectrometer NMS for RIDE Rocket Campaign

#Masahiro Yoneda[1)], Akinori Saito[1)], Yoshifumi Saito[2)], Oya Kawashima[2)], Satoshi Kasahara[3)], Shoichiro Yokota[4)]
([1]Kyoto University, [2]Institute of Space and Astronautical Science, Japan Aerospace Exploration Agency, [3]The University of Tokyo, [4]Osaka University

The RIDE rocket campaign plans to launch S-310-46 sounding rocket from the Uchinoura Space Center in Kagoshima Prefecture in the summer of 2025 to observe the ionospheric E region. The main objective is to reveal how sporadic E layers, the sporadic dense metal ion layers at about 100 km, develop during the daytime. Sporadic E layers at mid-latitudes are mainly caused by the bulk motion of metal ions dragged by the east-west neutral wind and subjected to the Lorentz force, accumulating at the altitude where the east-west wind switches. Since the bulk velocity of ions is affected by the neutral wind through collisions, the collision frequency between ions and neutrals is required in addition to the electric field, magnetic field, and neutral wind to calculate ion velocity from in situ observation data. Since the collision frequency depends on the composition of the neutral atmosphere, it is eventually necessary to measure the composition of the neutral atmosphere.

Therefore, we are developing a neutral mass spectrometer (NMS) to observe neutral atmospheric composition for the RIDE rocket campaign. The instrument is based on a neutral mass spectrometer called TRITON, developed at ISAS/JAXA to detect water in the lunar polar regolith. We have downsized the instrument and developed an antechamber to capture particles for the installation on the sounding rocket. The principle of mass spectrometry is based on time-of-flight mass spectrometry, which uses the fact that the time of flight depends on the mass-to-charge ratio when neutral particles taken from antechamber are ionized, accelerated, and flown a certain distance. In general time-of-flight mass spectrometers, the flight path is often folded back once, but in this system, the flight path is folded back three times to achieve higher mass resolution while maintaining the size. Since the instrument uses high voltage, measurements will be made during the rocket downleg, at an altitude of approximately 130 km to 100 km, to prevent electrical discharges before the beginning of observations.

The manufacture of the instrument has been completed, and the results of performance tests confirm that the mass resolution exceeds 200. This is sufficient to measure atomic oxygen O, molecular oxygen O_2, and molecular nitrogen N_2, which are the main neutral components at the observed altitudes.

In addition, it is possible in principle to limit the mass of particles reaching the detector by turning off the reflected electric field to fold back the flight path of the particles for a certain period in this system. Such a mode may be useful, for example, in detecting the spectrum of NO, which is assumed to be present in an amount less than 1% of that of the major component, separated from the spectrum of N_2, which has a relatively close mass. In this presentation, in addition to the test results on mass resolution and sensitivity, we will also report on the tests to validate this mass-limiting mode.

RIDE ロケットキャンペーンでは、2025 年夏に鹿児島県内之浦宇宙空間観測所から観測ロケット S-310-46 号機を打ち上げ、電離圏 E 領域を観測する予定である。特に、高度約 100km で散発的に発生する高密度金属イオン層であるスポラディック E 層が昼間にどのように発達するのかを解明することを目的としている。中緯度におけるスポラディック E 層は金属イオンが東西方向の中性風に引きずられてバルク運動してローレンツ力を受けることで、東西風が切り替わる高度に集積することで生じる。イオンのバルク速度は衝突を介して中性風の影響を受けることから、その場観測データからイオン速度を算出するためには電場、磁場、中性風に加えてイオンと中性の衝突周波数が必要となる。そして、衝突周波数は中性大気の組成に依存することから、最終的には中性大気組成の計測が必要となる。

そこで、本研究では RIDE ロケットキャンペーンに向けて中性大気組成を観測するための中性質量分析器 NMS（Neutral Mass Spectrometer）の開発を進めている。開発中の装置は宇宙科学研究所にて月極域レゴリス中の水を計測するために開発が進められている中性質量分析器 TRITON を基にしており、観測ロケット搭載に向けて装置の小型化と粒子を取り込むための前室部の開発を新たに行った。質量分析の原理として、前室部から取り入れた中性粒子をイオン化して加速し、一定の距離を飛行させた際の飛行時間が質量電荷比に依存することを利用する飛行時間型質量分析を採用している。一般的な飛行時間型質量分析器では飛行経路を 1 回折り返すことが多いが、本装置では飛行経路を 3 回折り返すことで大きさを維持したままより高い質量分解能を達成することが可能となっている。装置には高圧を用いることから、観測開始前の放電を防ぐために計測はロケットが下降する期間、高度約 130km から 100km にかけて行われる予定である。

装置の製造は完了しており、性能試験の結果から質量分解能は 200 を超えていることが確認されている。これは観測高度で主要な中性成分である原子状酸素 O や酸素分子 O_2、窒素分子 N_2 を計測する上で十分な数値である。

また、本装置では粒子の飛行経路を折り返すための反射電場をある期間だけ OFF とすることで、検出器に到達する粒子の質量を制限することが原理上可能となっている。このようなモードは、例えば主要成分と比較して 1% 以下の量しか存在しないと想定される NO のスペクトルを比較的質量が近い N_2 のスペクトルから分離して検出する場合等に有用であると考えられる。本発表では質量分解能や感度に関する試験結果に加えて、この質量制限モードを検証するための試験についても報告する。

R005-P38
ポスター 3 ：11/25　PM1/PM2 （13:15-18:15）

基本波型直交フラックスゲート磁力計の電子回路の小型化

#東村 敢 [1)], 村田 直史 [2)], 松岡 彩子 [3)], 栗田 怜 [4)], 小嶋 浩嗣 [5)]
([1] 京大, ([2]JAXA, ([3] 京都大学, ([4] 京都大学 生存研, ([5] 京大

Analog circuit chip dedicated to the Fundamental Mode Orthogonal Fluxgate Magnetometers

#Kan Higashimura[1)], Naofumi Murata[2)], Ayako Matsuoka[3)], Satoshi Kurita[4)], Hirotsugu Kojima[5)]
([1]Kyoto University Research Institute for Sustainable Humanosphere, ([2]Japan Aerospace Exploration Agency, ([3]Graduate School of Science, Kyoto University, ([4]Research Institute for Sustainable Humanosphere, Kyoto University, ([5]Kyoto university

The Fundamental Mode Orthogonal Fluxgate Magnetometers (FM-OFG) have a unique property in that the part of the sensor is much smaller than that of conventional fluxgates. The conventional “parallel” fluxgate magnetometers have contributed to many space missions. However, the sensor structure is complex, requiring a sufficiently large core to achieve a low noise level. Hence, it is unsuitable for the miniaturization of the instrument, considering the use of micro-/nanosatellites. FM-OFG is a new type of fluxgate magnetometer whose sensor consists of a pair of amorphous wire core and a pick-up/feedback coil. The FM-OFG sensor can be much lighter at about 1 gram per axis.

Miniaturizing electronic circuits is crucial to making the whole FM-OFG system smaller and lighter so that it can make best of its small sensor. An analog chip dedicated to the FM-OFG using a so-called ASIC (Application Specific Integrated Circuit) has been developed from this aspect. Its size is a few tens of millimeters square, and it contains the circuits that pick up signals from the sensor head and retrieve waveforms of detected magnetic fields based on a feedback configuration. As the first attempt, we developed the analog chip used for the FM-OFG onboard the sounding rocket called RIDE (Rocket Investigation of Daytime sporadic-E). The science target of the rocket campaign is to investigate the sporadic E layer in the ionosphere. The onboard instrument with our chip has been already developed, and we confirmed the instrument based on our chip shows performance enough to meet the requirements of this rocket experiment.

The remaining issue with the analog chip is its noise level. To expand the use of the chip in other space missions, the noise level should be lower by a factor of three. The noise in the low-frequency range is intrinsic to the MOS device. We are working to design a new ASIC chip to reduce the noise.

In the present paper, we introduce the design of the analog chip and show the performance that meets the specifications for the rocket experiment. We also discuss improving the design to reduce the chip’s noise.

R005-P39
ポスター 3 ：11/25　PM1/PM2 （13:15-18:15）

#熊本 篤志 [1)], 小嶋 浩嗣 [2)], 石坂 圭吾 [3)], 頭師 孝拓 [4)], 栗田 怜 [2)], 加藤 雄人 [1)], 阿部 琢美 [5)], 齋藤 義文 [5)]
([1] 東北大・理・地球物理, ([2] 京大, ([3] 富山県大・工, ([4] 奈良高専, ([5] ＪＡＸＡ宇宙科学研究所

Wideband impedance probe for measurements of lower hybrid resonance (LHR) in the ionosphere - Lessons Learned in SS-520-3

#Atsushi Kumamoto[1)], Hirotsugu Kojima[2)], Keigo Ishisaka[3)], Takahiro Zushi[4)], Satoshi Kurita[2)], Yuto Katoh[1)], Takumi Abe[5)], Yoshifumi Saito[5)]
([1]Department of Geophysics, Graduate School of Science, Tohoku University, ([2]Kyoto university, ([3]Faculty of Engineering, Toyama Prefectural University, ([4]National Institute of Technology (KOSEN), Nara College, ([5]Institute of Space and Astronautical Science, Japan Aerospace Exploration Agency

Wideband impedance probe (WNEI) was installed on SS-520-3 (launched in 2021) for determination of the ionospheric ion composition based on lower hybrid resonance (LHR) frequency. Design of the wide band impedance probe was based on that of the impedance probe for electron number density measurement (NEI) for the previous sounding rockets. The operation frequency range of WNEI was extended below up to 1 kHz in order to measure the probe capacitance decrease at LHR frequency around several kHz in the ionosphere. Determination of ion components using impedance probe operated around LHR frequency was already proposed by Miller and Schulte (1969). However, there was no report of actual applications of the wideband impedance probe to the ionospheric observations. The purpose of this study is to summarize the issues in application of WNEI to the ionospheric observations found in SS-520-3.

The WNEI was operated successfully during the flight of SS-520-3. The probe capacitance in a frequency range from 1 to 11 kHz could be measured in an altitude range from 160 to 740 km. However, in the analysis, the following issues were needed to be considered:

(i) Since the capacitance of the probe and surrounding ion sheath with a length of 1 m is about 30 pF, their impedance exceed 1 Meg ohm below 5.3 kHz. The signal level applied to WNEI capacitor bridge is several V. The currents in the loads of the bridge are therefore estimated to be less than several micro A below 5.3 kHz, which has little margin to the level of the surrounding noises. So, the datasets below 5.3 kHz are excluded from the analysis in this study.

(ii) Even above 5.3 kHz, the interference of the noises with odd harmonics of 156.5 Hz probably from the instruments installed on the rocket were also found in the WNEI data. The noises were also found in the prelaunch tests on the ground while their level was much smaller. They are more apparent when the probe was in the rocket wake. It is because the signal level proportional to the probe (with sheath) capacitance decrease in the rocket wake while the interfered noise level is constant.

(iii) In addition to the interfered noises, we could find another components of probe capacitance decrease with large deviation. They can be identified with criteria as probe capacitor decrease with a deviation of 2.5 sigma, where the sigma is standard deviation of probe capacitance in each profile with respect to the running average. They are around 7.6 kHz at an altitude around 730 km (400-500 s from the launch), and around 8.2 kHz at an altitude around 710 km (550-600 s from the launch), respectively, which are similar LHR frequency estimated from NEI data (electron number density) and IRI-2016 model with assuming the abundance of heavy ion as O+ is 95 and 90%, respectively. The reason why the large probe capacitance decrease can be found only in the wake is because the collision frequency of electrons with ions decrease in the rocket wake, which results in the probe capacitance decrease at LHR frequency with high Q value.

The future plans for solving the issues of WNEI found in SS-520-3 will be discussed in the presentation.

R005-P40
ポスター 3 ：11/25　PM1/PM2 （13:15-18:15）

#Qiu Lihui[1)], Liu Huixin[1)]
(1 九大

Modelling of three-dimensional structure and dynamics of the large-scale sporadic E layers over East Asia

#Lihui Qiu[1)], Huixin Liu[1)]
(1Kyushu University

Sporadic E (Es) layers are thin layers of concentrated metallic ions in the mesosphere and lower thermosphere (MLT) region. Their formation and evolution are deeply modulated by atmospheric dynamics, indicating that they can serve as indicators of atmosphere-ionosphere coupling processes. Currently, the three-dimensional (3-D) Es layer structure and evolution process have not yet been fully understood. In this study, we investigated the structural and dynamic characteristics of the large-scale Es layers over East Asia by using a 3-D Es layer numerical model driven by neutral winds from the Whole Atmosphere Community Climate Model with thermosphere and ionosphere eXtension model (WACCM-X). The simulation results show that the Es layer is a tilted structure rather than a narrow flat blanket. In addition, the Es layers mainly occur in the 3-D spatial position of the convergent vertical wind shear. The apparent velocity (˜300-400 m/s) of Es layers is mostly westward and northward, which is different from the ion drift velocity (˜100 m/s). This indicates that Es layer can develop rapidly over a large area rather than drifting gradually. This study systematically analyzed the physics of the 3-D Es layer, which can be helpful for understanding the observations recorded by different instruments, such as satellites and ground-based receiver networks.

R005-P41
ポスター 3 ：11/25　PM1/PM2 （13:15-18:15）

#安藤 慧 [1)], 齊藤 昭則 [2)], 品川 裕之 [3)]
([1]NICT, [2] 京都大・理・地球物理, [3] 九州大学国際宇宙惑星環境研究センター

The role of metal ion transport in the sporadic E layer occurrence in the Summer Southern Hemisphere

#Satoshi Andoh[1)], Akinori Saito[2)], Hiroyuki Shinagawa[3)]
([1]National Institute of Information and Communications Technology, [2]Department of Geophysics, Graduate School of Science, Kyoto University, [3]International Research Center for Space and Planetary Environmental Science, Kyushu University

The first simulation on the sporadic E (Es) occurrence distribution at middle and low latitudes in the summer Southern Hemisphere is presented. The Es distribution in the summer Southern Hemisphere, which shows a salient decrease around Southern Africa, has been considered owing to the geomagnetic configuration. Herein, we conducted Es simulations for the summer southern middle and low latitudes and for the first time reproduced the Es distribution. The geomagnetic westward wind region around 100–105 km altitudes corresponds well to the Es distribution in the summer Southern Hemisphere. Dense metal ions, that is Es layers, tend to move vertically into the geomagnetic westward wind regions. Geomagnetic zonal winds tend to be eastward around Southern Africa, which causes the decrease of Es occurrences there. Es distributions are also affected by horizontal ion transport due to winds and partially by the vertical ion convergence at 120–130 km altitudes, where Es layers start to form. Metal ion transport is the primary cause of the EsOR distribution and the genomagnetic configuration is the secondary cause.

R005-P42
ポスター 3 ：11/25　PM1/PM2 （13:15-18:15）

#Rifqi Farhan Naufal[1)], Liu Huixin[2)], Qiu Lihui[3)], 垰 千尋 [4)]
(1 九州大学理学府地球惑星科学専攻, (2 九州大学理学府地球惑星科学専攻, (3 九州大学理学府地球惑星科学専攻, (4 情報通信研究機構

Effects of doubling CO2 concentration on Sporadic E around Japan region based on GAIA

#Farhan Naufal Rifqi[1)], Huixin Liu[2)], Lihui Qiu[3)], Chihiro Tao[4)]
([1]Department of Earth and Planetary Science, Graduate School of Science, Kyushu University, [2]Department of Earth and Planetary Science, Graduate School of Science, Kyushu University, [3]Department of Earth and Planetary Science, Graduate School of Science, Kyushu University, [4]National Institute of Information and Communications Technology

This study utilizes the Ground-to-topside Atmosphere Ionosphere model for Aeronomy (GAIA) to investigate the effects of doubling CO2 concentration on the occurrence of Sporadic E (Es) layers around Japan region. Using two datasets, representing normal and doubled CO2 conditions for the year 2001, the vertical ion convergence (VIC) and other related parameters were calculated during the Summer Solstice. The VIC distribution around Japan was examined in terms of daily variations at four ionosonde stations around Japan: Wakkanai, Kokubunji, Yamagawa, and Okinawa. Based on our analysis, a general increase in the magnitude of VIC around Japan under doubled CO2 conditions are observed, while the altitude of VIC magnitude maxima decreases. Potential physical processes driving vertical ion convergence under these conditions are identified. At altitudes of 90-100 km, the increase in VIC magnitude is primarily driven by zonal wind and a decreasing ratio of ion-neutral collision frequency to ion gyrofrequency. At 100-105 km, the increase is mainly influenced by the aforementioned ratio. These mechanisms are clearly observed at Kokubunji, Yamagawa, and Okinawa, but not as evident at Wakkanai, of which mechanism mainly driven by zonal wind, regardless of altitude difference. The results revealed in this study suggest that the climate change will enhance Es and its occurrence.

R005-P43
ポスター 3 ：11/25　PM1/PM2 （13:15-18:15）

酸素原子のイオン-中性衝突断面積：電離圏温度での関数フィットの改良

#家田 章正 [1)]
(1 名大宇宙地球研

Improved Fit of Atomic Oxygen Ion – Neutral Collision Cross Section at Ionospheric Temperatures

#Akimasa Ieda[1)]
(1Institute for Space-Earth Environmental Research, Nagoya University

Atomic oxygen and its ion are major species in the ionospheres of Earth, Venus, and Mars. Collisions between them control the structure and dynamics of the ionosphere. An accurate collision cross-section model is thus a prerequisite for a quantitative study of the ionosphere. Fits of recent wide-energy models are reasonable for the quiet-time F-region ionosphere of Earth near 1000 K. However, their valid temperature range has been unclear and limited because of physically inaccurate fitting basis functions. We improved the classic charge-exchange fitting basis function by introducing the curved-trajectory and quantum oxygen-atom fine-structure effects. The resultant fit is accurate between 40 and 9000 K and thus can be robustly used for the ionospheres of Earth, Venus, and Mars.

Ieda (JGR, 2021), https://doi.org/10.1029/2020ja028441
Ieda (JGR, 2022), https://doi.org/10.1029/2021ja029612

酸素原子とそのイオンは、地球・金星・火星の電離圏を構成する主要な粒子種である。両粒子間の衝突は、衝突断面積モデルとして表現される。最近、教科書的な high-energy タイプのモデルでなく、wide-energy タイプのモデルが正しいことが示された (Ieda, 2021)。この wide-energy タイプのモデルの、有効な温度範囲は 300-2000 K 程度である。本研究で、カーブ軌道効果 (Ieda, 2022) を考慮することにより、関数フィットの基底関数を改良した。この結果、有効温度範囲は 75-9000 K と広がり、地球・金星・火星の電離圏に十分となった。

Ieda (JGR, 2021), https://doi.org/10.1029/2020ja028441
Ieda (JGR, 2022), https://doi.org/10.1029/2021ja029612

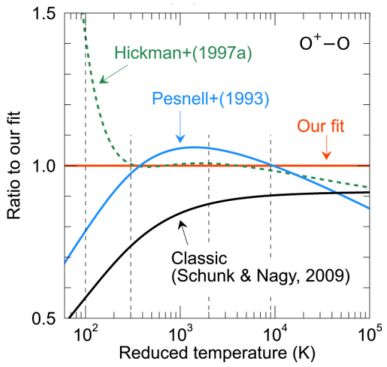

Figure 1.
O^+-O collision frequency or momentum-transfer cross section. Our concluding fit is shown by the red line. Various models are shown as the ratio to our concluding fit.

Below 300 K, only our fit is accurate because low temperatures were not concerned in previous fits. The collision frequency is underestimated in the classic model by 16% at 1000 K and by 35% at 200 K.